University of Massachusetts Amherst
ScholarWorks@UMass Amherst

Doctoral Dissertations 1896 - February 2014

1-1-2006

Surface modification by adsorption of macromolecules : organosilane/metal oxide chemistry.

Ilke Anac
University of Massachusetts Amherst

Follow this and additional works at: https://scholarworks.umass.edu/dissertations_1

Recommended Citation
Anac, Ilke, "Surface modification by adsorption of macromolecules : organosilane/metal oxide chemistry." (2006). *Doctoral Dissertations 1896 - February 2014*. 1092.
https://doi.org/10.7275/gnce-gv71 https://scholarworks.umass.edu/dissertations_1/1092

This Open Access Dissertation is brought to you for free and open access by ScholarWorks@UMass Amherst. It has been accepted for inclusion in Doctoral Dissertations 1896 - February 2014 by an authorized administrator of ScholarWorks@UMass Amherst. For more information, please contact scholarworks@library.umass.edu.

UMASS/AMHERST
312066 0325 6442 1


University of
Massachusetts
Amherst

LIBRARY

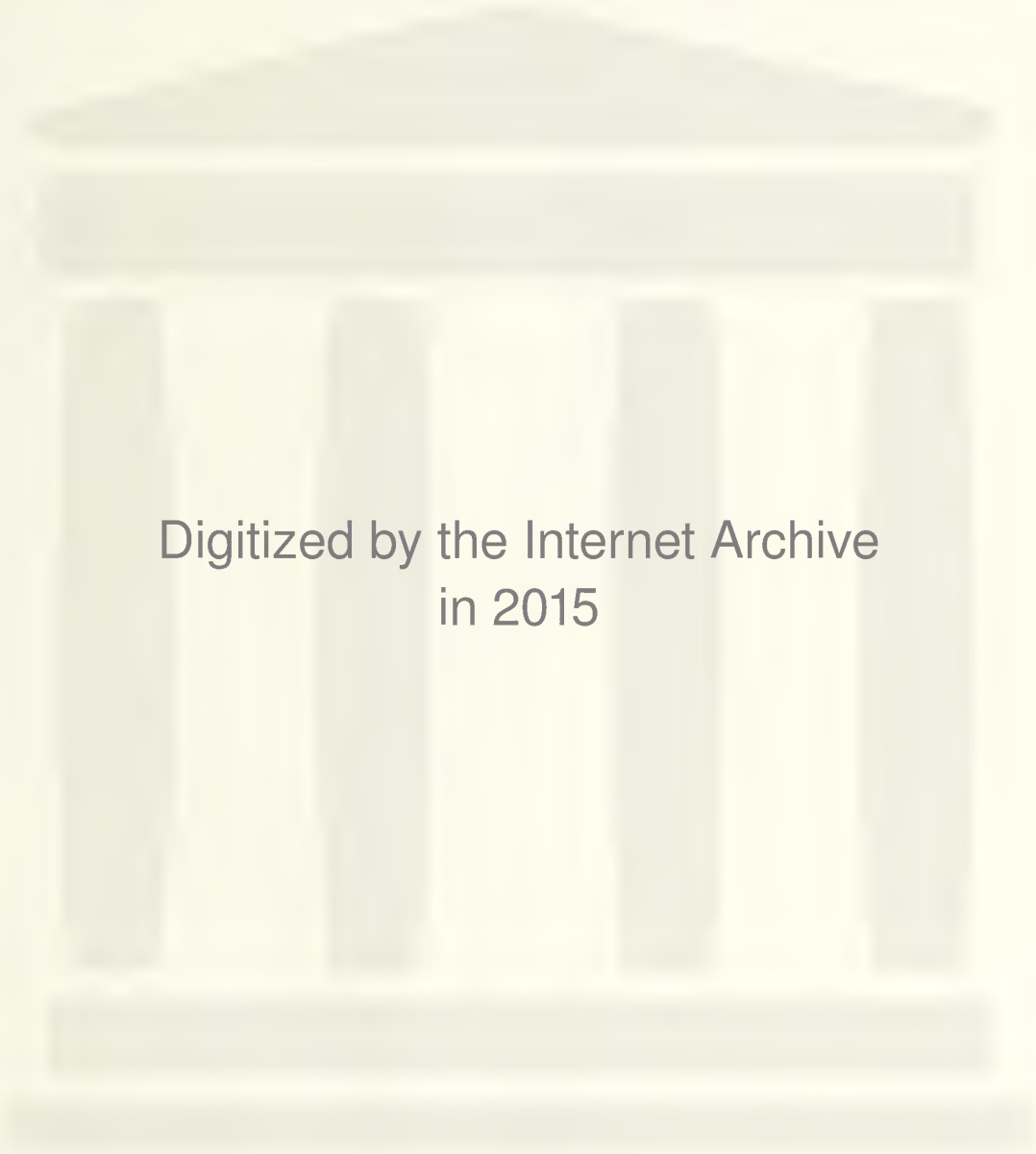

Digitized by the Internet Archive
in 2015

https://archive.org/details/surfacemodificat00anal

This is an authorized facsimile, made from the microfilm master copy of the original dissertation or master thesis published by UMI.

The bibliographic information for this thesis is contained in UMI's Dissertation Abstracts database, the only central source for accessing almost every doctoral dissertation accepted in North America since 1861.

UMI® Dissertation Services

From:ProQuest COMPANY

300 North Zeeb Road
P.O. Box 1346
Ann Arbor, Michigan 48106-1346 USA

800.521.0600 734.761.4700
web www.il.proquest.com

Printed in 2007 by digital xerographic process
on acid-free paper

SURFACE MODIFICATION BY ADSORPTION OF MACROMOLECULES; ORGANOSILANE/METAL OXIDE CHEMISTRY

A Dissertation Presented

by

İLKE ANAÇ

Submitted to the Graduate School of the
University of Massachusetts Amherst in partial fulfillment
of the requirements for the degree of

DOCTOR OF PHILOSOPHY

September 2006

Polymer Science and Engineering

UMI Number: 3242302

Copyright 2006 by
Anac, Ilke

All rights reserved.

INFORMATION TO USERS

The quality of this reproduction is dependent upon the quality of the copy submitted. Broken or indistinct print, colored or poor quality illustrations and photographs, print bleed-through, substandard margins, and improper alignment can adversely affect reproduction.

In the unlikely event that the author did not send a complete manuscript and there are missing pages, these will be noted. Also, if unauthorized copyright material had to be removed, a note will indicate the deletion.

UMI Microform 3242302
Copyright 2007 by ProQuest Information and Learning Company.
All rights reserved. This microform edition is protected against unauthorized copying under Title 17, United States Code.

ProQuest Information and Learning Company
300 North Zeeb Road
P.O. Box 1346
Ann Arbor, MI 48106-1346

© Copyright by İlke Anaç 2006

All Rights Reserved

SURFACE MODIFICATION BY ADSORPTION OF MACROMOLECULES; ORGANOSILANE/METAL OXIDE CHEMISTRY

A Dissertation Presented

by

İLKE ANAÇ

Approved as to style and content by:

_____

Thomas J. McCarthy, Chair

_____

David A. Hoagland, Member

_____

S. Thayumanavan, Member

_____

Shaw Ling Hsu, Department Head
Polymer Science and Engineering

SURFACE MODIFICATION BY ADSORPTION OF MACROMOLECULES: ORGANOSILANE/METAL OXIDE CHEMISTRY

A Dissertation Presented

by

İLKE ANAÇ

Approved as to style and content by:

Thomas J. McCarthy, Chair

David A. Hoagland, Member

S. Thayumanavan, Member

Shaw Ling Hsu, Department Head
Polymer Science and Engineering

DEDICATION

My parents, Nevres and Özdemir Anaç

ACKNOWLEDGMENTS

I would like to thank all the people who made this thesis possible and enjoyable experience for me. Most of all, I would like to acknowledge my thesis advisor, Professor Tom McCarthy. His wide knowledge and his logical way of thinking have been of great value for me. Thank you, Tom, for your understanding, support and guidance: it was a great pleasure for me to conduct this thesis under your supervision. I also want to thank my committee Professor David Hoagland and Professor S. Thayumanavan for their time and helpful suggestions that they have given me in the last year.

I want to thank past and present McCarthy group members because this thesis would not be possible without them. I had wonderful time with them both in lab and outside lab. Thanks to Margarita (for the wonderful memories, your endless help and your real friendship). Jung Ah (for your help, input and friendship), Jack (for your help with many things in the lab), Ebru (for the support during my qualifiers), Jay (for interesting conversations), Zhixiang (for your kindness and joyful personality), Kevin, Ted, Misha, Wei, Yufeng, Lichao, Dalton, Bokyung, Joonsung, Scott, Xiaoying and Jiaxin. Thanks to PS&E Faculty and staff for all the kindness and support. Special thanks to Vivien Venskowski, Eileen Besse, and Anita Hassenfratz. Some of my friends from PSE department also deserve acknowledgment. Thanks to Manuel, Sian, Matt, Sterling, Kishore, and especially to Ali and Damla who made the graduation year easier for me with their friendship and great support.

I would also like to thank my teachers in Boğaziçi University for their support during my undergraduate and graduate years. Special thanks to Eliza Kalvo, Nihan and Turgut Nugay.

During my years in Amherst, I had wonderful friends outside the department who made the life easier and so enjoyable. I want to thank to Pilar, Tim, John, Ceren, Başak, Barbara, Güneş, Genti, Belma, Gökhan, Cahide and Serkan. Special thanks to my forever-supportive family in Amherst: Gökhan Abi, Kaan (my little and cute love), Özgür (your strong personality and encouragement was so helpful for me) and my great sister, Betül, (your endless support about everything made my life in Amherst so meaningful).

Special thanks to my aunt, Nurdan , my uncle, Ahmet, my grandmothers, my cousins, Didem and Evren, my sister, Emek, my best friends, Ezel and Şeyda who always provided me love, support and care on the other side of the world.

I feel very special and blessed to have unconditional love, patience and support of wonderful parents, Nevres and Özdemir Anaç. I could not make it this far without their endless encouragement, friendship, understanding and self-sacrifice. I know saying thank you to them will never be enough.

ABSTRACT

SURFACE MODIFICATION BY ADSORPTION OF MACROMOLECULES:

ORGANOSILANE/METAL OXIDE CHEMISTRY

SEPTEMBER 2006

İLKE ANAÇ, B.S., BOĞAZİÇİ UNIVERSITY

M.S., UNIVERSITY OF MASSACHUSETTS AMHERST

Ph.D., UNIVERSITY OF MASSACHUSETTS AMHERST

Directed by: Professor Thomas J. McCarthy

Poly(trifluoroethylene) (PF_3E) irreversibly adsorbs to oxidized silicon and covalently attached amine monolayers supported on silicon, producing hydrophobic thin films in the thickness range of 8-40 Å. The ultra-thin films of adsorbed PF_3E were characterized here by means of contact angle, ellipsometry and X-ray photoelectron spectroscopy (XPS). Adsorption conditions such as reaction time, polymer concentration and solvent composition were also investigated. The adsorption behavior of PF_3E can be explained by its ability to crystallize and form hydrogen bonds with proton acceptors, due to highly polar C-H bonds throughout the backbone.

The hydrogen bonding - directed layer-by-layer assembly technique was used to build multilayers of poly(trifluoroethylene) (PF_3E) and poly(4-vinylpyridine) (P4VP) from methanol solution. It was difficult to build up layers subsequent to the second layer, due to the replacement of an already formed layer by the adsorbing polymer.

The remainder of this thesis describes the modification of metal oxide surfaces with organosilanes. Silicon-supported titanium oxide is modified by the reaction of

hydridosilane ($R_{3-n}SiH_{n+1}$) in the vapor phase and in heptane solution at elevated temperatures. Surfaces are characterized by contact angle measurements and XPS.

The preparation of hydrophobic alkylsiloxane layers on chromium surfaces by reaction of organosilanes $R_{3-n}SiX_{n+1}$ (where X=Cl, OEt and H) was examined under two conditions: (1) in the vapor phase and (2) in toluene in the presence of ethyldiisopropylamine (EDIPA) using chloro- or ethoxysilanes, or in heptane using hydridosilanes. Surfaces were again characterized by contact angle analysis and XPS. Silicon-supported alkylsiloxane layers are prepared by the reaction of tri-n-hexylsilane and octylsilane in the vapor phase, in toluene and in $ScCO_2$ at elevated temperatures, and octadecylsilane in the vapor phase and in toluene solution. It is shown that the layer structure depends on the reaction conditions. The kinetics of vapor phase reactions using tri-n-hexylsilane and octylsilane and $ScCO_2$ phase reaction using octylsilane are described.

TABLE OF CONTENTS

LIST OF TABLES

LIST OF FIGURES

CHAPTER 1

ADSORPTION OF POLY(TRIFLUOROETHYLENE)

1.1 Introduction

Adsorption is a phenomenon in which molecules in solution spontaneously form a concentrated layer at an interface, changing surface properties. Polymers readily adsorb to solid surfaces[1], creating a rather diffuse layer with polymer segments. The adsorption of polymers (e.g. homo-, block and graft polymers) plays a vital role in many scientific and technological applications such as colloid stabilization [2-5](e.g. formulation of paints, coatings, and printing inks), flocculation[6], corrosion[1,7], adhesion[1,8], and lubrication[9].

The ultimate goal of polymer adsorption research is to fabricate materials with tailored surface properties. To reach this goal we need to understand how the nature of the polymer, the substrate, the type of solvent, and the concentration of polymer affect the macroscopic properties of the interface. This field of research has received great interest from experimental[10-19] and theoretical groups[20-24] for many years.

The McCarthy Group reported adsorption of the polar homopolymer poly(L-lysine) (PLL) to a fluoropolymer[25] / poly(tetrafluoroethylene-co-hexafluoropropylene) (FEP) surface / from aqueous solution, adsorption of thiol terminated polystyrene and styrene-propylene sulfide block polymers to a gold surface from tetrahydrofuran (THF)[26], adsorption of terminally functionalized (-COOH and -OH) polystyrenes on alumina and silicon thin layers[27], and adsorption of poly(vinylalcohol) (PVOH) onto hydrophobic surfaces from aqueous solutions[28,29].

The heterogenous (gas-solid) chlorination and fluorination of poly(trifluoroethylene) (PF_3E) has been investigated (Figure 1.1 A) by Vipavee Phuvarnartnuruks[30]. Besides this report, there is no literature reporting the use of poly(trifluoroethylene) (PF_3E) in surface modification.

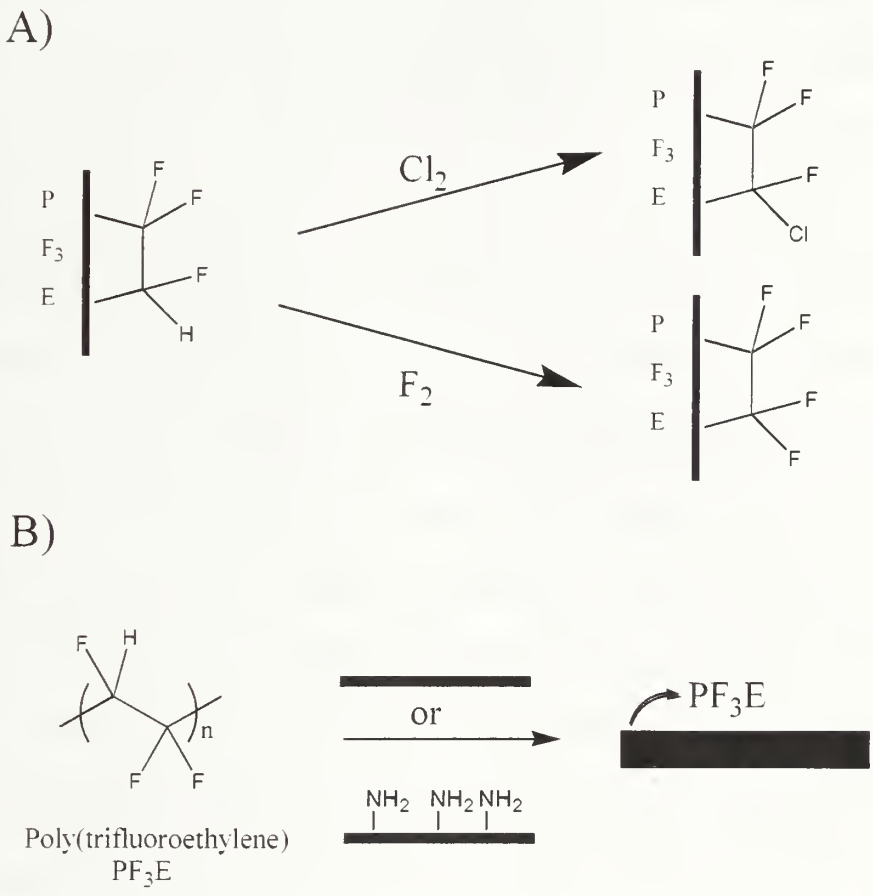

Figure 1.1 Schematic representation of reactions of poly(trifluoroethylene) thin films (A) and adsorption of poly(trifluoroethylene) (PF_3E) onto silicon and a silicon-supported covalently attached amine monolayer (B)

In this chapter, the adsorption of poly(trifluoroethylene) (PF_3E) from solution onto hydrophilic (bare oxidized silicon wafer) and slightly hydrophilic (silicon-supported covalently attached amine monolayer) surfaces is described. (Figure 1.1 B).

1.1.1 Homopolymer Adsorption[30,31]

When a polymer molecule is brought in the vicinity of a surface, it will either be attracted to the surface and form an adsorption layer, or be repelled from the surface and form a depletion layer (Concentration near the surface is lower than in solution). Three energetic contributions determine whether a polymer will adsorb to or deplete. They are solvent- and polymer- segment interactions with the surface and with each other, conformational losses of an isolated polymer chain incurred upon adsorption and osmotic (crowding) effects in the adsorbed layer. The energy difference between the polymer-surface interaction and polymer segment-solvent interaction is defined as surface interaction parameter (exchange free energy) χ_s[20,32,33]. It is the energy that makes the polymer adsorb to the surface by replacing a solvent molecule on the surface with a polymer segment. This predicts a number of different results. High interaction energy (exothermic) between polymer segments and the surface can drive the adsorption. In another scenario both solvent and polymer interactions with the surface can be endothermic (as is the case with many low energy solids), and the polymer can adsorb. The choice of a solvent is very important because a solvent with a high interaction with the surface can prevent adsorption of the chain. When the polymer chain is attached to the surface, the total number possible conformations decreases with respect to a chain in solution, thus the conformational entropy of the polymer chain decreases with respect to a chain in free solution. The entropy loss is described in terms of a critical surface interaction parameter χ_{sc}[20,32-34]. The osmotic term (crowding term) is determined by how much polymer segment density can be forced to the surface and it tends to limit adsorption by diluting the polymer segments as much as possible. The

adsorption, which is a negative energy change, can take place if the surface interaction parameter, χ_s, is greater than the critical surface interaction parameter, χ_{sc}, which means that loss of configurational entropy upon adsorption is compensated by the gain of enthalpy due to multiple polymer segment-surface interactions.

Polymers can adsorb on surfaces and have only a fraction of their segments on the surface while a substantial fraction of segments is projecting into the solution. The segments on the surface are termed trains, the ones with both ends in contact with the surface are termed loops, and one or two tails can be present at the end of the adsorbed molecule. The distribution of loops, trains and tails largely determines the physical properties of the system, and this distribution varies with polymer concentration and molecular weight of the polymer. The adsorbed amount per unit surface area, Γ, fractional surface coverage, θ, and the bound fraction, p, can be measured experimentally. Spectroscopic methods such as infrared, nuclear magnetic resonance and electron spin resonance spectroscopies illuminate adsorbed amounts and configurations with the surface. Ellipsometry can be used to determine the amount of the adsorbed amount and thickness on optically reflecting surfaces. Radiotracer labeling followed by scintillation also can be used to determine the adsorbed amounts[17]. Small-angle neutron scattering[35] shows the spatial distribution of adsorbed layers and determines the overall size of polymer chains. The layer thickness can also be determined by the layer's hydrodynamic response by the viscosity change upon adsorption or the change in solvent flux[36].

The theory of Scheutjens and Fleer (S&F)[20,23,32] for homopolymers has been shown to agree well with experimental results. They evaluated the partition function for

a mixture of polymer chains and molecules near an interface assuming random mixing within an adsorption layer (the mean field approximation) based on a quasi-crystalline lattice model. The theory can predict the distribution of individual chain segments, the concentration profile due to the loops and tails, the root-mean square layer thickness, the numbers and average lengths of trains, loops, and tails, and the train, loop and tail size distribution.

De Gennes'[37] scaling argument predicts polymer adsorption tendencies from good solvents. In their theory, they took into consideration the correlations between polymer segments, and claimed that the Scheutjens and Fleer theory doesn't consider the swelling of a polymer chains in good solvent conditions or overlapped polymers in concentrated solutions.

It was proven experimentally and predicted theoretically that homopolymer adsorption can be enhanced by decreasing solvent quality[14,38] (decreasing solvent-polymer segment interaction) or increasing surface affinity[27,39,40] (increasing the polymer segment-surface interaction).

1.1.2 Poly(trifluoroethylene)

Poly(trifluoroethylene) (PF_3E) is soluble in several solvents (e.g. THF, methanol and acetone) and can be conveniently cast as a film or coating. It is a practical precursor[30] to fluoropolymers (PCTFE and PTFE) for surface or coating applications. It is the least studied fluoropolymer, particularly with regard to its stereo- and regioirregularity. It gained more attention after it was found[41-45] that copolymers of trifluoroethylene and vinylidene fluoride are piezo- and pyroelectric over a range of compositions and, additionally, display distinct ferroelectric transitions that, so far , have not been seen in PVF_2 itself. This has stimulated interest in the synthesis, structure, crystallization and properties of poly(trifluoroethylene).

1.1.2.1 Synthesis of Poly(trifluoroethylene)

Direct polymerization of trifluoroethylene using free radical polymerization forms polymers with regioirregular defects as a result of head-to-head and tail-to-tail addition of monomeric units. Cais et al[46] have proposed a synthetic route to isoregic (stereochemical structure in which monomeric units have the same directional orientations) PF_3E by reductive dechlorination or debromination of the precursor polymers, poly(bromotrifluoroethylene) or poly(chlorotrifluoroethylene). PF_3E in this study was synthesized by the reductive dechlorination of poly(chlorotrifluoroethylene) in tetrahydrofuran (THF) at 65 ^{o}C using azo(bisisobutyronitrile)(AIBN) as an initiator and tributyltin hydride (Bu_3SnH) as a reducing agent. (Figure 1.2)

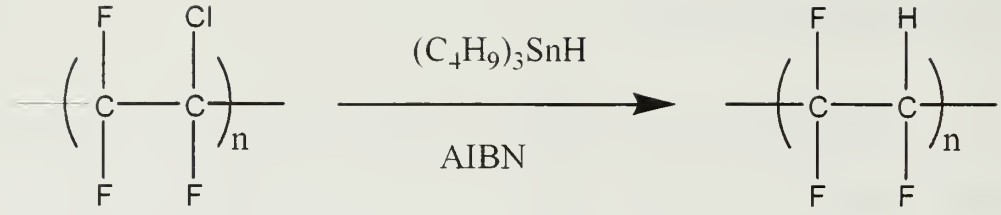

Figure 1.2 Reductive dechlorination of poly(chlorotrifluoroethylene)

1.1.2.2 Properties of Poly(trifluoroethylene)

Even though PF_3E[47] is essentially atactic, the polymer chains are able to crystallize as a result of the similarity between C-F and C-H bond lengths, as well as the van der Walls radii of fluorine and hydrogen. These elements behave isomorphically in PF_3E, allowing development of significant crystallinity. The melting behavior of PF_3E reflects its thermal history, polydispersity and molecular weight. Isoregic polymer with fairly high molecular weight and low polydispersity displays a single melting endotherm ranging from 175-180 °C that depends on crystallization temperature. The glass transition temperature is reported as 30-40 °C.[48] The structure and morphology of the polymer have been studied by X-ray and electron diffraction. It has been shown that variations in isoregicity from 86.2% to 98% have no effect on the crystalline structure of PF_3E. X-ray results show hexagonal packing of polymer chains with a diffuse meridional reflection observed at 2.29 Å. This indicates a disordered conformation comprised of an irregular succession of TGTG and TT groups.

1.1.2.3 Adsorption of Poly(trifluoroethylene)

In the research studies reported here, adsorption of poly(trifluoroethylene) (PF_3E) from solution was chosen to fabricate thin coatings of poly(trifluoroethylene) (PF_3E) on oxidized silicon and covalently attached silicon-supported amine monolayers.

The polymer's ability to crystallize and form hydrogen bonds with proton acceptors were two driving forces to study the adsorption of PF_3E on different substrates. Since PF_3E does not contain specific functionality which will promote the adsorption onto the surfaces. two approaches can be chosen: (1) the addition of non-solvent to the polymer solution (that is dissolved in good solvent) to adjust the solvent quality or (2) incorporation of polar functionality to polymer backbone. In this chapter. the first approach is described to promote the adsorption on two different substrates. Tetrahydrofuran (THF) and toluene were chosen as a good and non-solvent. respectively.

1.2 Surface Analytical Techniques

1.2.1 X-ray Photoelectron Spectroscopy

X-ray photoelectron spectroscopy[49,50],XPS. is a versatile surface analytical technique that provides a total elemental analysis. except for hydrogen and helium. of the top 10-200 Å (depending on the sample and instrumental conditions) of any solid surface which is vacuum stable or can be made vacuum stable by cooling. From photoemission spectra. quantitative (surface concentrations) and qualitative (functional group) information can be obtained. During an XPS experiment. a sample surface is irradiated with monochromatic X-rays. X-ray photons transfer their energy to inner-shell electrons. forcing them to leave the surface of the sample. These electrons are referred to as photoelectrons. (Figure 1.3)

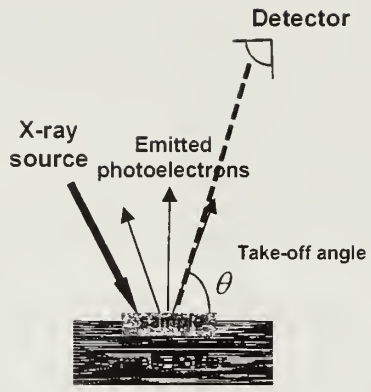

Figure 1.3 Schematic Diagram of XPS

The kinetic energy E_k of the photoelectron is determined by the difference between the X-ray photon energy ($h\nu$) and the binding energy E_b of the electron. Since the kinetic energy of the photoelectron is measured experimentally, the binding energy of the inner shells electrons can be determined by the following equation:

$$E_b = h\nu - E_k$$

where h is Planck's constant and ν is the X-ray frequency. The element can be easily identified due to the uniqueness of the binding energy of a particular shell of an atom for each element. That is why XPS is also known as electron spectroscopy for chemical analysis (ESCA). After the ejection of an electron from an inner shell of an atom, the hole can be filled by an electron from the outer shell, releasing an amount of energy. This energy can be emitted as a quantum of X-ray radiation (X–ray fluorescence) or the energy can be given to another electron in the same level or a lower level. This electron (Auger electron) is then emitted (Auger Emission) with a certain kinetic energy. The kinetic energy of Auger electrons is also characteristic of the elemental composition and independent of the excitation energy while E_k depends on X-ray energy.

The photoelectrons can experience elastic and inelastic interactions due to excitation of valance and inner electrons, as well as vibrational interactions. The

inelastic interactions produce decreases in kinetic energy, which limits no-loss emission to a mean depth of only a few atomic layers below the surface and makes the technique surface sensitive. The intensity of photoelectrons which show no loss in their kinetic energy after traveling a distance z can be shown by the following equation[51]:

$$I(z) = I' \exp\left(\frac{-z}{\lambda_a(E_k)\sin\theta}\right)$$

where I' is the initial photoelectron energy. $\lambda_a(E_k)$ is the attenuation length of photoelectron with a certain kinetic energy E_k, and θ the angle between the analyzer and the surface. There are four distances to be defined. Inelastic mean free path is defined to be the average distance (in nanometers) that an electron having a given energy travels between successive inelastic collisions. Attenuation length, λ_a, is defined to be the average distance (in nanometers) that an electron having a given energy travels between successive inelastic collisions as derived from a model in which the elastic electron scattering is assumed to be insignificant. The measured attenuation length is shorter than the inelastic mean free path by an amount depending on the differential cross section for elastic scattering. The escape depth (ς) is defined as the distance normal to the surface at which the probability of an electron being emitted without significant energy loss is $e^{-1}(36.8\%)$ of its original value. It is equal to $\lambda_a \sin\theta$. Finally, the sampling depth is the distance (in nanometers) normal to the surface from which a specific percentage of the detected electrons originate. Sampling depth is usually taken as three times the escape depth $(3\lambda_a \sin\theta)$. Changing the θ allows characterization at various depths within the substrate.

By measuring the relative intensities of photoelectron peaks with respect to appropriate sensitivity factors, the atomic composition of the surface can be determined. Small "chemical shifts" in binding energies are observed due to the chemical environment of an element, since the binding energy is sensitive to the electronegativity of the substituents. The more electronegative the substituents are, the higher will be the binding energy of the peak. This difference in binding energies allows the identification of functional groups.

1.2.2 Contact Angle Measurements –Wettability

Contact angle measurement is the simplest, but still powerful, surface characterization tool. When a drop of liquid is placed on a solid surface and the surface tension of the liquid is larger than the surface tension of the solid, it makes a definite angle of contact between the liquid and solid phases. Throughout this text, references to contact angle will refer to this method of measurement which is termed the "sessile drop" method. The contact angle[51-53], (Figure 1.4) is governed by force balance at the three – phase boundary and defined by Young's equation:

$$\gamma_{LV} \cos\theta = \gamma_{SV} - \gamma_{SL}$$

where γ_{LV} the surface tension of the liquid in its saturated vapor. γ_{SV} is the surface tension of the solid saturated with the saturated vapor of the liquid and γ_{SL} is the interfacial tension between the solid and the liquid.

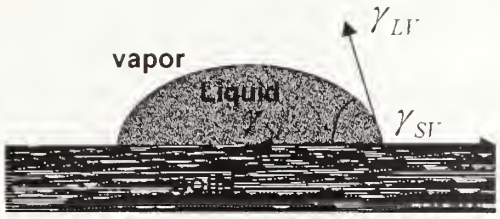

Figure 1.4 Contact Angle Measurement by Sensile Drop Method

There are two types of contact angle: static and dynamic. A static angle, which is determined by the equilibrium of interfacial tensions, is formed at a stationary liquid front. A dynamic contact angle, which is the balance of interfacial driving force and viscous force, is formed at a moving liquid front. More accurate information about the surface can be gathered through the use of dynamic contact angle. In a dynamic contact angle experiment, the liquid is added to (advancing) and withdrawn from (receding) the drop during the measurement of the angle. Dynamic contact angle is measured when the three phase contact line is in motion. The advancing angle, which is the observed maximum value, gives information about the surface functional groups and the surface energy of a fresh surface which has not been changed by the probe liquid through surface reconstruction or fluid adsorption. The receding angle, which is the observed minimum value, and hysteresis, the difference between the advancing angle and receding angle, together give information about surface heterogeneity, both chemically and physically (roughness). Contact angle hysteresis is also a measure of liquid dissolution of the surface, adsorption on the solid, and surface reorientation. Hysteresis also plays an important role in determining hydrophobicity[54]. Together, much information can be gained about the top couple of angstroms of the sample. Even more

information can be assessed when dynamic contact angle data from a variety of probe fluids are used.

Surface	γ_c (dyne/cm)	Liquid	γ_{LV} (dyne/cm)
$-CF_3$ (densely packed monolayer)	6	Ethanol	21.4
Poly(tetrafluoroethylene)	18.5	Tetrahydrofuran	27.4
$-CH_3$ (densely packed monolayer)	22	n-Hexadecane	27.6
Poly(vinylidene fluoride)	25	Ethylene Glycol	47.0
Polyethylene	31	Methylene Iodide	50.8
Poly(ethylene terephthalate)	43	Water	72.8
SiO_2(silicon surface)	73		

Table 1.1 Critical Surface tension values for common polymeric surfaces and liquid surface tensions for some liquid probe fluids at 25 °C[55,56]

Many researchers use contact angle data of water, methylene iodide, and n-hexadecane to cover a broad range of liquid surface tensions. The critical tension of a surface can be obtained if the values of $\cos\theta$ for a series of homologous liquids are plotted against the surface tension of liquids (Zisman Plot). The intercept of the line at $\cos\theta = 1$ is the critical surface tension (γ_c). Table 1.1 shows the critical surface tension values for common polymeric surfaces and surface tension values for common liquids. A surface is completely wetted by a fluid with a surface tension equal to or less than the critical surface tension.

1.2.3 Ellipsometry

Ellipsometry[57,58] is a common technique for determination of the thickness and refractive index of thin homogeneous films. The sample thickness can be measured from a few angstroms to microns. The advantages of this technique are that the measurement does not require special conditions such as vacuum, heat and electron

bombardment, and the presence of an optical liquid does not affect the results. In a typical ellipsometer, the surface is irradiated at a known angle of incidence with a collimated beam of monochromatic light. If the surface contains a thin film and substrate properties are known, the thickness and refractive index of the thin film can be deduced. In order to make an accurate measurement, it is assumed that the film is smooth and isotropic over an area of 2 mm^2 to 10 mm^2. A large difference between film and substrate refractive indices is important[59].

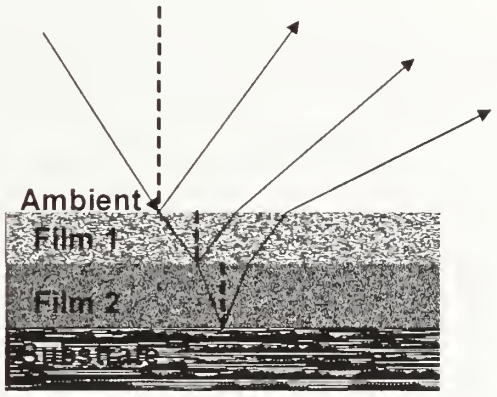

Figure 1.5 Ellipsometric determination of film thickness

When a plane-polarized monochromatic light (p= angle of polarization) interacts with the surface at some angle, it can be resolved into its parallel and perpendicular components (s- and p- polarized, respectively). These components are reflected from the surfaces in a different way; i.e., the amplitude and phase of both components are changed. When s- and p- polarized light beams are combined, the result is elliptically polarized light. A compensator changes the elliptically polarized light to plane polarized light (a = angle of polarization). These two angles (p and a) give the phase shifts between the parallel and perpendicular components (Δ) and the change in the ratio of

amplitudes of the two components ($\tan\Psi$). By applying fundamental physics, the basic equation of ellipsometry can be derived:

$$\rho = \tan\Psi e^{i\Delta}$$

where $\Delta = 2p + \pi/2$ and $\Psi = a$ and ρ is the ratio between r_p and r_s, the reflection coefficients of the p- and the s- polarized light, respectively. For a clean surface, Δ and Ψ are related to the complex index of reflection of the surface.

$$\hat{n}` = n`\left(1 - ik`\right)$$

where $n`$ is the ordinary reflection index and $k`$ is the extinction coefficient. The fit of $\tan\Psi$ and $\cos\theta$ allows the calculation of thickness.

1.2.4 Atomic Force Microscopy

Atomic Force Microscopy[51] (AFM) can produce three-dimensional images of solid surfaces at very high resolution. An advantage of using an atomic force microscope is that it can image non-conducting materials such as ceramics and polymers. A typical AFM consists of a piezoelectric scanner, which controls the scanning motion, an optical head, which senses the cantilever detection, and a base, which supports the scanner, the head and includes a circuit for detection.

AFM operates by scanning across the surface with a sharp tip mounted on a soft cantilever spring. The cantilever and tip are microfabricated from silicon, silicon oxide, or silicon nitride. AFM operates in two modes: Contact mode and Tapping mode. Contact mode AFM operates by scanning a tip attached to the cantilever across the sample surface while monitoring the change in cantilever deflection with a split photodiode detector. Tapping mode AFM operates by scanning a tip attached to the end

of oscillating cantilever across the sample surface. The tip lightly "taps" on the surface during scanning, contacting the surface at the bottom of its swing. The surface damage is less in tapping mode.

1.3 Experimental

1.3.1 Materials and Methods

All materials were used as obtained unless mentioned otherwise.

Poly(chlorotrifluoroethylene) (PCTFE) powder (3M Kel-F 81) was obtained from 3M. Tributyltinhydride (Bu_3SnH), azo(bisisobutyronitrile) (AIBN), aminopropyldimethylethoxysilane (APDMES), anhydrous tetrahydrofuran (THF) and anhydrous toluene were obtained from Aldrich. Hexane (HPLC grade) and heptane (HPLC grade) were purchased from Fisher. Silicon wafers were obtained from International Wafer Service (<100> orientation, P/B doped, 20-40 Ω cm, thickness 450-575 μm) and cleaned by a Harrick Scientific O_2 plasma cleaner at high power settings for 5 minutes prior to use. The oxide layer on the wafers after plasma treatment was determined to be ~25 Å by ellipsometry. Water was purified using a Millipore Milli-Q water system that involves reverse osmosis, ion exchange and filtration steps (10^{18} Ω/cm). Products obtained after synthesis were dissolved in THF and analyzed by ^{19}F NMR on a Bruker DPX300. Gel permeation chromatography (GPC) was performed with a Polymer Laboratories LC1120 high performance liquid chromatography (HPLC) pump equipped with a Waters differential refractometer detector. The mobile phase was tetrahydrofuran (THF) with a flow rate 1 mL/min. Transmission Infrared spectra (FT-IR) were recorded on a Bio Rad FTS 175C FT-IR spectrometer equipped with a

mercury cadmium telluride (MCT) detector. Differential scanning calorimetry (DSC) measurements were performed using a TA Instruments 2190 DSC under nitrogen gas flow. The heating rate was 10 °C/min. Thermogravimetric analysis was performed on a Dupont TGA 2950. X-ray photoelectron spectra (XPS) were obtained on a Physical Electronics Quantum 2000 Scanning ESCA Microprobe. Depth profiling was done by collecting spectra at 15° and 75° take-off angles with respect to the plane of the sample surface. The analysis at 15° has a penetration depth of ~10 Å and that at 75° corresponds to a penetration depth of ~40 Å. Contact angle measurements were made with a Ramè-Hart telescopic goniometer and a Gilmont syringe with a 24-gauge flat-tipped needle. Water was used as a probe liquid. Advancing and receding contact angles were recorded while the water was added and withdrawn from the drop, respectively. Ellipsometric measurements were done using a Rudolph Auto El-II automatic elipsometer. The light source is He-Ne laser $(\lambda = 623.8 \text{ nm})$, the incident angle is 70° and the compensator is-45°. The thicknesses were calculated using the transparent double layer model using a dafBM software (silicon substrate / silicon oxide + APDMES layer / PF_3E /air and silicon substrate / silicon oxide + PF_3E / air) with the following parameters: silicon substrate $n_s = 3.858$, $k_s = 0.018$ (imaginary part of the refractive index); air, $n_o = 1$; PF_3E, $n_1 = 1.42$; silicon oxide + APDMES layer: $n_2 = 1.462$. AFM images were obtained with a Digital Instruments Dimensions 3100 scanning probe microscope with a NanoScope III controller operated in tapping mode.

1.3.2 Synthesis of Poly(trifluoroethylene)

22.7 g (0.078 mol) Bu_3SnH in 112 mL THF solution and 1.2 g AIBN (0.0073 mol) in 30 mL THF solution were added to a nitrogen-purged round bottom flask containing 6 g PCTFE (0.052 mol, Mn~700.000-800.000) respectively. The mixture was refluxed at 65-70 °C for 24 hours. An additional 1.2 g AIBN in 30 mL THF was added to the mixture after the reaction had proceeded for 12 hours. The product was precipitated in 600 mL cold hexane (in dry ice) and purified by Soxhlet extraction using heptane for a day. The product was dried under vacuum at 80 °C for 48 hours. The obtained product and reaction yield were 3.5 g and 82% respectively.

1.3.3 Preparation of Silicon-Supported Amine Surfaces

Silanization with aminopropyldimethylethoxysilane (APDMES) was performed in the vapor phase at 70 °C for a day using ~ 0.5 mL of silane. There was no contact between the liquid silane and the cleaned silicon wafers. After silanization, the wafers were rinsed with toluene, 2-propanol, ethanol and water (in this order) and dried under vacuum at room temperature for half an hour. (Figure 1.6).

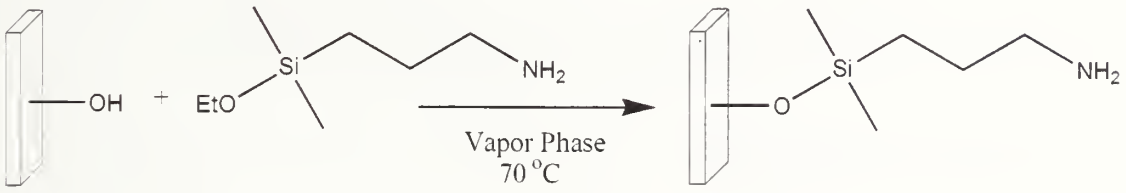

Figure 1.6 Reaction scheme for the preparation of NH_2-terminated covalently attached monolayers supported on silicon

1.3.4 Preparation of Poly(trifluoroethylene) Films

PF_3E (5 mils) films were prepared on glass microscope slides by casting a THF solution of PF_3E (5% mg/mL) with an application blade. The slide was put in a Petri dish and the Petri dish was covered with aluminum foil with holes to let the solvent slowly evaporate at room temperature overnight. Films were dried in a vacuum oven at 75 °C for 24 hours.

1.3.5 Adsorption Studies

PF_3E solutions of different concentration in THF and THF:Toluene mixtures (25:75; 50:50; 30:70) were prepared. PF_3E solutions in THF:Toluene mixtures were made by addition of the desired amount of toluene to a homogenous solution of PF_3E in THF. PF_3E dissolves in THF very slowly upon heating so the solutions were prepared a day prior to adsorption studies and toluene was added at the last minute. Substrates were submerged in the PF_3E solutions at room temperature for 24 h. Then the samples were rinsed with the same solvent used for adsorption, and dried under vacuum overnight. Desorption studies were done by immersing the samples (adsorption from 1 mg/mL THF solution) in THF for 24 h. PF_3E is irreversibly attached to the silicon surface and no desorption is observed after exposure to THF fora day.

1.4 Results and Discussion

1.4.1 Synthesis and Characterization of Polytrifluoroethylene

PF_3E is synthesized by the reductive dechlorination of poly(cholorotrifluoroethylene) (PCTFE) (Figure 1.2). This radical reaction is conducted in THF at 65 °C where AIBN and tributyltin hydride are used as an initiator and

reducing agent respectively. An excess molar ratio of tritinbutyl hydride is used to assure the complete dechlorination. The weight of the obtained product and yield of the reaction were 3.5 g and 82% respectively. The product had a weight average molecular weight (M_w) of 570.000 and a polydispersity of 1.3 by gel permeation chromatography (GPC). PF_3E is thermally stable up to 440 °C. as indicated by thermal gravimetric analysis (TGA) (Figure 1.7) Differential scanning calorimetry was used to analyze the melting transitionof the polymer (DSC, using a 10 °C/min heating rate, under nitrogen in the range of room temperature to 250 °C). T_m was ~177.40 °C. (Figure 1.8) The glass temperature (Tg), which was expected to be in the range of 30-50 °C. was not observed by DSC analysis. [48]

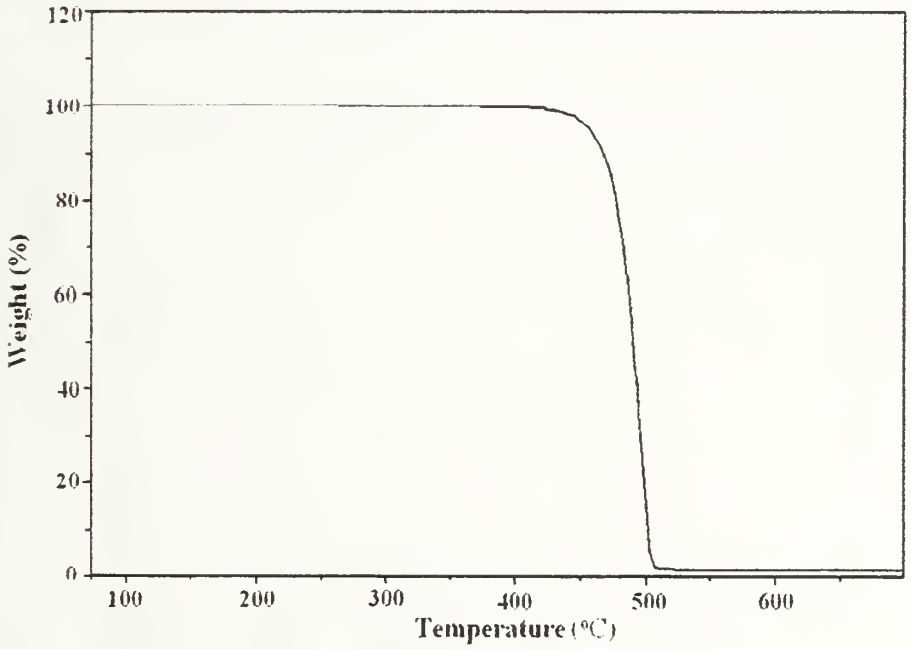

Figure 1.7 Thermal gravimetric analysis of poly(trifluoroethylene)

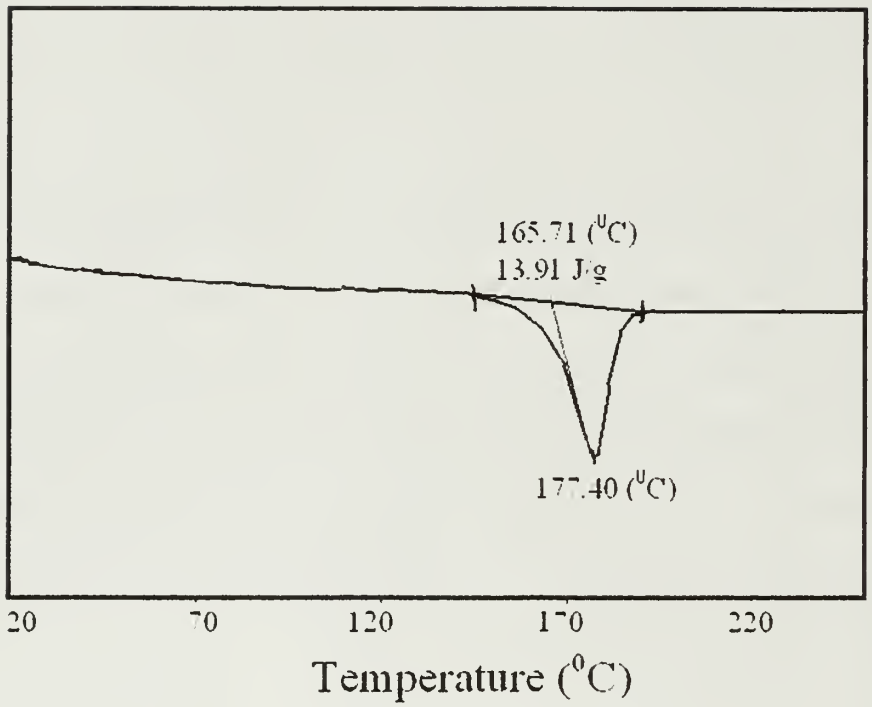

Figure 1.8 Differential Scanning Calorimetry profile of poly(trifluoroethylene)

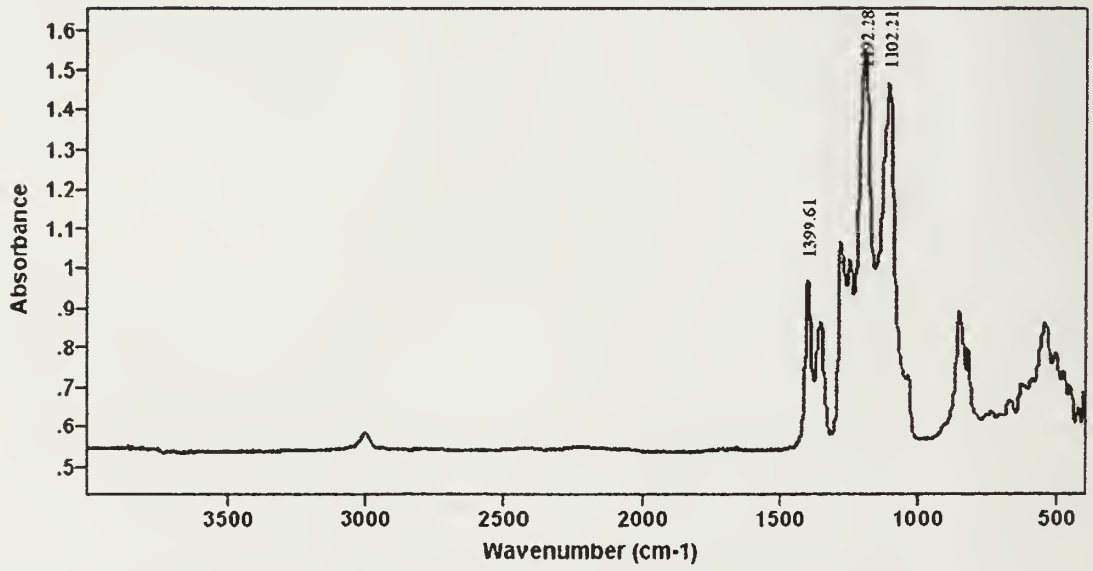

Figure 1.9 Infrared spectrum of solution-cast poly(trifluoroethylene)

Complete dechlorination can be confirmed by the absence of the 950 cm^{-1} absorbance to the C-Cl vibration in the infrared spectrum of poly(trifluoroethylene). (Figure 1.9). A small peak at at ~3000 cm^{-1} on the spectrum is due to the C-H stretching. The other bands that are observable in the spectrum at 1399 and at 1192-1102 cm^{-1} are due to the stretching of C-F and out-of-plane deformation of CF_2 units on the polymer backbone, respectively.

Figure 1.10 shows the ^{19}F NMR Spectra of poly(trifluoroethylene). The spectrum shows two peaks of interest that are assigned to two kinds of fluorine atoms such as –CHF-CF^*_2- CHF- and -CF_2-CHF^*-CF_2-. The absence of peaks, due to head-to-head or tail-to-tail addition (such as-CFH-CF^*_2-CF_2-CFH- or –CF_2-CHF^*-CFH-CF_2-) of the monomeric units throughout the reaction, proves the isoregic character of the polymer.

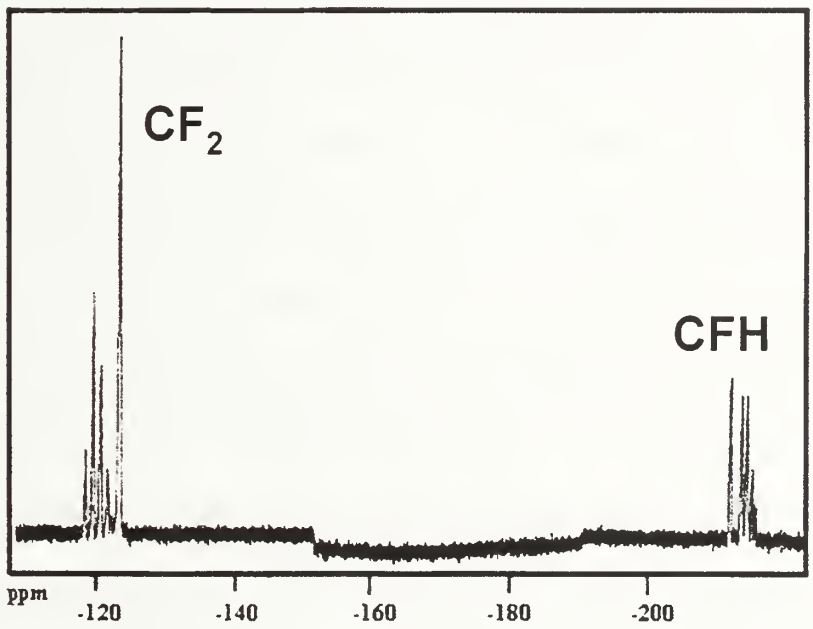

Figure 1.10 ^{19}F NMR spectra of poly(trifluoroethylene)

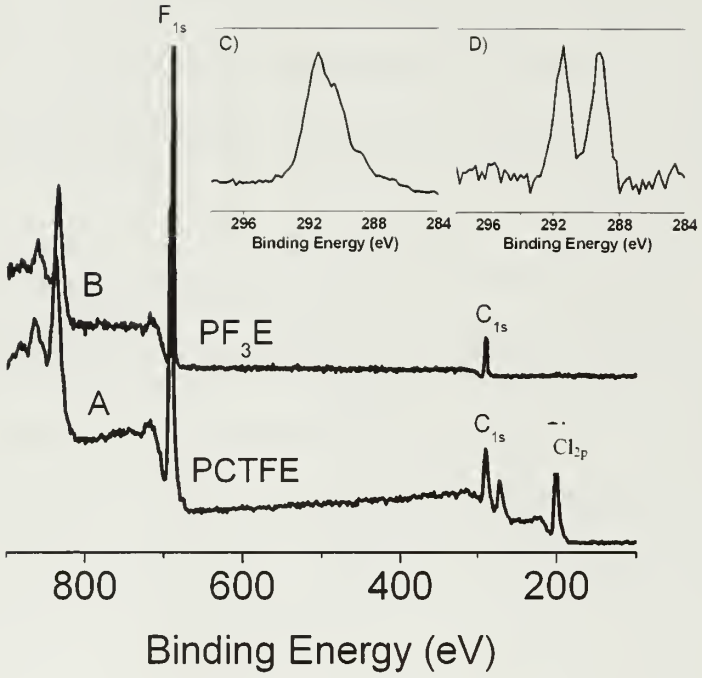

Figure 1.11 XPS survey and C_{1s} high resolution spectra of PCTFE (A,C) and PF_3E (B.D) films analyzed using 75° take-off angle

Figure 1.11 shows the XPS survey and C_{1s} spectra of PF_3E and PCTFE solution cast films at 75° take-off angle. The stoichiometry of the PF_3E product deduced from quantitative XPS (75° take-off angle) is C=29.1%. F=70.8% O=0.2% Sn~0% and Cl~%0. (Table 1.2) This stiochiometry and the disappearance of the Cl_{2p} peak prove the complete removal of residual tin compounds (Bu_3SnCl and unreacted Bu_3SnH) and complete dechlorination. The C_{1s} peak of PCTFE appears as a broad spectrum which is a combination of carbons from CF_2 and CFCl. This broad spectrum (Figure-1.11-C) turns into a spectrum (Figure-1.11-D) which consists of two peaks at 289.25 eV (47.65%) and 291.47 eV (52.35%) that correspond to $(-FC^*HCF_2-)_n$ and $(-FCHC^*F_2)_n$ carbons respectively after dechlorination.

$\theta_A/\theta_R(^o)$	λ (mil)	XPS atomic concentration (%)[a]				
		C	F	O	Cl	Sn
94/68	5	29.1	70.8	0.2	~0	~0

[a] 75° take-off angle data

Table 1.2 Water contact angle (θ_A/θ_R), thickness (λ) and elemental composition of solution-cast poly(trifluoroethylene)

PF_3E films were prepared as explained in experimental section. The films are transparent, colorless, and flexible. The PF_3E film exhibits contact angles of $94^o \pm 2^o/68^o \pm 2^o$. Our dynamic contact angle data is very close to the static angle (92^o) data obtained by Neumann and coworkers [60] using a computer program, which evaluates in terms of solid surface tensions using experimental contact angle patterns.

1.4.2 Adsorption Studies

1.4.2.1 Kinetics of Adsorption

Figure 1.12 and 1.13 show the kinetics of adsorption of PF_3E to Si/SiO_2 from THF solution containing 1 mg/mL PF_3E at room temperature determined by ellipsometry and XPS measurements respectively. Ellipsometry results (Figure 1.12) show that the adsorption is not very fast and reaches its final state in 8 hours. It is very hard to control thickness of PF_3E from THF solution and results are not reproducible.

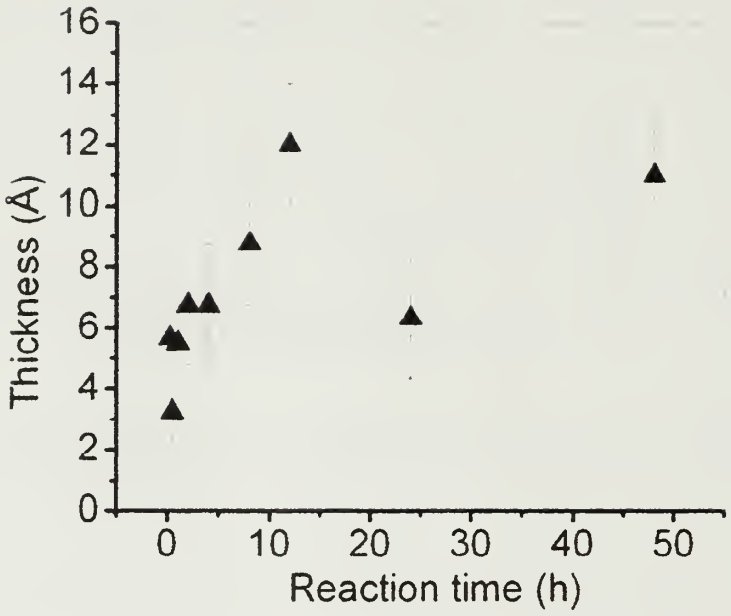

Figure 1.12 Kinetics of adsorption of PF_3E (1 mg/mL) to Si/SiO_2 from (100:0):(THF:Toluene) mixture determined by ellipsometry

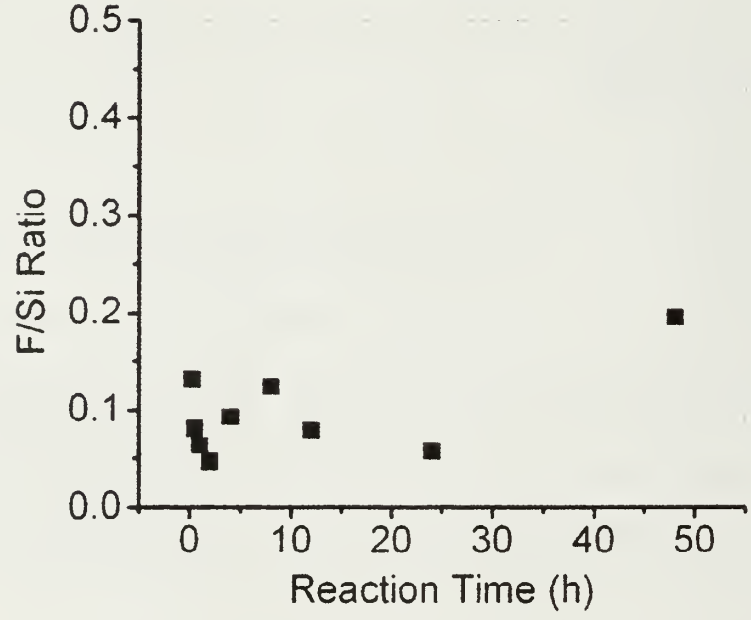

Figure 1.13 Kinetics of adsorption of PF_3E (1 mg/mL) to Si/SiO_2 from (100:0):(THF:Toluene) mixture determined by XPS (F/Si is calculated from XPS composition data at 75° take-off angle)

The adsorbed amount is determined by the ratio of F/Si calculated from XPS composition data at 75° take-off angle. (Figure 1.13) Unlike elllipsometry results. XPS results show that the adsorption is very rapid but the adsorbed amount does not reach a plateau and decreases and increases without any trend. This also supports the idea that it is very hard to control the adsorbed amount and the thickness of PF_3E from THF solution.

The kinetics of adsorption of PF_3E from (50:50);(THF:Tolune) and (30:70);(THF:Tolune) mixtures was not studied. 24 hours was chosen to study the effect of solvent quality and effect of concentration on adsorption. (One day of adsorption time was found to be the most reproducible.)

1.4.2.2 Adsorption Isotherms

The effect of concentration on PF_3E adsorption onto Si/SiO_2 from (10:0);(THF:Toluene). (50:50);(THF:Toluene). and (30:70);(THF:Toluene) solutions were investigated by XPS. contact angle measurements and ellipsometry. The adsorption isotherms are presented as a change in F/Si ratio determined by XPS analysis after one day adsorption as a function of solution concentration. (Figure 1.14) In all cases. the F/Si ratio is constant until high polymer concentration and then increases significantly except for the (50:50);(THF:Toluene) solution. At lower concentrations. PF_3E adsorbs to silicon surfaces whereas at higher concentrations the polymer precipitates from the solution. As the quality of solvent decreases. the adsorbed amount

increases in the regime of adsorption as assessed by XPS analysis. The increase is more pronounced at higher toluene concentrations.

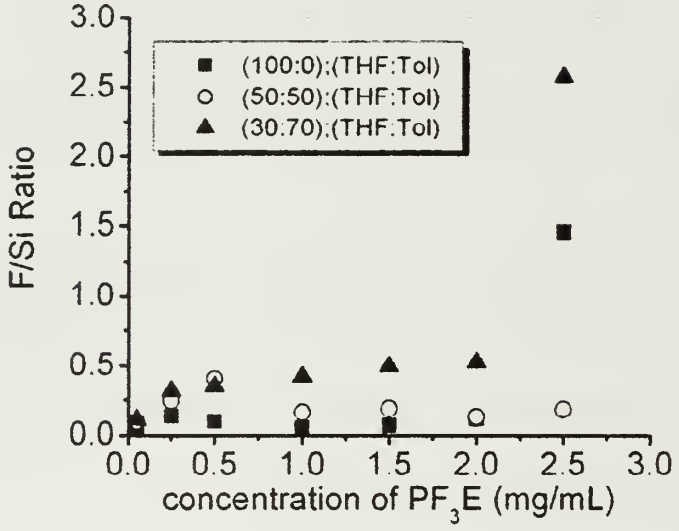

Figure 1.14 F/Si ratio (calculated from XPS composition data at 75° take-off angle) of PF_3E adsorbed to Si/SiO_2 from (100:0);(THF:Toluene) (■). (50:50):(THF:Toluene) (○) and (30:70):(THF:Toluene) (▲) mixtures as a function of PF_3E concentration at room temperature

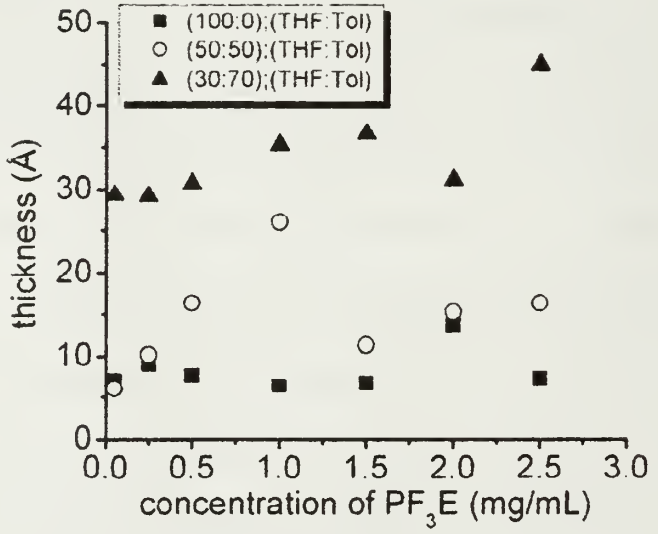

Figure 1.15 Ellipsometric thickness of PF_3E adsorbed to Si/SiO_2 from (100:0):(THF:Toluene) (■), (50:50):(THF:Toluene) (○) and (30:70):(THF:Toluene) (▲) mixtures as a function of PF_3E solution concentration at room temperature

Figure 1.15 shows the ellipsometric thickness of adsorbed PF_3E layers on Si/SiO_2 as a function of PF_3E concentration from (100:0):(THF:Toluene), (50:50):(THF:Toluene) and (30:70):(THF:Toluene) mixtures at room temperature. It was found out that concentration does not have an effect on PF_3E adsorption onto Si/SiO_2 in all cases. The adsorbed layer thickness remains nearly the same in all cases as the concentration of PF_3E increases.

Ellipsometry results also support that the adsorption of PF_3E onto Si/SiO_2 surfaces can be enhanced by the addition of toluene (non-solvent) to the PF_3E that is dissolved in THF (good solvent). Addition of toluene (non-solvent) to PF_3E that is dissolved in THF (good solvent) decreases the solvent-polymer interaction and this enhances the adsorbed amount.

Figure 1.16 shows the advancing and receding contact angle results as a function of PF_3E concentration from (100:0):(THF:Toluene), (50:50):(THF:Toluene) and (30:70):(THF:Toluene) mixtures at room temperature. In all cases, advancing and receding contact angles increase from low concentration to high concentration and become constant as the concentration increases. As the solvent quality decreases, the advancing contact angles increase and receding contact angles remains the same at higher concentrations. High contact angle hysteresis shows that the PF_3E surfaces are rough and the surfaces become rougher as the solvent quality decreases. The advancing contact angle results from (30:70):(THF:Toluene) mixture at higher concentrations become similar to the solution cast PF_3E film, and this indicates that the adsorbed PF_3E thickness has reached the sampling depth of contact angle.

A)

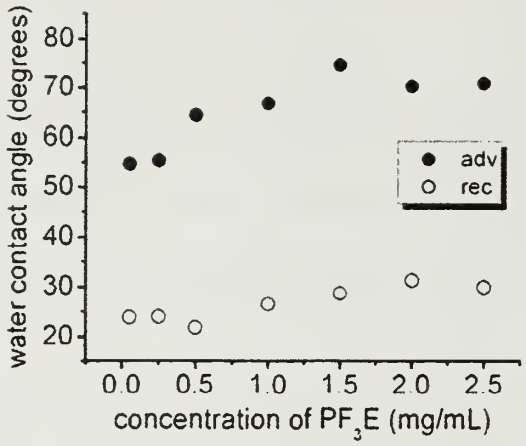

B)

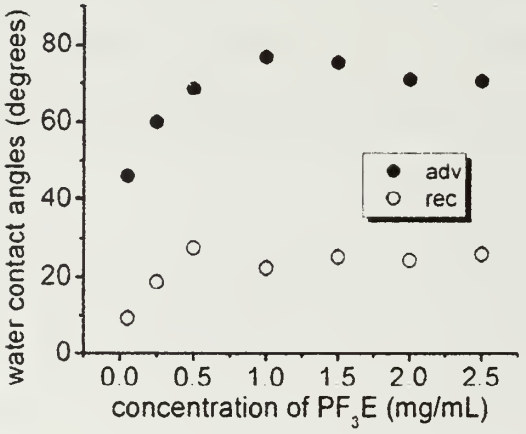

C)

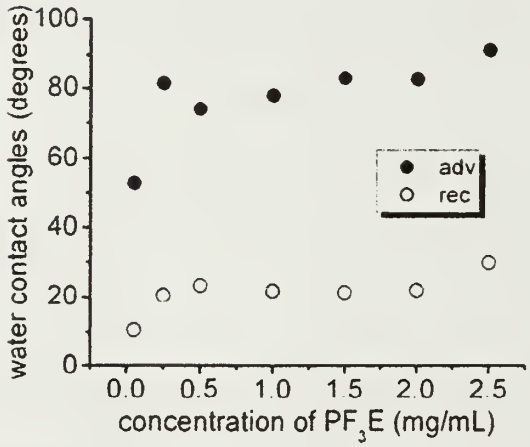

Figure 1.16 Advancing (●) and receding (○) contact angle data for PF_3E adsorbed to Si/SiO_2 from (100:0):(THF:Toluene) (A), (50:50):(THF:Toluene) (B), (30:70):(THF:Toluene) (C) mixtures at room temperature as a function of PF_3E concentration

A)

B)

C)

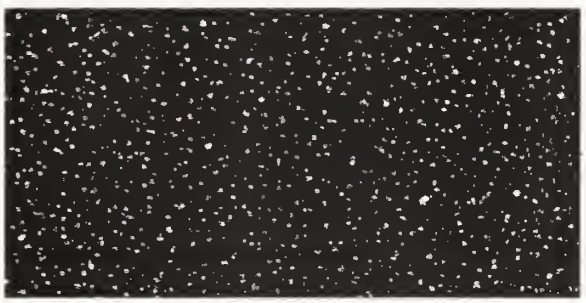

D)

Figure 1.17 AFM images (5x2.5 μm) of a clean silicon wafer (A) and PF_3E adsorbed to Si/SiO_2 from 1.5 mg/mL solution as a function of solvent composition (B) (100:0):(THF:Toluene), (C) (50:50):(THF:Toluene).(D) (30:70):(THF:Toluene)

Figure 1.17 shows the AFM pictures of a clean silicon surface and PF_3E adsorbed to Si/SiO_2 surface from 1.5 mg/mL solution as a function of non-solvent (toluene) composition (B) (100:0);(THF:Toluene), (C) (50:50);(THF:Toluene), (D) (30:70);(THF:Toluene). As the composition of the toluene increases, a change in the surface images is observed. The AFM pictures in B and C don't really confirm that we have a continuous layer of PF_3E on the surfaces. The continuous layer formation is observed when the adsorption is done from (30:70);(THF:Toluene) mixture. From the AFM pictures it can be concluded that, as the solvent quality decreases, the PF_3E layers become continuous on the Si/SiO_2.

1.4.3 Preparation of Amine Surfaces

The amine monolayer supported on silicon was prepared by the reaction of n-aminopropyldimethylethoxysilane in the vapor phase. (Figure 1.6) The reaction occurs between silanol groups on the surface and APDMES, and ethanol is the by product. The reaction can be proven by the appearance of nitrogen on the surfaces. The amine surfaces exhibit advancing and receding contact angles of $75^o/37^o$ and the thickness of the amine monolayer is 8 Å. (Table 1.3)

Surface	θ_A/θ_R (^{o})	λ(Å)	XPS atomic concentration (%)[a]			
			C	N	O	Si
SiO_2-APDMES	75/37	8.1	57.50	3.07	22.46	13.87
			18.14	1.80	37.06	42.00

[a] upper row is 15^0 take-off angle data and lower row is 75^0 take-off angle data

Table 1.3 Water contact angle (θ_A/θ_R), ellipsometric thickness (λ) and elemental composition of amine monolayer supported on silicon

1.4.4 Adsorption of PF_3E on Amine Surfaces

The adsorption of PF_3E (2 g/mL) on silicon-supported covalently attached amine monolayer was studied as a function of solvent quality. The adsorbed amount (determined by XPS) is plotted in figure1.18 as a function of solvent quality. The adsorbed amount on amine surfaces is more than on the silicon surfaces. due to the strong interactions between the amine surface and PF_3E through hydrogen bonding. As the solvent quality decreases. an increase in the adsorbed amount is observed.

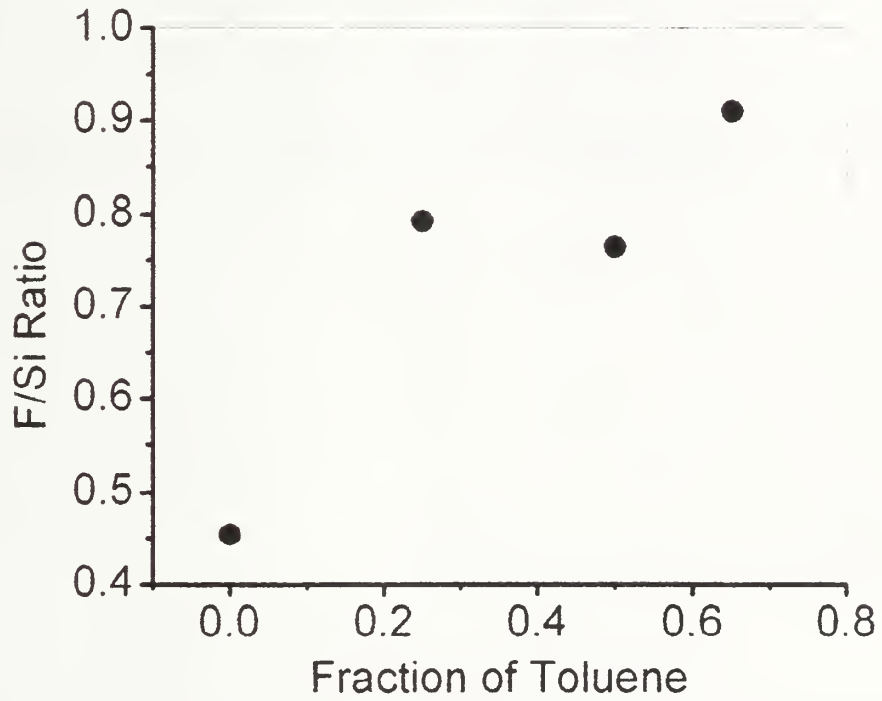

Figure 1.18 F/Si ratio (calculated from XPS composition data at 75° take-off angle) for PF_3E adsorbed to Si/SiO_2-APDMES from 2 mg/mL PF_3E solution as a function of solvent composition

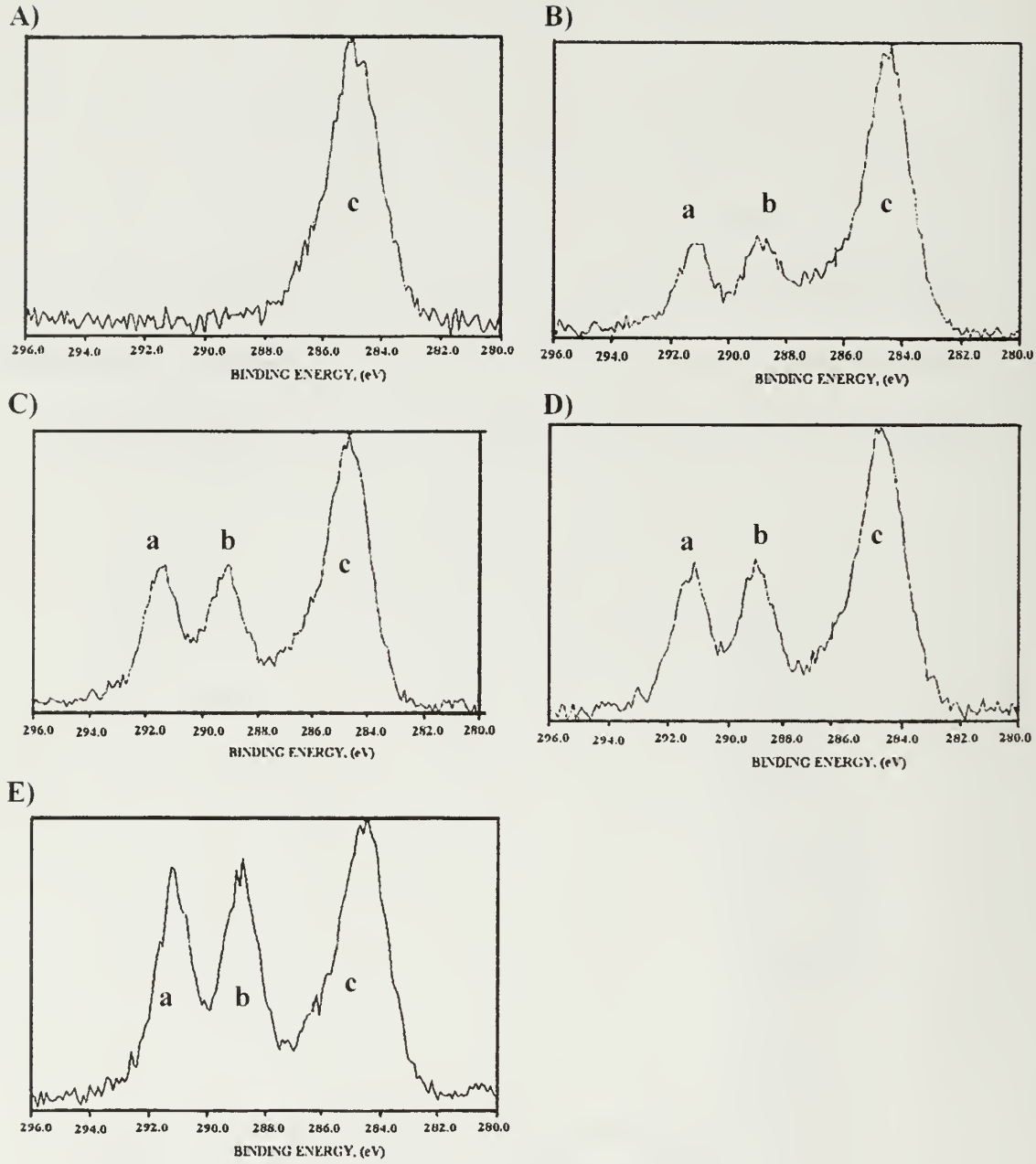

a= -(CHFC*F$_2$)-, b=-(C*HFCF$_2$)- c=-(CH$_2$)-

Figure 1.19 High resolution XPS spectra of the C_{1s} signal (75° take-of angle) of Si/SiO_2-APDMES surface (A) and PF_3E adsorbed to Si/SiO_2/APDMES from 2 mg/mL solution as a function of solvent composition (B) (100:0);(THF:Toluene), (C) (75:25);(THF:Toluene), (D) (50:50);(THF:Toluene), (E) (35:65);(THF:Toluene)

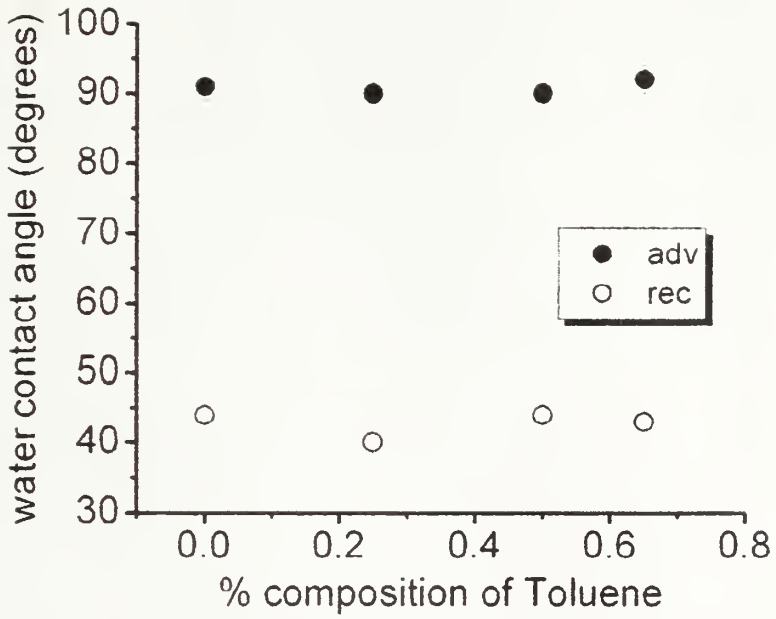

Figure 1.20 Advancing (●) and receding (○) contact angle data for PF_3E adsorbed to Si/SiO_2-APDMES from 2 mg/mL PF_3E solution as a function of solvent composition

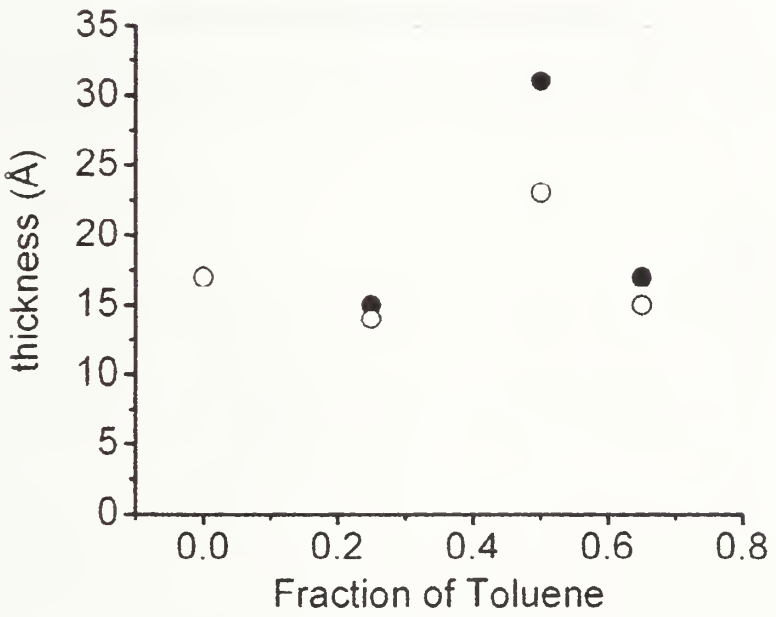

Figure 1.21 Ellipsometric thickness of PF_3E adsorbed to Si/SiO_2-APDMES from 2 mg/mL PF_3E solution as a function of solvent composition (● and ○ represent the results from two sets of experiments under the same conditions)

Figure 1.19 shows the high resolution XPS spectra of the C_{1s} signal (75° take-of angle) of Si/SiO_2-APDMES surface and PF_3E adsorbed to Si/SiO_2/APDMES from 2 mg/mL solution as a function of non-solvent composition. Two new peaks appear at higher binding energy after adsorption of PF_3E. The peaks at ~289 eV and ~291 eV are due to $(-FC^*HCF_2-)_n$ and $(-FCHC^*F_2-)_n$ carbons respectively. Figure 1.20 shows the advancing (θ_A) and receding (θ_R) contact angle data as a function of non-solvent composition on amine surfaces. The advancing contact angle (θ_A) did not change as the non-solvent composition increased on SiO_2-APDMES-PF_3E surfaces because the contact angle sampling depth was reached before the addition of non-solvent. The contact angle of an amine-PF_3E surface (adsorption from THF solution) was 90°/44° (θ_A/θ_R), which is similar to the solution cast PF_3E films contact angle data 94°/68° (θ_A/θ_R). The difference between receding angles indicates that the PF_3E layers on amine surfaces are rougher than the free standing PF_3E films. The thickness of PF_3E layers on amine surfaces changes between 14-27 Å as the solvent quality changes. (Figure 1.21).

1.5 Conclusions

Poly(trifluoroethylene) was prepared by reduction of poly(chlorotrifluoro-ethylene). The properties of solution-cast PF_3E films were investigated. PF_3E films show hydrophobic character and the films are transparent. colorless and easily drawable. It is also shown that PF_3E irreversibly adsorbs to oxidized silicon wafers and covalently attached amine monolayers supported on silicon. The covalently attached amine monolayer supported on silicon is prepared by reaction of APDMES in the vapor phase. By controlling the solvent quality. the adsorbed amount on the surfaces can be

controlled. The adsorbed amount on the amine surfaces is higher than the adsorbed amount on SiO_2 due to the stronger hydrogen bonding interactions between the surface amine groups and highly polar C-H groups throughout the polymer backbone.

1.6 References

(1) Lee, L.-H. *Adhesion and Adsorption of Polymers*; Plenum Press: New York, 1980.

(2) Napper, D. H. *Polymeric Stabilization of Colloidal Dispersions*; Academic Press: London ; New York, 1983.

(3) Tseng, C. M.; Lu, Y. Y.; Elaasser, M. S.; Vanderhoff, J. W. *Journal of Polymer Science Part A-Polymer Chemistry* **1986**, *24*, 2995-3007.

(4) Awan, M. A.; Dimonie, V. L.; Elasser, M. S. *Polymer Preprints (American Chemical Society, Division of Polymer Chemistry)* **1994**, *35*, 551-552.

(5) Ober, C. K.; Hair, M. L. *Journal of Polymer Science Part A-Polymer Chemistry* **1987**, *25*, 1395-1407.

(6) Dobiáš, B. *Coagulation and Flocculation : Theory and Applications*; M. Dekker: New York, 1993.

(7) Nathan, C. C.; Bregman, J. I. *Corrosion Inhibitors*; National Association of Corrosion Engineers: Houston, Tex., 1973.

(8) Mittal, K. L.; MST Conferences. *Adhesion aspects of polymeric coatings*; Utrecht; Boston, 2003.

(9) Dorinson, A.; Ludema, K. C. *Mechanics and Chemistry in Lubrication*; Elsevier: New York, 1985.

(10) Takahashi, A.; Kawaguchi, M. *Advances in Polymer Science* **1982**, *46*, 1-65.

(11) Kawaguchi, M.; Mikura, M.; Takahashi, A. *Macromolecules* **1984**, *17*, 2063-2065.

(12) Kawaguchi, M.; Maeda, K.; Kato, T.; Takahashi, A. *Macromolecules* **1984**, *17*, 1666-1671.

(13) Kawaguchi, M.; Hayashi, K.; Takahashi, A. *Macromolecules* **1984**, *17*, 2066-2070.

(14) Luckham, P. F.; Klein, J. *Macromolecules* **1985**, *18*, 721-728.

(15) Hadziioannou, G.; Patel, S.; Granick, S.; Tirrell, M. *Journal of the American Chemical Society* **1986**, *108*, 2869-2876.

(16) Guzonas, D. A.; Boils, D.; Tripp, C. P.; Hair, M. L. *Macromolecules* **1992**, *25*, 2434-2441.

(17) Parsonage, E.; Tirrell, M.; Watanabe, H.; Nuzzo, R. G. *Macromolecules* **1991**, *24*, 1987-1995.

(18) Coupe, B.; Evangelista, M. E.; Yeung, R. M.; Chen, W. *Langmuir* **2001**, *17*, 1956-1960.

(19) Coupe, B.; Chen, W. *Macromolecules* **2001**, *34*, 1533-1535.

(20) Scheutjens, J. M. H. M.; Fleer, G. J. *Journal of Physical Chemistry* **1979**, *83*, 1619-1635.

(21) Ploehn, H. J.; Russel, W. B. *Macromolecules* **1989**, *22*, 266-276.

(22) Muthukumar, M.; Ho, J. S. *Macromolecules* **1989**, *22*, 965-973.

(23) Scheutjens, J. M. H. M.; Fleer, G. J. *Macromolecules* **1985**, *18*, 1882-1900.

(24) Degennes, P. G. *Macromolecules* **1982**, *15*, 492-500.

(25) Shoichet, M. S.; Mccarthy, T. J. *Macromolecules* **1991**, *24*, 1441-1442.

(26) Stouffer, J. M.; Mccarthy, T. J. *Macromolecules* **1988**, *21*, 1204-1208.

(27) Iyengar, D. R.; McCarthy, T. J. *Polymer Preprints (American Chemical Society, Division of Polymer Chemistry)* **1989**, *30*, 154-155.

(28) Kozlov, M.; Quarmyne, M.; Chen, W.; McCarthy, T. J. *Macromolecules* **2003**, *36*, 6054-6059.

(29) Kozlov, M.; McCarthy, T. J. *Langmuir* **2004**, *20*, 9170-9176.

(30) Phuvanartnuruks, V.; *Polymer surface chemistry surface mixtures, supported polyelectrolyte multilayers and heterogeneous chemical modification.* PhD Dissertation, University of Massachusetts, 1997

(31) Kolb, B. U.; *Synthesis of Specifically Functionalized Polymers and Their Adsorption at the Solid-Solution Interface.* PhD Dissertation, University of Massachusetts, 1993

(32) Scheutjens, J. M. H. M.; Fleer, G. J. *Journal of Physical Chemistry* **1980**, *84*, 178-190.

(33) Silberbe,A. *Journal of Chemical Physics* **1968**, *48*, 2835-&.

(34) Roe, R. J. *Journal of Chemical Physics* **1974**, *60*, 4192-4207.

(35) Tadros, T. F. *The Effect of Polymers on Dispersion Properties*; Academic Press: London, 1982.

(36) Gramain, P.; Myard, P. *Macromolecules* **1981**, *14*, 180-184.

(37) Degennes, P. G. *Macromolecules* **1981**, *14*, 1637-1644.

(38) Marra, J.; Hair, M. L. *Macromolecules* **1988**, *21*, 2349-2355.

(39) Iyengar, D. R.; McCarthy, T. J. *Macromolecules* **1990**, *23*, 4344-4346.

(40) Vanderbeek, G. P.; Stuart, M. A. C.; Fleer, G. J.; Hofman, J. E. *Macromolecules* **1991**, *24*, 6600-6611.

(41) Higashihata, Y.; Sako, J.; Yagi, T. *Ferroelectrics* **1981**, *32*, 85-92.

(42) Furukawa, T.; Johnson, G. E.; Bair, H. E.; Tajitsu, Y.; Chiba, A.; Fukada, E. *Ferroelectrics* **1981**, *32*, 61-67.

(43) Lovinger, A. J.; Davis, G. T.; Furukawa, T.; Broadhurst, M. G. *Macromolecules* **1982**, *15*, 323-328.

(44) Davis, G. T.; Furukawa, T.; Lovinger, A. J.; Broadhurst, M. G. *Macromolecules* **1982**, *15*, 329-333.

(45) Yamada, T.; Kitayama, T. *Journal of Applied Physics* **1981**, *52*, 6859-6863.

(46) Cais, R. E.; Kometani, J. M. *Macromolecules* **1984**, *17*, 1932-1939.

(47) Lovinger, A. J.; Cais, R. E. *Macromolecules* **1984**, *17*, 1939-1945.

(48) Yagi, T. *Polymer Journal* **1979**, *11*, 711-719.

(49) Andrade, J. D. *Surface and Interfacial Aspects of Biomedical Polymers*; Plenum Press: New York, 1985.

(50) Garbassi, F.; Morra, M.; Occhiello, E. *Polymer Surfaces : From Physics to Technology*; Wiley: New York, 1998.

(51) Chan, C. M. *Polymer surface modification and characterization*; Hanser; Cincinnati, 1994.

(52) Berg, J. C. *Wettability*; M. Dekker: New York, 1993.

(53) Youngblood, J. P.; *Wettability of Polymer Surfaces : Effects of Chemistry and Topography*, PhD Dissertation, University of Massachusetts, 2001

(54) Chen, W.; Fadeev, A. Y.; Hsieh, M. C.; Oner, D.; Youngblood, J.; McCarthy, T. J. *Langmuir* **1999**, *15*, 3395-3399.

(55) Adamson, A. W. *Physical Chemistry of Surfaces*; Wiley: New York, 1990.

(56) Fowkes, F. M.; Zisman, W. A. *Contact Angle, Wettability and Adhesion*; American Chemical Society: Washington, 1964.

(57) Ulman, A. *An Introduction to Ultrathin Organic Films : From Langmuir-Blodgett to Self-assembly*; Academic Press: Boston, 1991.

(58) Tompkins, H. G. *A User's Guide to Ellipsometry*; Academic Press: Boston, 1993.

(59) Azzam, R. M. A.; Bashara, N. M. *Ellipsometry and Polarized Light*; North-Holland Pub. Co.: New York, 1977.

(60) Kwok, D. Y.; Neumann, A. W. *Colloids and Surfaces A-Physicochemical and Engineering Aspects* **2000**, 161, 49-62.

CHAPTER 2

HYDROGEN BONDING - DIRECTED LAYER-BY-LAYER ASSEMBLY OF POLY(4-VINYLPYRIDINE) AND POLY(TRIFLUOROETHYLENE)

2.1 Introduction

The layer-by-layer (LbL) assembly process, which was introduced by Decher et.al[1], is a method for preparing multilayer ultrathin films by alternating the deposition of oppositely charged polymers from dilute aqueous solutions onto charged surfaces. Layer-by-layer assembly produce has been intensively investigated in recent years[1-4] due to its simpilicty, versatility, and systematic control over the structure and thickness of the resulting multilayer. In addition, a variety of materials can be used in LbL studies such as small organic molecules[5].inorganic compounds[6-9], proteins[10.11], DNA[12] and colloids.[13] LbL assembled films have a variety of proposed applications including as biosensors[3,14], light emitting diodes and photovoltaic cells[15-18], optical strorage devices and magnetic films[19-21], separation membranes and chromatopgraphy columns[22,23], controlled particle and catalyst preparation[24-26], etc.[27]

Different substrates, from inorganic to polymeric ones, have been used to prepare multilayer assemblies. Depending on the application, the multilayer can be fabricated on planar surfaces, latex particles, or custom surfaces. It has been reported that multilayers can be grown on defined areas of patterned surfaces.[28] Inorganic substrates include fused quartz, silicon single crystals, and glass. For instance, a positively charged surface can be produced on a glass surface by reaction of silane coupling reagent containing an amine group[1,29,30]. In the McCarthy group, layer-by-layer deposition has been performed by using poly(4-methyl-1 pentene) (PMP)[31],

poly(ethylene terephthalate) (PET)[32], poly(chlorotrifluoroethyelene) (PCTFE)[33], low density polyethylene (LDPE)[34] and Teflon (PTFE)[35] as polymeric substrates.

The driving forces for LbL assembly are primarily electrostatic and covalent bonds, charge transfer interactions and van der Waals interactions. Hydrogen bonding as the driving force of LbL self-assembled films was first introduced by Rubner *et. al.*[29] and Zhang *et. al*[36]. Multilayer assemblies were produced by successively alternating the deposition of two kinds of polymers, one with hydrogen donating groups and the other with hydrogen accepting groups.[29,36-38] Rubner *et.al.*[29] reported LbL assembly of polyaniline with a variety of different nonionic water soluble polymers (poly(vinylpyrolidine), (poly(vinyl alcohol), poly(acrylamide) and poly(ethylene oxide)). The hydrogen-bonding-directed layer-by-layer assembly has advantages over the electrostatically formed polyelectrolyte multilayers. The multilayer formation can be obtained in organic solvents and it facilitates the preparation of multilayers using nonionic and water insoluble polymers. The layer structure in multilayer materials can be controlled readily by altering the relatively weak hydrogen bonds between the layered films. Erasable hydrogen bonded multilayers containing weak polyacids were prepared by Granik *et al.*. [39,40] The layers assembled at low pH and dissolved at higher pH because of the increasing ionization degree of weak polyacids.[39,40] Lian[41]*et. al.* prepared polymer and nanocomposite multilayers based on hydrogen bonding. Thermal and photochemical techniques were used to stabilize hydrogen-bonded multilayers, and by using this technique, micro-patterned surfaces were produced. The competitive role of hydrogen bonding and electrostatic interactions in the growth and stability of polyelectrolyte multilayers over a wide range of pH were reported by Sukhishvili *et. al.*

[42]. Caruso *et. al.* reported the preparation of heterogeneous multilayer films comprised of alternating stacks of hydrogen bonded (poly-4-vinylpyridine) (P4VP) and poly(acrylic acid, sodium salt) (PAA) and electrostatically formed (poly(sodium 4-styrenesulfonate) (PSS) and poly(allyaminehydrochloride) (PAH) layers via LbL assembly techniques and their high pH sensitivity toward deconstruction.[43] Hydrogen bonding - directed poly(4-vinylpyridine)/poly(4-vinylphenol) (P4VP/PVPh) multilayer films were prepared by the LbL assembly process from ethanol solutions.[44]

The multilayer structures can be controlled by different factors. Among these factors, pH values[45] and ionic strength of adsorption solutions[46] are important in multilayer assembly based on electrostatic interactions. In multilayer assemblies based on hydrogen bonding, varying the solvent composition provides an additional means to control the multilayer structure. The structure and properties of hydrogen bonding - directed multilayer films of P4VP/PVPh were tuned by Zhang *et. al* when the the solvent composition of the adsorption solutions was changed.[44]

Polymers containing tertiary amine groups are good proton acceptors because of the basic nature of the functional groups. Poly(4-vinylpyridine) (P4VP) is one of thestronger proton acceptors with a basic nitrogen at the 4-position of pyridine ring. The ability of P4VP to interact through hydrogen bonding was used to prepare micelles with modified styrene in a selective solvent[47], spherical micelles with poly(ethyelneglycol)-block-poly(acrylic acid)[48].In addition , P4VP forms miscible blends with poly(amide-enaminonitrile).[49] Poly(trifluoroethylene) (PF_3E) is capable of forming hydrogen bonds with proton acceptors due to the highly polar carbon-hydrogen bonds throughout its backbone.

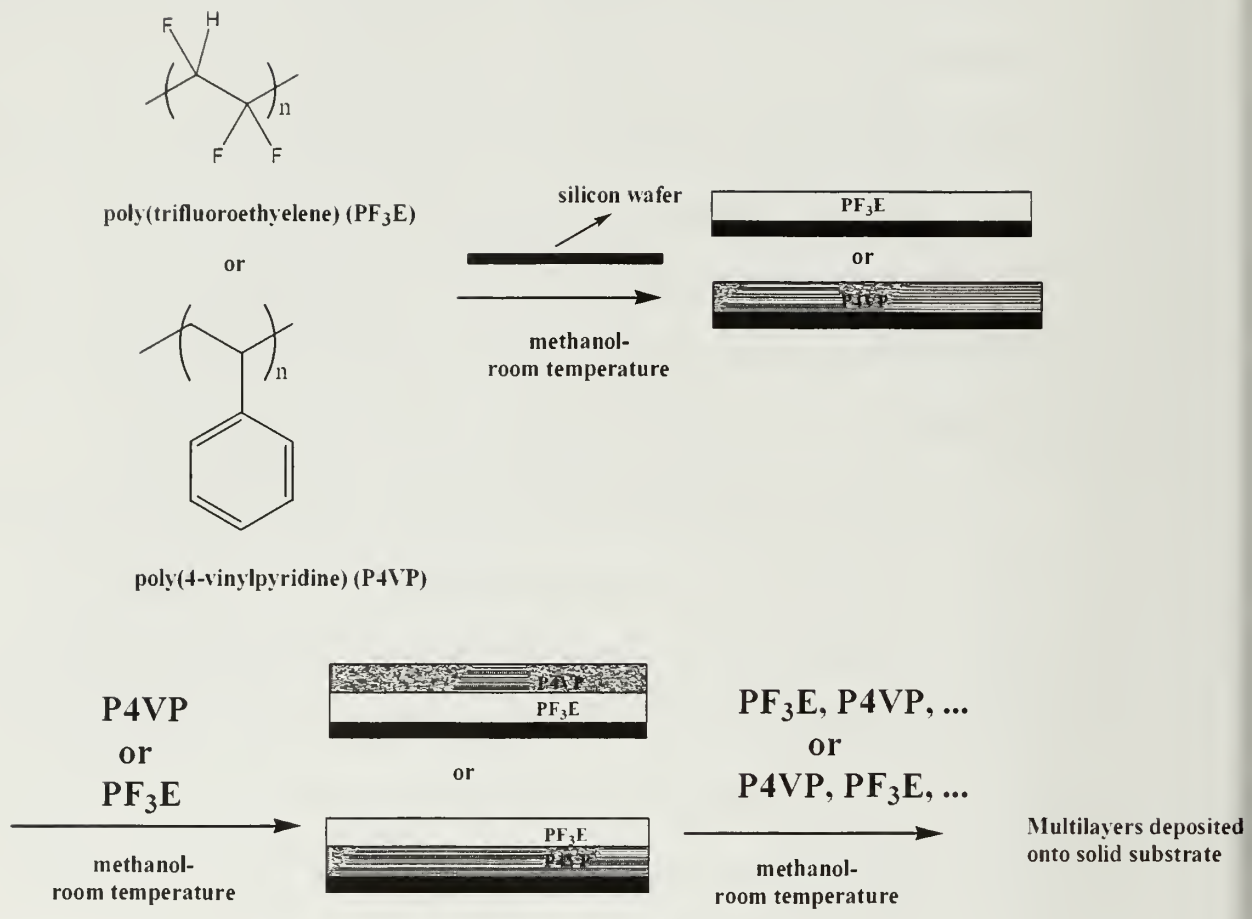

Figure 2.1 Schematic representation poly(trifluoroethylene) (PF_3E) and poly (4-vinylpyridine) (P4VP) adsorption onto Si/SiO_2 from methanol solution at room temperature and subsequent layer-by-layer deposition by alternating the deposition of P4VP and PF_3E

In this chapter, the layer-by-layer assembly of PF_3E and P4VP by alternating the deposition of P4VP (hydrogen bonding - accepting group) and PF_3E (hydrogen bonding - donating group) from methanol solution is described. Methanol is a good solvent both for P4VP and for PF_3E.

2.2 Experimental

2.2.1 Materials and Methods

All reagents were used without further purification. Poly(trifluoroethylene) was synthesized as described in Chapter 1. Poly(4-vinylpyridine) (P4VP) (M_w = 160.000 g/mol), was obtained from Aldrich. Methanol (HPLC grade) was purchased from Fisher. Silicon wafers were obtained from International Wafer Service (<100> orientation, P/B doped, 20-40 Ω cm, thickness 450-575 μm) and cleaned by a Harrick Scientific O_2 plasma cleaner at high power settings for 5 minutes prior to use. The oxide layer on the wafers after plasma treatment was determined to be ~25 Å by ellipsometry. Water was purified using a Millipore Milli-Q water system that involves reverse osmosis, ion exchange and filtration steps (10^{18} Ω/cm). X-ray photoelectron spectra (XPS) were obtained on a Physical Electronics Quantum 2000 Scanning ESCA Microprobe. Depth profiling was done by collecting spectra at 15° and 75° take-off angles with respect to the plane of the sample surface. The analysis at 15° has a penetration depth of ~10 Å and that at 75° corresponds to a penetration depth of ~40 Å. Contact angle measurements were made with a Ramè-Hart telescopic goniometer and a Gilmont syringe with a 24-gauge flat-tipped needle. Water was used as a probe liquid. Advancing and receding contact angle were recorded while the water was added and withdrawn from the drop, respectively. Ellipsometric measurements were done using a Rudolph Auto El-II automatic elipsometer. The light source is He-Ne laser($\lambda = 623.8$ nm), the incident angle is 70° and the compensator is -45°. The

thicknesses were calculated using the transparent double layer model using a dafBM software (silicon substrate / silicon oxide + PF_3E /air, silicon substrate / silicon oxide + P4VP/ air, silicon substrate / silicon oxide + P4VP / PF_3E / air and silicon substrate / silicon oxide + PF_3E / P4VP / air) with the following parameters: silicon substrate n_s = 3.858, k_s = 0.018 (imaginary part of the refractive index); air, n_o = 1; PF_3E, n_1 = 1.42; P4VP; n_2 = 1.549.

2.2.2 Adsorption of Poly(4-vinylpyridine)(P4VP) and Poly(trifluoroethylene) (PF_3E) to Silicon Surfaces

1 mg/mL (0.0122 M, based on repeat units) PF_3E and (0.0082 M, based on repeat unit) P4VP solutions in methanol were prepared. Adsorptions were carried out at room temperature for 24 hours. The clean silicon wafers were placed in polystyrene vials and PF_3E or P4VP solution (1 mL) was added. After the adsorption, the wafers were rinsed with methanol. Samples were dried under reduced pressure at room temperature for 2 hours. Desorption studies were done by immersing the samples in methanol for a day.

2.2.3 Adsorption of Poly(4-vinylpyridine)(P4VP) to Poly(trifluoroethylene) Surface (Si/SiO_2-PF_3E)

P4VP solutions of different concentrations in methanol were prepared. The samples (Si/SiO_2-PF_3E) were placed in polystyrene vials and P4VP solutions were added (1 mL). Adsorptions were carried out at room temperature for a desired amount of time. After the adsorption, the wafers were rinsed with methanol. Samples were dried under reduced pressure at room temperature for 2 hours.

2.2.4.Adsorption of Poly(trifluoroethylene) (PF_3E) to Poly(4-vinylpyridine) Surface (Si/SiO_2-P4VP)

PF_3E solutions of different concentrations in methanol were prepared. The samples (Si/SiO_2-P4VP) were placed in polystyrene vials and P4VP solutions were added (1 mL). Adsorptions were carried out at room temperature for a desired amount of time. After the adsorption, the wafers were rinsed with methanol. Samples were dried under reduced pressure at room temperature for 2 hours.

2.2.5 Multilayer Preparation

The multilayers were prepared by subsequent adsorption of polymers at room temperature for a desired amount of time by the same procedures mentioned above.

2.3 Results and Discussion

Initially, thin layers of poly(trifluoroethylene) (PF_3E) and poly(4-viynlpyridine) (P4VP) on silicon wafers were prepared from 1 mg/mL methanol solution. Adsorptions were carried out at room temperature for 24 hours. The SiO_2-PF_3E and SiO_2-P4VP samples exhibit contact angles of $81^o/30^o$ (θ_A/θ_R) and $62^o/9^o$ (θ_A/θ_R) and thicknesses of 10 Å and 9 Å, respectively (Table 2.1). The desorption experiments were performed by immersing the samples in methanol for a day. Thickness and XPS atomic composition data prove that the PF_3E and P4VP irreversibly attach to silicon surfaces. Figure 2.2 and Figure 2.3 show the XPS survey spectra and high-resolution spectra of C_{1s} signals of SiO_2-PF_3E and SiO_2-P4VP at 15^o and 75^o take-off angles, respectively. Appearance of fluorine (after PF_3E adsorption) and nitrogen (after P4VP adsorption) on the surfaces support the formation of polymer layers on the silicon surface.

	Contact angle (θ_A/θ_R) (^{o})	Thickness (λ)(Å)	XPS Atomic Composition			
			F (%)		N (%)	
			15°	75°	15°	75°
SiO_2-PF_3E[a]	81/30	10 10[c]	31.70 28.35[c]	20.00 15.55[c]	-	-
SiO_2-P4VP[a]	62/9	9 9[c]	-	-	5.25 5.75[c]	2.65 2.60[c]
SiO_2-PF_3E[a]+P4VP[b]	76/11	23	19.25	10.70	3.90	2.55
SiO_2-P4VP[a]+PF_3E[b]	71/11	24	11.30	4.60	3.10	2.90

[a] adsorptions were carried out at room temperature for 24 h
[b] adsorptions were carried out at room temperature for 4 h
[c] after adsorptions were carried out, the wafers were left in methanol for 24 h

Table 2.1 Water contact angle (θ_A/θ_R), thickness (λ) and elemental composition of poly(trifluoroethylene) adsorbed from methanol at room temperature onto Si/SiO_2 and Si/SiO_2-P4VP and poly(4-vinylpyridine) adsorbed onto Si/SiO_2 and Si/SiO_2 -PF_3E from methanol at room temperature

Adsorption of P4VP from 1 mg/ml methanol solution at room temperature to a SiO_2-PF_3E surface decreases the contact angles of the layer to 76°/11° and increases the thickness by 13 Å. Adsorption of PF_3E from 1 mg/ml methanol solution at room temperature to a SiO_2-P4VP surface increases the contact angles of the layers to 71/11 and increases the thickness by 15 Å. (Table 2.1) Figure 2.4 shows the XPS survey spectra and high resolution the C_{1s} spectra of a SiO_2-PF_3E-P4VP surface. The appearance of nitrogen on the surface after P4VP adsorption and the decrease in fluorine content support the adsorption of P4VP on PF_3E. (Table 2.1 and Figure 2.4). XPS survey spectra and high resolution C_{1s} and N_{1s} spectra of a SiO_2-P4VP-PF_3E

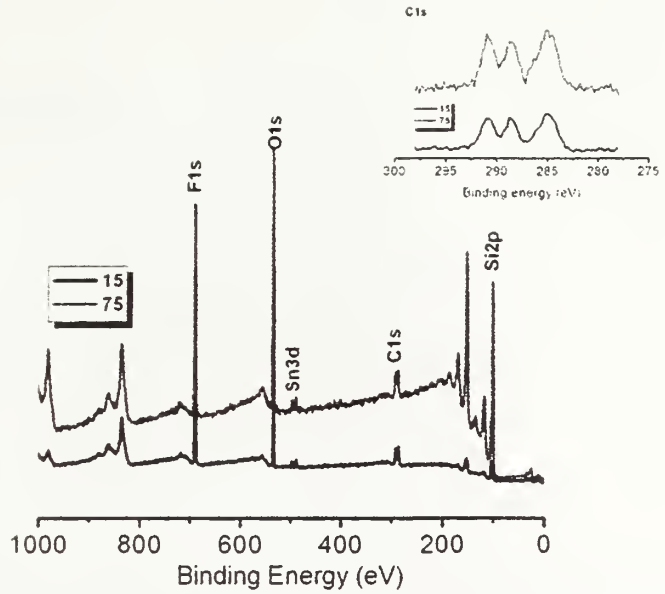

Figure 2.2 XPS survey and high resolution C_{1s} spectra of poly(trifluoroethylene) (1 mg/mL) adsorbed to Si/SiO_2 from methanol at room temperature

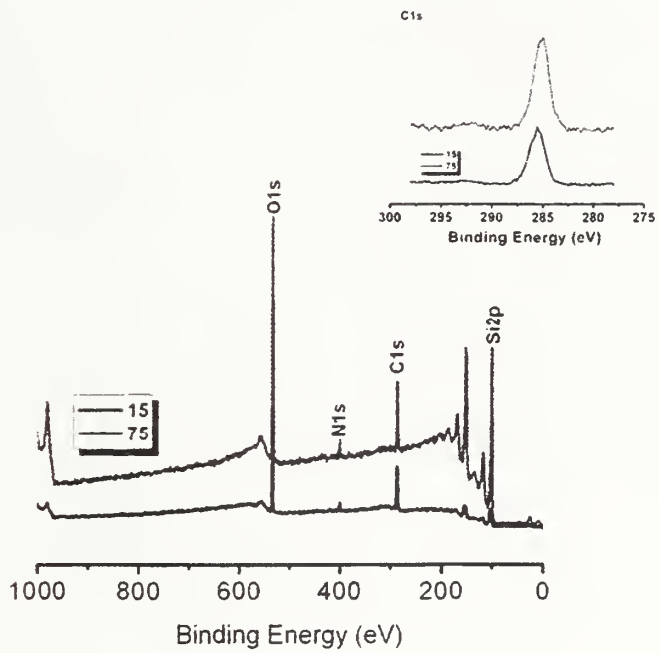

Figure 2.3 XPS survey and high resolution C_{1s} spectra of poly(4-viynlpyridine) (1 mg/mL) adsorbed to Si/SiO_2 from methanol at room temperature

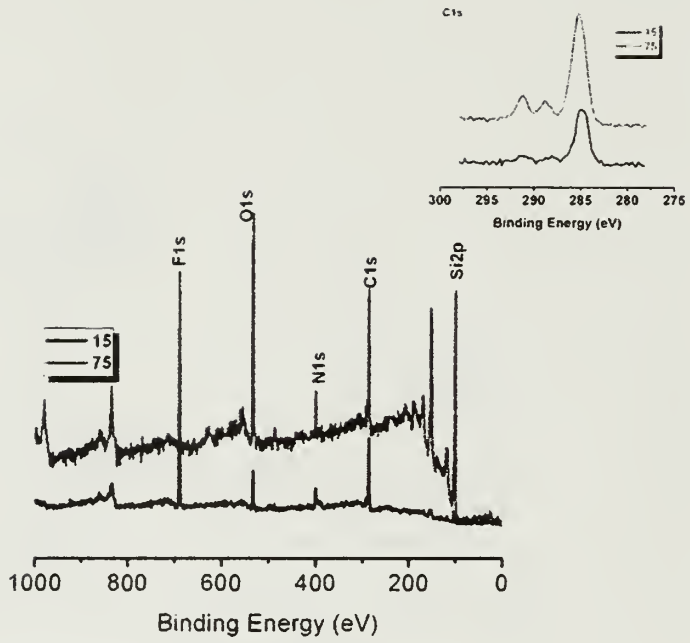

Figure 2.4 XPS survey and high resolution C_{1s} spectra of poly(4-vinylpyridine) (1 mg/mL) adsorbed to Si/SiO_2-PF_3E from methanol at room temperature for 4 h

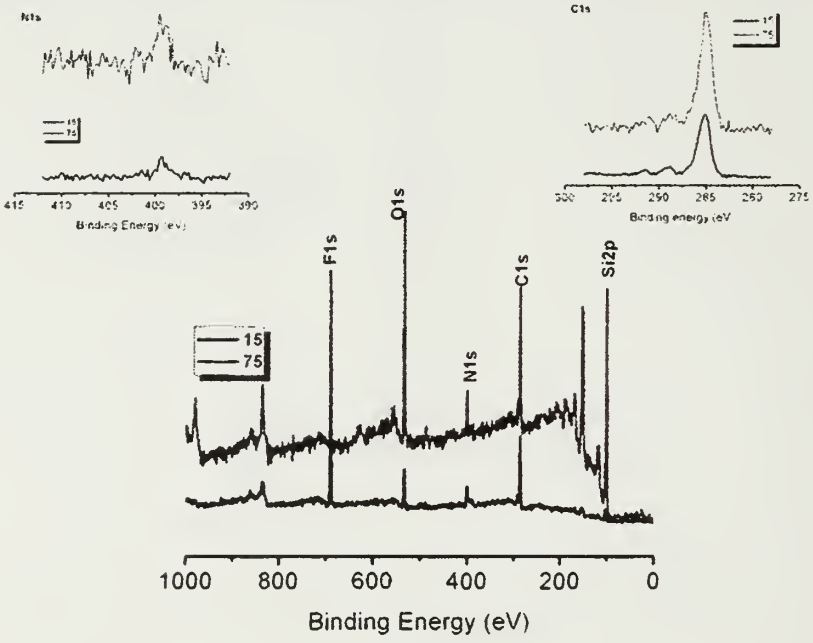

Figure 2.5 XPS survey and high resolution C_{1s} and N_{1s} spectra of poly(trifluoroethylene) (1 mg/mL) adsorbed to Si/SiO_2-P4VP from methanol at room temperature for 4 h

surface are shown in figure 2.5. The appearance of fluorine on the surface supports the adsorption of PF_3E to P4VP.

2.3.1. Kinetics of Poly(4-vinylpyridine) Adsorption to Poly(trifluoroethylene) Surface (Si/SiO_2-PF_3E)

Figure 2.6 and Figure 2.7 show the kinetics of the P4VP adsorption to Si/SiO_2-PF_3E as monitored by XPS and ellipsometry. The P4VP concentration was 1 mg/mL. The XPS indicates that the adsorption is fast, reaching a final state in 15 minutes. (Figure 2.6) The nitrogen concentration remains the same after 15 minutes. However, although no additional P4VP adsorption is observed, the fluorine percentage decreases after 15 minutes of adsorption and reaches a plateau only after 4 hours.

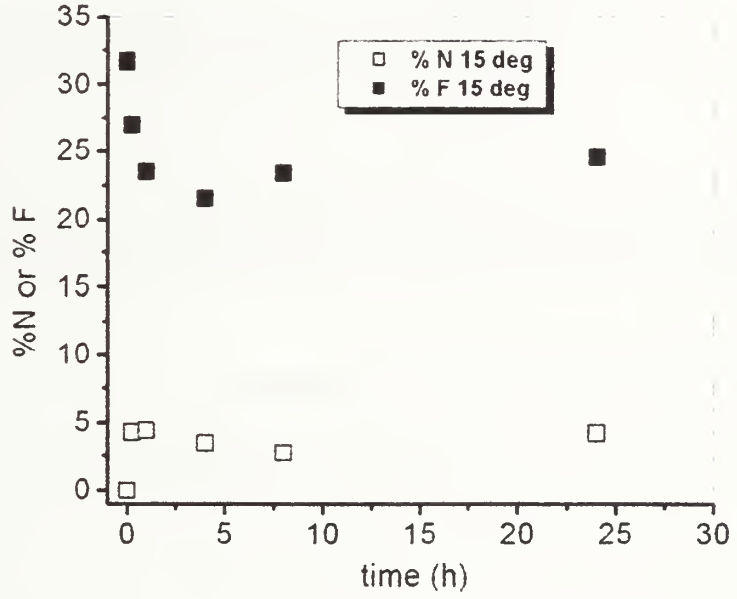

Figure 2.6 Kinetics of adsorption poly(4-vinylpyridine) (P4VP) (1 mg/mL) to Si/SiO_2-PF_3E from methanol at room temperature determined by XPS (%F and %N is determined from XPS composition data at 15° take-off angle)

In addition, layer thickness increases as the adsorption time increases beyond 15 minutes. (Figure 2.7) This argues for another adsorption mechanism after this point, which reconstructs the adsorbed layer. This also explains why a decrease in fluorine percentage is observed.

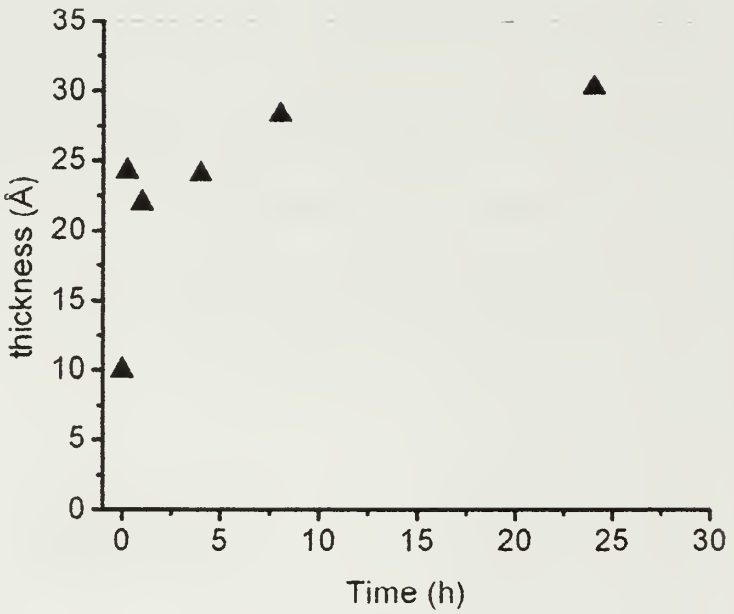

Figure 2.7 Kinetics of poly(4-vinylpyridine) (P4VP) (1 mg/mL) adsorption to Si/SiO_2-PF_3E from methanol solution at room temperature determined by ellipsometry

2.3.2 Effect of Concentration on Adsorption

The effect of concentration on the adsorption of PF_3E to the SiO_2-P4VP surface and of P4VP to the SiO_2-PF_3E surface was monitored by XPS, ellipsometry and contact angle measurements. The adsorption time was chosen as 4 hours. Figure 2.8-A shows the advancing and receding contact angle data for P4VP adsorbed to a SiO_2-PF_3E surface as a function of P4VP concentration. As the concentration of P4VP increases, both advancing and receding contact angles decreases initially, and then level at around 1 mg/mL.

A)

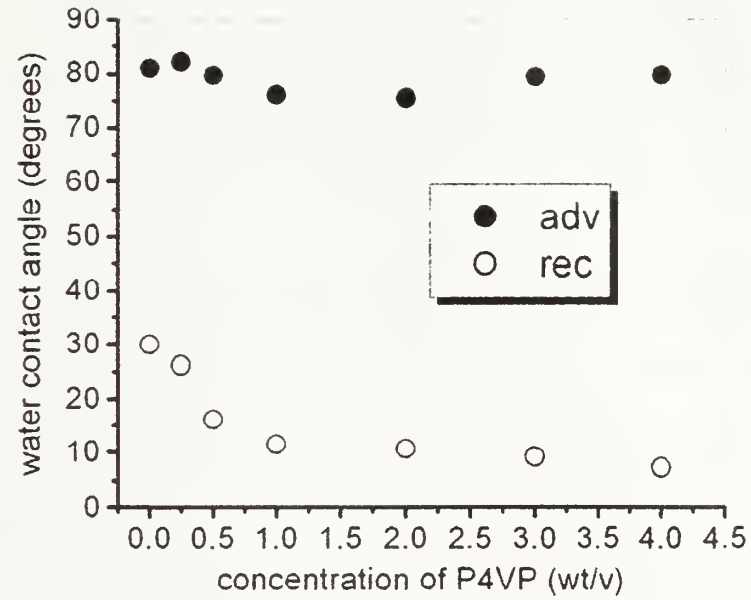

B)

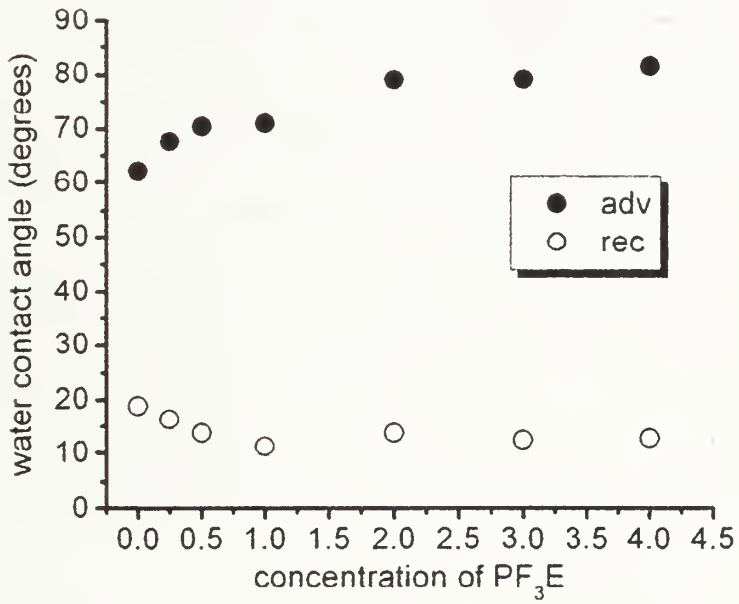

Figure 2.8 Advancing and (●) and receding (○) contact angle data for P4VP adsorbed to SiO_2-PF_3E from methanol solution at room temperature for 4 hours as a function of P4VP concentration (A) and PF_3E adsorbed to SiO_2-P4VP from methanol solution at room temperature for 4 hours as a function of PF_3E concentration (B)

The water contact angle data as a function of PF_3E concentration for PF_3E adsorbed to a SiO_2-P4VP surface from methanol solution at room temperature are shown in figure 2.8-B. Initially, an increase in advancing and a decrease in receding contact angles are observed as the concentration of PF_3E increases. Both of them reach a plateau at 2 mg/mL.

Figure 2.9 shows fluorine and nitrogen content determined by XPS at 15^0 take off angle for P4VP adsorbed to SiO_2-PF_3E as a function of P4VP concentration (A) and PF_3E adsorbed to SiO_2-P4VP as a function of PF_3E concentration (B). As the P4VP concentration increases, nitrogen content increases and fluorine content decreases and both level at 1 mg/mL. (Figure 2.9-A). In the case of PF_3E adsorption, the fluorine concentration increases and nitrogen content decreases as the PF_3E concentration increases. Both level at high concentrations (Figure 2.9-B).

In addition to XPS and contact angle measurements, the concentration effect on P4VP adsorption on SiO_2-PF_3E and PF_3E adsorption on SiO_2-P4VP was monitored by ellipsometry. Ellipsomtery results show that as the P4VP concentration increases, the layer thickness increases until 1 mg/ mL and then does not change as the concentration increases (Figure 2.10-A). In the case of PF_3E adsorption, the layer thickness is not affected by the PF_3E concentration (Figure 2.10-B) and this is not very consistent with the XPS data. (Figure 2.9-B)

A)

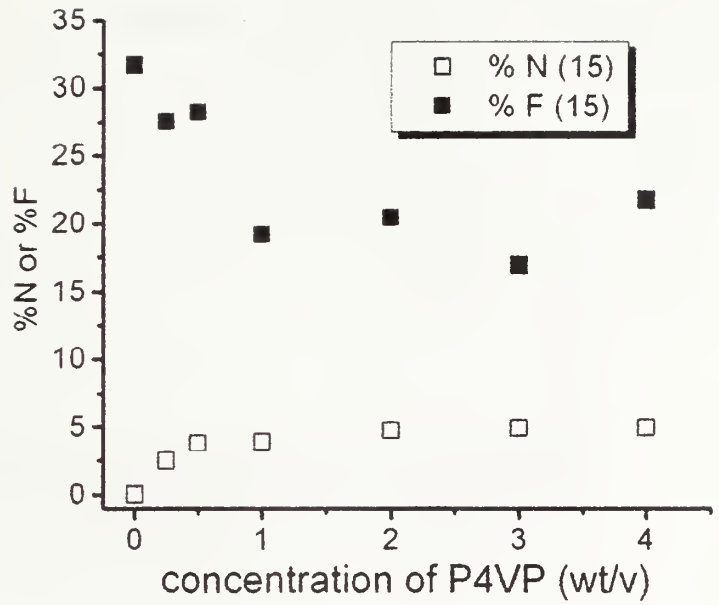

B)

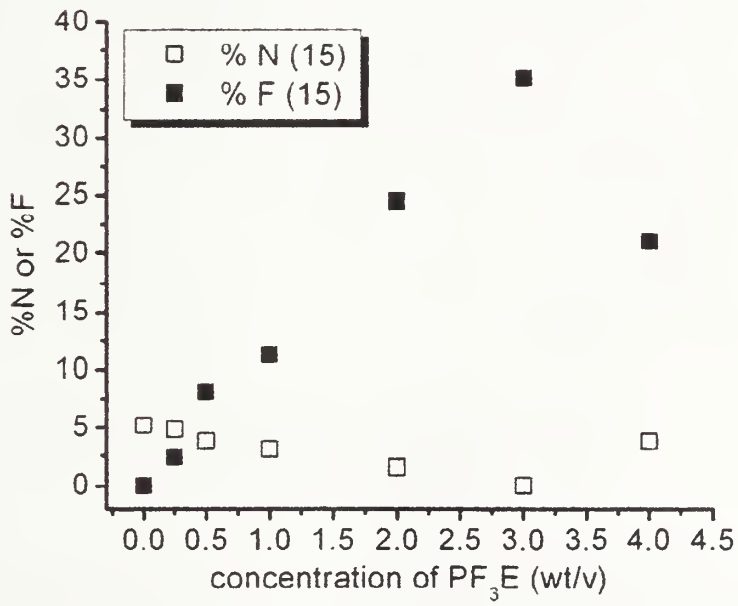

Figure 2.9 Fluorine (■) and nitrogen (□) concentrations (determined from XPS composition data at 15° take-off angle) of P4VP adsorbed to Si/SiO_2–PF_3E (A) from methanol solution at room temperature for 4 h as a function of P4VP concentration and PF_3E adsorbed to Si/SiO_2-P4VP (B)) from methanol solution at room temperature for 4 h as a function of PF_3E concentration

A)

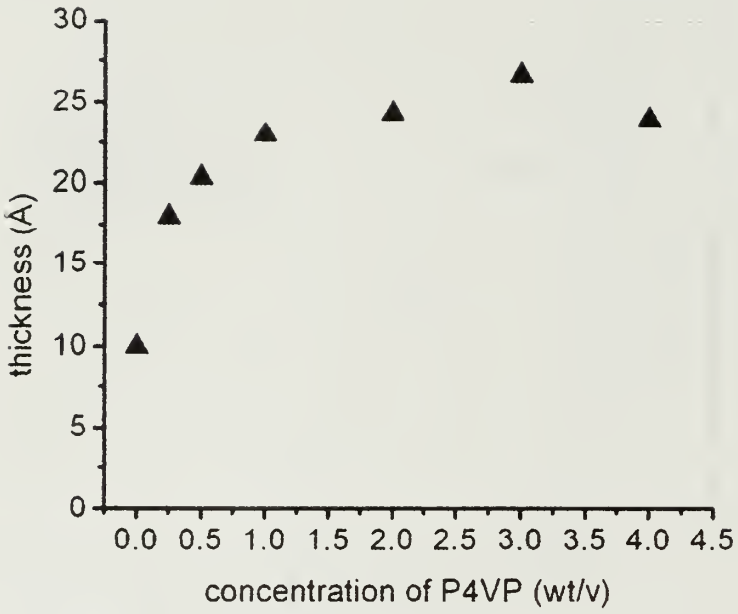

B)

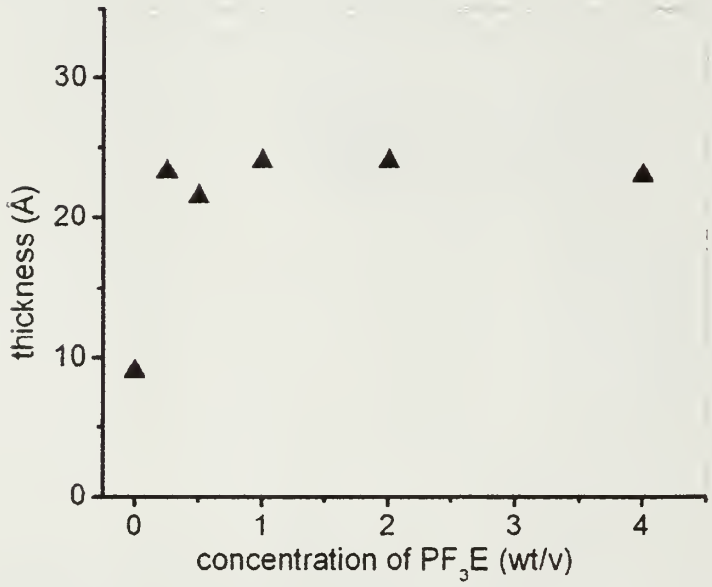

Figure 2.10 Ellipsometric thickness data for P4VP adsorbed to Si/SiO_2–PF_3E (A) from methanol solution at room temperature for 4 h as a function of P4VP concentration and PF_3E adsorbed to Si/SiO_2-P4VP (B) from methanol solution at room temperature for 4 h as a function of PF_3E concentration

2.3.3 Multilayer studies

Two sets of multilayer adsorption studies were performed. The first layer was always PF_3E. The first layer adsorptions were carried out at room temperature for a day from 1 mg/mL PF_3E methanol solution. The initial layer thickness was 10 Å.

In the first set, polymer concentrations were held at 1 mg/mL and all adsorptions are carried out for 1 hour except the first layer. Figure 2. 11 show XPS and ellipsomtery results as a function of number of layers. After the second layer formation. (P4VP adsorption), we did not observe any significant change in thickness and nitrogen concentration remains the same as the number of adsorption steps increases. The fluorine content decreases, due to some reconstruction of the adsorbed layer. These results show that P4VP strongly adsorbs on PF_3E. However, PF_3E does not adsorb on P4VP to form the third layer due to non-availability of P4VP nitrogens to form hydrogen bonding with PF_3E.

In the second set, polymer concentrations were held at 3 mg/mL and all adsorption were carried out for 4 hours except the first layer. XPS and ellipsomtery results as a function of layers are shown in Figure 2.12. With alternating adsorption steps, when the fluorine content increases, the nitrogen content decreases and visa versa. This means that when P4VP adsorption takes place, a decrease in fluorine content and an increase in nitrogen content are seen, and when PF_3E adsorption takes place, a decrease in nitrogen content and an increase in fluorine content are observed. This indicates that multilayer formation is successful. However, ellipsmetry results are not very promising. As the number of adsorption steps increases, after the first two layers,

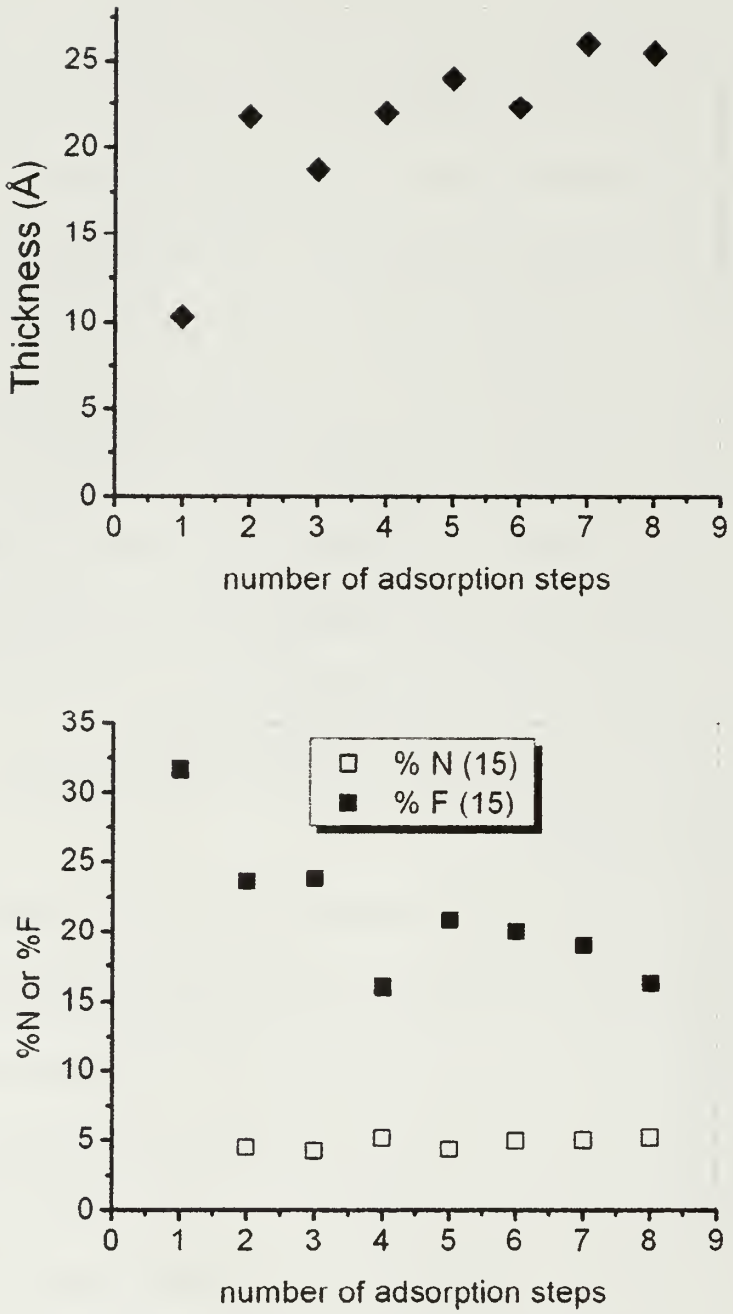

Figure 2.11 Thickness of the multilayer (♦). and nitrogen (□) and fluorine (■) atomic concentrations determined at 15° take-off angle as a function of number of adsorption steps in the multilayer film formation (first layer is prepared by adsorption of PF_3E on clean silicon wafer from 1 mg /mL methanol solution at room temperature for 24 hours. The subsequent layers are prepared by adsorption of P4VP (1 mg /mL) or PF_3E (1 mg /mL) from methanol solution at room temperature for an hour)

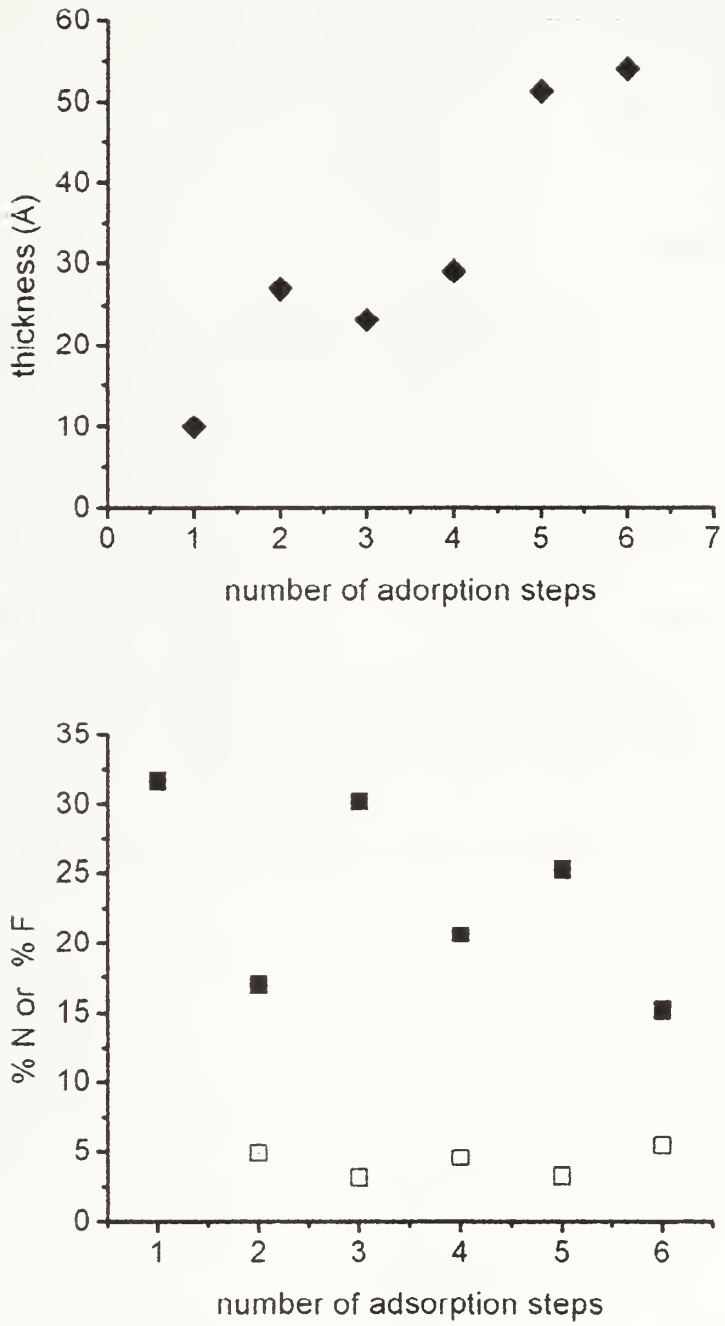

Figure 2.12 Thickness of the multilayer (♦). and nitrogen (□) and fluorine (■) atomic concentrations determined at 15° take-off angle as a function of number of adsorption steps in the multilayer film formation (first layer is prepared by adsorption of PF_3E on clean silicon wafer from 1 mg /mL methanol solution at room temperature for 24 hours. The subsequent layers are prepared by adsorption of P4VP (3 mg /mL) or PF_3E (3 mg /mL) from methanol solution at room temperature for 4 hours.)

no change is observed until 5th adsorption step. This suggests that, while adsorption of one kind of polymer (P4VP or PF_3E) takes place in each step, dissolution of already formed layers occurs.

2.3 Conclusions

In this chapter, thin layers of poly(4-vinylpyridine) and poly(trifluoroethylene) on silicon wafers were prepared by adsorption from methanol solution. It has been shown that poly(4-vinylpyridine) adsorbs on poly(trifluoroethyelene) and poly(trifluoroethyelene) adsorbs on poly(4-vinylpyridine) through hydrogen bonding interactions. The adsorption of poly (4-vinylpyrine) on poly(trifluoroethylene) is fast and reaches its limiting amount in 15 minutes. Multilayer adsorption studies show that the multilayer formation is complex. Adsorbing polymer replaces the already formed layer and no increase or a small increase in layer thickness is observed.

2.4 References

(1) Decher, G.; Hong, J. D.; Schmitt, J. *Thin Solid Films* **1992**, *210*, 831-835.

(2) Decher, G. *Science* **1997**, *277*, 1232-1237.

(3) Decher, G.; Lehr, B.; Lowack, K.; Lvov, Y.; Schmitt, J. *Biosensors & Bioelectronics* **1994**, *9*, 677-684.

(4) Decher, G.; Schlenoff, J. B. *Multilayer Thin Films : Sequential Assembly of Nanocomposite Materials*, Wiley-VCH: Weinheim, 2003.

(5) Zhang, X.; Gao, M. L.; Kong, X. X.; Sun, Y. P.; Shen, J. C. *Journal of the Chemical Society-Chemical Communications* **1994**, 1055-1056.

(6) Kleinfeld, E. R.; Ferguson, G. S. *Science* **1994**, *265*, 370-373.

(7) Lvov, Y.; Ariga, K.; Ichinose, I.; Kunitake, T. *Langmuir* **1996**, *12*, 3038-3044.

(8) Ostrander, J. W.; Mamedov, A. A.; Kotov, N. A. *Journal of the American Chemical Society* **2001**, *123*, 1101-1110.

(9) Liu, S. Q.; Kurth, D. G.; Bredenkotter, B.; Volkmer, D. *Journal of the American Chemical Society* **2002**, *124*, 12279-12287.

(10) He, J. A.; Valluzzi, R.; Yang, K.; Dolukhanyan, T.; Sung, C. M.; Kumar, J.; Tripathy, S. K.; Samuelson, L.; Balogh, L.; Tomalia, D. A. *Chemistry of Materials* **1999**, *11*, 3268-3274.

(11) Kong, W.; Zhang, X.; Gao, M. L.; Zhou, H.; Li, W.; Shen, J. C. *Macromolecular Rapid Communications* **1994**, *15*, 805-805.

(12) Taton, T. A.; Mucic, R. C.; Mirkin, C. A.; Letsinger, R. L. *Journal of the American Chemical Society* **2000**, *122*, 6305-6306.

(13) Schmitt, J.; Decher, G.; Dressick, W. J.; Brandow, S. L.; Geer, R. E.; Shashidhar, R.; Calvert, J. M. *Advanced Materials* **1997**, *9*, 61-&.

(14) Yang, X.; Johnson, S.; Shi, J.; Holesinger, T.; Swanson, B. *Sensors and Actuators B-Chemical* **1997**, *45*, 87-92.

(15) Sun, J. Q.; Zou, S.; Wang, Z. Q.; Zhang, X.; Shen, J. C. *Materials Science & Engineering C-Biomimetic and Supramolecular Systems* **1999**, *10*, 123-126.

(16) Sun, J. Z.; Sun, J. Q.; Ma, Y. G.; Zhang, X.; Shen, J. C. *Materials Science & Engineering C-Biomimetic and Supramolecular Systems* **1999**, *10*, 83-86.

(17) Tian, J.; Wu, C. C.; Thompson, M. E.; Sturm, J. C.; Register, R. A. *Chemistry of Materials* **1995**, *7*, 2190-2198.

(18) Tian, J.; Wu, C. C.; Thompson, M. E.; Sturm, J. C.; Register, R. A.; Marsella, M. J.; Swager, T. M. *Advanced Materials* **1995**, *7*, 395-398.

(19) Voigt, A.; Lichtenfeld, H.; Sukhorukov, G. B.; Zastrow, H.; Donath, E.; Baumler, H.; Mohwald, H. *Industrial & Engineering Chemistry Research* **1999**, *38*, 4037-4043.

(20) Viswanathan, N. K.; Balasubramanian, S.; Li, L.; Kumar, J.; Tripathy, S. K. *Journal of Physical Chemistry B* **1998**, *102*, 6064-6070.

(21) Caruso, F.; Caruso, R. A.; Mohwald, H. *Chemistry of Materials* **1999**, *11*, 3309-3314.

(22) Graul, T. W.; Schlenoff, J. B. *Analytical Chemistry* **1999**, *71*, 4007-4013.

(23) Van Ackern, F.; Krasemann, L.; Tieke, B. *Thin Solid Films* **1998**, *329*, 762-766.

(24) Dante, S.; Hou, Z. Z.; Risbud, S.; Stroeve, P. *Langmuir* **1999**, *15*, 2176-2182.

(25) Sukhorukov, G.; Dahne, L.; Hartmann, J.; Donath, E.; Mohwald, H. *Advanced Materials* **2000**, *12*, 112-115.

(26) Liu, Y. J.; Wang, A. B.; Claus, R. O. *Applied Physics Letters* **1997**, *71*, 2265-2267.

(27) Bertrand, P.; Jonas, A.; Laschewsky, A.; Legras, R. *Macromolecular Rapid Communications* **2000**, *21*, 319-348.

(28) Hammond, P. T.; Whitesides, G. M. *Macromolecules* **1995**, *28*, 7569-7571.

(29) Stockton, W. B.; Rubner, M. F. *Macromolecules* **1997**, *30*, 2717-2725.

(30) Ferreira, M.; Cheung, J. H.; Rubner, M. F. *Thin Solid Films* **1994**, *244*, 806-809.

(31) Levasalmi, J. M.; McCarthy, T. J. *Macromolecules* **1997**, *30*, 1752-1757.

(32) Chen, W.; McCarthy, T. J. *Macromolecules* **1997**, *30*, 78-86.

(33) Phuvanartnuruks, V.; McCarthy, T. J. *Macromolecules* **1998**, *31*, 1906-1914.

(34) Hsieh, M. C.; *Polyelectrolyte Multilayer Assemblies*, PhD Dissertation, University of Massachusetts, 1999

(35) Hsieh, M. C.; Farris, R. J.; McCarthy, T. J. *Polymer Preprints (American Chemical Society, Division of Polymer Chemistry)* **1997**, *38*, 670-671.

(36) Wang, L. Y.; Wang, Z. Q.; Zhang, X.; Shen, J. C.; Chi, L. F.; Fuchs, H. *Macromolecular Rapid Communications* **1997**, *18*, 509-514.

(37) Wang, L. Y.; Fu, Y.; Wang, Z. Q.; Wang, Y.; Sun, C. Q.; Fan, Y. G.; Zhang, X. *Macromolecular Chemistry and Physics* **1999**, *200*, 1523-1527.

(38) Fu, Y.; Bai, S. L.; Cui, S. X.; Qiu, D. L.; Wang, Z. Q.; Zhang, X. *Macromolecules* **2002**, *35*, 9451-9458.

(39) Sukhishvili, S. A.; Granick, S. *Journal of the American Chemical Society* **2000**, *122*, 9550-9551.

(40) Sukhishvili, S. A.; Granick, S. *Macromolecules* **2002**, *35*, 301-310.

(41) Hao, E. C.; Lian, T. Q. *Chemistry of Materials* **2000**, *12*, 3392-3396.

(42) Kharlampieva, E.; Sukhishvili, S. A. *Langmuir* **2003**, *19*, 1235-1243.

(43) Cho, J.; Caruso, F. *Macromolecules* **2003**, *36*, 2845-2851.

(44) Zhang, H. Y.; Wang, Z. Q.; Zhang, Y. Q.; Zhang, X. *Langmuir* **2004**, *20*, 9366-9370.

(45) Shiratori, S. S.; Rubner, M. F. *Macromolecules* **2000**, *33*, 4213-4219.

(46) Dubas, S. T.; Schlenoff, J. B. *Macromolecules* **1999**, *32*, 8153-8160.

(47) Wang, M.; Jiang, M.; Ning, F. L.; Chen, D. Y.; Liu, S. Y.; Duan, H. W. *Macromolecules* **2002**, *35*, 5980-5989.

(48) Zhang, W. Q.; Shi, L. Q.; Gao, L. C.; An, Y. L.; Li, G. Y.; Wu, K.; Liu, Z. *Macromolecules* **2005**, *38*, 899-903.

(49) Moore, J. A.; Kaur, S. *Macromolecules* **1998**, *31*, 328-335.

CHAPTER 3

TITANIUM SURFACE MODIFICATION USING HYDRIDOSILANES

3.1 Introduction

The covalent modification of solid surfaces is a powerful technique in designing materials with a desired level of solid-liquid and solid-vapor interactions. Selective surface modification has been the focus of research and technology in different applications such as sorption and separation media, wetting and adhesion, pigments, sensors, biomaterials, polymer composites, and optical and electronic devices.[1-4]

Organosilanes that have a general formula $R_{3-n}SiX_{n+1}$ (n=0-3), where X is a reactive leaving group, have been used for surface modification and as coupling agents for different substrates including metal oxides, oxidized metals and so forth.[3-10] Films derived from organosilanes have good thermal and chemical stability due to robust Si-O linkages between the silane and the surface[8,9] (realized in covalently attached monolayers, CAMs) or between the neighboring silane molecules[4-7] (realized in self-assembled monolayers SAMs). It has been shown that the self-assembly reaction is not the only reaction possible between alkyltrichlorosilanes and the silica surfaces. Under some conditions the alklytrichlorosilanes can react with the surface silanols in a covalent attachment manner or can condense into 3-D siloxanes grafted to the surface.[10]

Titanium is very reactive toward oxygen and forms an oxide layer on the surface when it is exposed to air.[11,12] The oxide layer is mostly composed of titanium dioxide TiO_2, though Ti_2O_3 and other forms may also be present.[11,13] There are three crystalline phases of TiO_2, rutile, anatase and brookite and TiO_2 can also be amorphous.[14,15]

TiO_2[16]forms a native oxide layer spontaneously at room temperature and the oxide layer is amorphous and has a thickness of 2-6 nm.[11] The crystalline phases form at higher temperatures and the transition temperature from one crystalline state to another varies with the preparation method. For example, when TiO_2 thin films are prepared by atomic layer deposition, amorphous, anatase and rutile structures grow below 440 K, at 440-625 K and above 625 K, respectively.[17] Owing to its low density, high mechanical resistance, and protective surface thin oxide layer, titanium is useful in aerospace and biomedical applications.[18]

The modification of titanium surfaces with organosilanes has been studied with different active groups.[19-21] Cossement *et al.* modified polycrystalline titanium surfaces with chlorosilanes and ethoxysilanes.[19] The reaction of (3,3,3-trifluoropropyl)trimethoxysilane with titanium surfaces was studied by Gamble *et al.*[21]

In the reaction of commonly used chloro- (X=Cl), N,N-dimethyamino ($X=N(CH_3)_2$), and alkoxy- (X=OAlk) silanes, the by products are corrosive and highly reactive compounds such as HCl, $HN(CH_3)_2$, and alcohol. They can adsorb and react with the surfaces. This corrodes the substrate and slows down the reaction and decreases the uniformity of the surface coverage. The liberation of HCl is troublesome for surface modification of high surface area substrates. The use of hydridosilanes (X=H)[22] in surface modification has advantages over other silane coupling agents. The monolayer production occurs in a clean environment because the byproduct is hydrogen gas or water. Hydridosilanes ($R_{3-n}SiH_{n+1}$ (n=0-3)) are less moisture sensitive than chlorosilanes ($R_{3-n}SiCl_{n+1}$(n=0-3)) and alkoxysilanes ($R_{3-n}SiOAlk_{n+1}$ (n=0-3)). Hydridosilanes have lower boiling points and this facilitates the reaction in vapor phase.

The $-SiH_3$ (or $-SiH_2$ or -SiH) group is the smallest among $-SiCl_3$ (or $-SiCl_2$ or -SiCl) and-$SiOAlk_3$ (or $-SiOAlk_2$ or -SiOAlk) groups so the highest surface coverage can be achieved. The reactions of hydridosilanes with various metals, including Zr, Fe, Ni, Mn, Nb, Cr, Mo, and W, are quite general.[16]

Organosilicon hydrides (silicones with Si-H groups) were used in 1949 for water proofing of construction materials by Andrinanov and Sobolevsky.[23] Then low-and high-molecular weight organosilicon hydrides for water repellency and protective coatings were used by Voronkov *et al* .[24-26] In the early publications[23-26], they emphazised the importance of Si-H group in the hydrophobizing agents, but did not study the structure of the films or the mechanism of the surface binding in detail. Tada, et al.[27,28] studied the chemisorption of 1,3,5,7-tetramethylcyclotetrasiloxane on titania. The reaction of octadecylsilane with titania in the presence of ultrasound was studied by Grunze *et al*.[29] The reaction of hydridosilanes with titanium and other metal oxides was reported by Fadeev *et al.*[16,22] and other groups[30]. In earlier studies, they used several mono-, di- and tri-hydridosilanes and used only one kind of reaction condition (solution phase), and did not study the reaction kinetics.

In this chapter, the modification of silicon-supported titanium surfaces with mono-, di- and tri- hydridosilanes under two conditions (1) in the vapor phase and (2) in heptane is described. The kinetics of the solution phase reaction with octadecylsilane is also described.

3.2 Thickness determination by XPS

Electrons do not travel very large distances in matter due to inelastic scattering processes with the matrix or solid medium. This is the basis for surface sensitivity of XPS. The attenuation of photoelectron intensity in solids as a function of sampling depth is expressed in below equation where N_0 is the number of electrons that originate at depth t. N is the number of photoelectrons emitted from solid that have not been inelastically scattered. λ is the mean free path of the electron and θ is the take-off angle.

$$N = N_o \exp\left(-\frac{t}{\lambda \sin\theta}\right)$$

The expression indicates that 95% of detected photoelectrons originate in the outermost $3\lambda\sin\theta$. In another words, the electron should be attenuated to 5% of its original intensity when the thickness is $3\lambda\sin\theta$.

In this work, the thickness of the monolayers is determined using the attenuation of the Ti_{2p} signal and the equation below.

$$t = Ln\left(\frac{N_0}{N}\right)\lambda \sin\theta$$

where N_0 and N are the intensity of the Ti_{2p} peak for bare sample and monolayers, respectively, θ is the take-off angle, and λ is the Ti_{2p} photoelectron mean free path. A literature value[21] of λ=20 Å will be assumed for the calculations.

3.3 Experimental

3.3.1 Materials and Methods

All chemicals were used as received unless noted otherwise. Heptane (HPLC), methylene chloride (HPLC), ethanol and acetone were purchased from Fisher. All silane reagents (n-octadecylsilane (n-$C_{18}H_{37}SiH_3$), diphenylsilane ($(C_6H_5)_2SiH_2$), tri-isopropylsilane ($(i\text{-}C_3H_7)_3SiH$), tri-n-propylsilane ($(n\text{-}C_3H_7)_3SiH$), hexylsilane ($C_6H_{13}SiH_3$), triphenylsilane ($(C_6H_5)_3SiH$), diphenylmethylsilane ($(C_6H_5)_2CH_3SiH$), and trihexylsilane ($(C_6H_{13})_3SiH$) were purchased from Gelest with the exceptions of n-octadecyldimethylsilane (n-$C_{18}H_{37}(CH_3)_2SiH$),phenylmethylsilane ($C_6H_5CH_3SiH_2$) and t-butyldimethylsilane (t-$C_4H_9(CH_3)_2SiH$) which were purchased from Aldrich. Anhydrous heptane was purchased from Aldrich. Water was purified using a Millipore Milli-Q system that involves reverse osmosis, ion exchange and filtration steps. Silicon-supported titanium wafers (the titanium layer on the silicon was ~1000 Å thick) were obtained from Schick and cleaned with a Harrick Scientific O_2 plasma cleaner at high power settings for 5 minutes prior to use. X-ray photoelectron spectra (XPS) were obtained on a Physical Electronics Quantum 2000 Scanning ESCA Microprobe. Depth profiling was done by collecting spectra at 15° and 75° take-off angles with respect to the plane of the sample surface. The analysis at 15° has a penetration depth of ~10 Å and that at 75° corresponds to a penetration depth of ~40 Å. Contact angle measurements were made with a Ramè-Hart telescopic goniometer and a Gilmont syringe with a 24-gauge flat-tipped needle. Water was used as the probe liquid. Advancing and receding contact angle were recorded while water was added and

withdrawn from the drop, respectively. Reported values are averages of 4-5 measurements made on different areas of a sample.

3.3.2 Reaction of Titanium Surfaces with Hydridosilanes in Solution

Titanium wafers were cleaned as described above. The wafers were immediately placed into the reaction flask. The reaction flask was similar to the one that was used for vapor phase reactions with the exception that the top included a 4 mm Teflon stopcock and joint capped with a rubber septum to facilitate cannulation and additions via syringe under an inert atmosphere. Anhydrous heptane (~25 mL) was cannulated into the reaction tube and the hydridosilane (1 mL) of the choice was added via syringe. The reaction tube was placed in an oil bath and heated to 65-70 °C for 2 days, unless otherwise noted. After the reaction, the wafers were rinsed with heptane, methylene chloride, ethanol, acetone, and distilled water in this order, and then dried in a clean oven at 125 °C for 10 min.

3.3.3 Reaction of Titanium Surfaces with Hydridosilanes in the Vapor Phase

Titanium wafers were cleaned as described above. The wafers were immediately placed in the reaction tube containing the hydridosilane of choice. Samples were placed in a custom-made wafer holder and suspended in a schlenk tube containing 1 mL of silane (Figure 3.1). There was no contact between the silane and the silicon substrates. The reaction tube was placed in an oil bath and heated to 65-70 °C for a day. After the reaction, the wafers were rinsed with heptane, methylene chloride, ethanol, acetone, and distilled water in this order, and then dried in a clean oven at 125°C for 10 min.

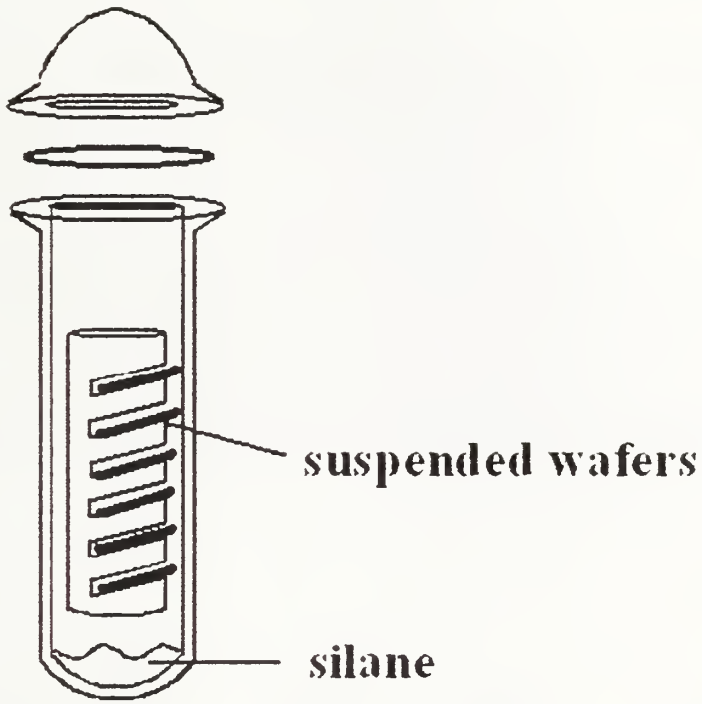

Figure 3.1 Schematic of the Schlenk tube used for the vapor phase reaction of hydridosilanes.

3.4 Results and Discussion

Two types of reaction conditions were used to prepare covalently attached monolayers on silicon-supported titanium surfaces: (1) in heptane at 65-70 °C for 2 days and (2) in vapor phase at 65-70 °C for a day.

3.4.1 Reaction of TiO_2 with Hydridosilanes in Solution

Reaction of silicon-supported titanium wafers with hydridosilanes (mono-, di- and trihydridosilanes) was conducted in heptane solution at 65-70 °C (Figure 3.2). Table 3.1 shows the water contact angle and thickness data for a number of the monolayers. All mono-, di-and tri-hydridosilanes react with titanium surfaces, as assessed by high water contact angle results (Table 3 1). N-octadecylsilane-derived monolayers exhibits water

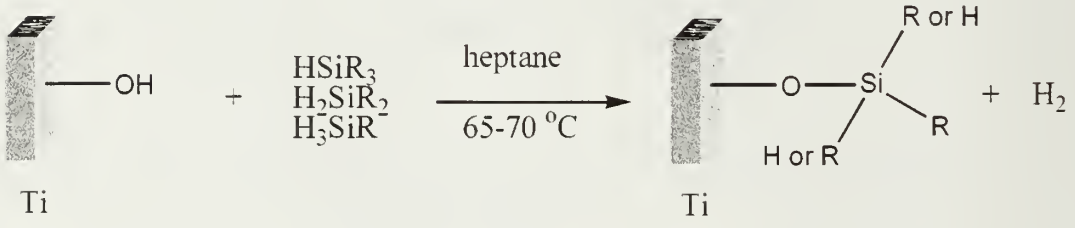

Figure 3.2 Schematic representation of the reaction of hydridosilanes with titanium surfaces

contact angle values that are very close to the water contact angle data of self-assembled, closed packed monolayers reported in literature.[4,7,10] Hysterises in contact angle data for n-octadecylsilane-derived monolayer is high (16°) but not so much different than the reported octadecyl supported monolayers in the literature.[7,10]

Monolayer thicknesses are calculated from XPS using attenuation of the Ti_{2p} signal at two different angles. The thickness results also prove formation of monolayers on titanium surfaces from hydridosilanes in heptane.

Oxygen plasma-cleaned silicon-supported titanium surfaces contain low percentages of silicon and carbon as assessed by XPS at 15° and 75° take-off angles. After silanization in heptane, the titanium surfaces all show an increase in carbon and silicon content. In addition, the titanium content decreases (Table 3.2).

Hydridosilanes	Contact Angle (θ_A/θ_R(°))	Thickness[b] (λ(Å))	
		(XPS-15°)	(XPS-75°)
None (TiO_2) O_2 cleaned	Spreads	------	-------
n-$C_{18}H_{37}SiH_3$	107/91	18	15
$(C_6H_5)_2SiH_2$	87/52	3	6
$C_6H_5MeSiH_2$	93/65	7	11
(i-$C_3H_7)_3SiH$	91/64	4	7
(n-$C_3H_7)_3SiH$	91/57	5	8

All reactions were carried out in heptane at 65-70 °C for two days
[b] Determined by XPS using the attenuation of Ti2p signal at 15° and 75° take-off angles

Table 3.1 Water contact angle data (θ_A/θ_R) in degrees (deg) and layer thickness (from XPS) in angstroms (Å) for silicon-supported titanium surfaces treated with hydridosilanes in heptane

Hydridosilanes	XPS Atomic (%)[a]			
	Ti	C	Si	O
None (TiO_2)	29.80	<.1	0.10	70.10
O_2 cleaned	31.30	1.00	0.20	67.60
n-$C_{18}H_{37}SiH_3$	5.40	73.90	2.60	18.10
	15.10	39.50	1.50	43.90
$(C_6H_5)_2SiH_2$	15.70	39.70	2.60	41.90
	23.40	14.20	1.40	61.00
$(C_6H_5)_2MeSiH$	7.30	63.30	4.40	25.00
	17.40	33.10	1.80	47.60
$(i\text{-}C_3H_7)_3SiH$	14.60	25.80	7.60	52.00
	21.80	10.40	2.90	64.90
$(n\text{-}C_3H_7)_3SiH$	11.40	55.65	2.60	30.40
	21.00	23.10	0.80	55.10

[a] Upper rows are 15° takeoff angle data and lower rows are 75° data.
All reactions are carried out in heptane at 65-70 °C for two days

Table 3.2 XPS analysis for silicon-supported titanium surfaces treated with hydridosilanes in heptane

3.4.2 Reaction Kinetics

Octadecysilane was chosen to study the reaction kinetics in heptane solution. Reaction kinetics were monitored by water contact angle measurements. The data are plotted in Figure 3.3. From the contact angle graph it is very clear that significant hydrophobization occurs in an hour, but the reaction is not complete until 1-2 days. The hysterises decreases as the time increases, and the minimum hysterises is obtained for samples reacted for 3 days (11°). Beyond 3 days, a slight increase in hysterises is observed.

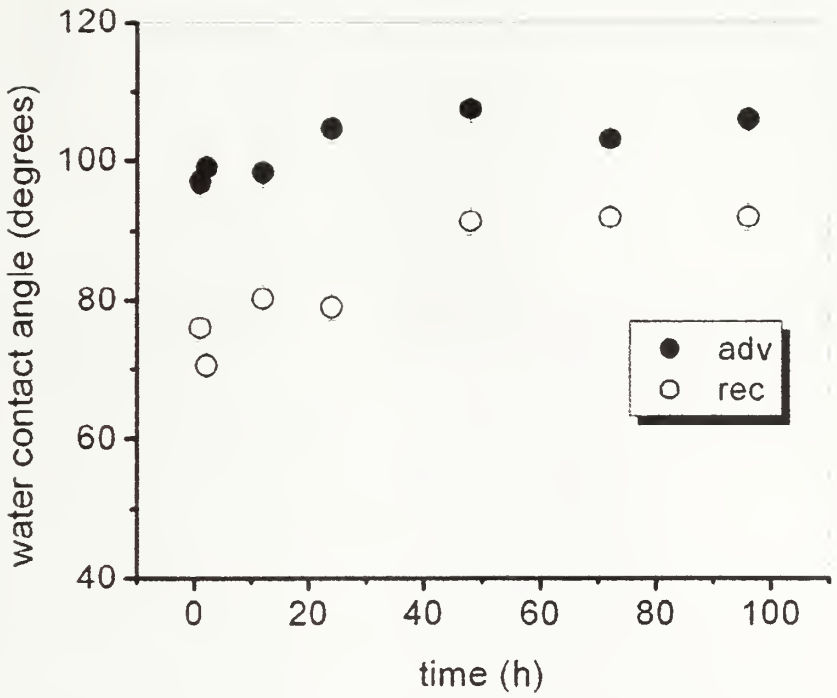

Figure 3.3 Water contact angle data (θ_A/θ_R) data versus reaction time of grafted octadecylsilane (Samples were prepared in heptane at 65-70 °C. Prior to reaction the wafers are cleaned by O_2 plasma.) silicon-supported titanium surfaces. The closed symbols are advancing angles and the open symbols are receding angles.

Figure 3.4 shows high-resolution spectra of the O_{1s} signal at 15° (take-off angle) of a clean titanium surface (Å) and octadecylsilane-derived monolayers prepared in heptane for different reaction periods. Clean titanium shows two peaks of interest. The lower binding energy peak is due to oxygen bonded to two titaniums and the higher binding energy peak is due to surface oxygen species. Upon reaction with octadecylsilane, the substrate signal (the lower binding energy peak) decreases. The octadecylsilane-derived monolayer prepared by two days of reaction completely attenuates the substrate signal.

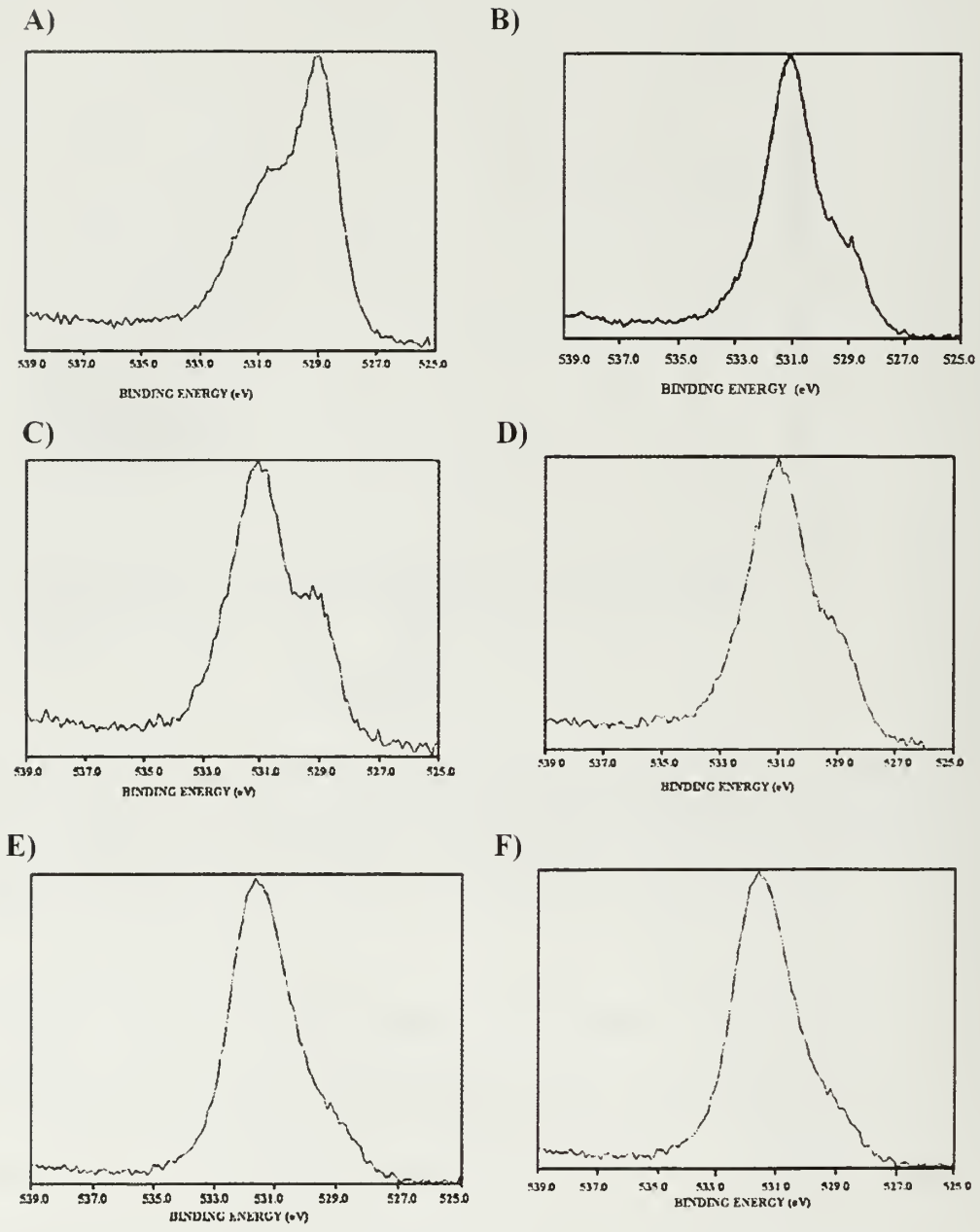

Figure 3.4 High resolution XPS spectra of the O_{1s} signal (15° take-of angle) of a clean silicon supported titanium surface (A) and a silicon-supported titanium surface treated with octadecylsilane silane in heptane at 65-70 °C for 1 h (B), 12 h (C), 24 h (D). 48 h (E) and 72 h (F)

3.4.3 Reaction of Titanium Surfaces with Hydridosilanes in the Vapor Phase

Reactions of silicon-supported titanium surfaces with mono- , di- and trihydridosilanes were conducted at 65-70 °C for a day. All mono- , di- and trihydridosilanes react with titanium surfaces in vapor phase conditions as assessed by the contact angle results (Table 3.3). The monolayers prepared in the vapor phase show, for the most part, higher contact angles than the monolayers prepared in heptane. The octadecylsilane monolayer on silicon-supported titanium shows higher contact angles than the ones prepared in the literature.[10] The monolayers prepared from hexylsilane and trihexylsilane have similar contact angles, and the contact angle values for the trihexylsilane-derived monolayer decreases as the reaction time increases. This can be ascribed to oxidative degradation of the already modified surface. The thickness of the monolayers is also calculated by the attenuation of the Ti_{2p} signal (Table 3.3).

Table 3.4 shows XPS data of layers prepared by vapor phase reaction. The reaction of titanium surfaces with hydridosilanes is indicated by the XPS results. After silanization in the vapor phase, increase in carbon and silicon concentration and decrease in titanium concentration are observed. The decrease in titanium concentration is due to the monolayer formation.

Hydridosilanes	Contact Angle ($\theta_A/\theta_R(^o)$)	Thickness (λ(Å))	
		(XPS 15°)	(XPS-75°)
None (TiO_2) O_2 cleaned	Spreads	------	-------
n-$C_{18}H_{37}SiH_3$	112/88	13	15
$C_6H_{13}SiH_3$	104/80	6	11
$(C_6H_5)_2SiH_2$	92/64	9	12
n-$C_{18}H_{37}(Me)_2SiH$	93/60	6	10
$(C_6H_5)_3SiH$	87/56	6	9
$(C_6H_5)_2MeSiH$	96/67	9	12
(i-$C_3H_7)_3SiH$	102/62	10	19
(n-$C_3H_7)_3SiH$	89/50	6	12
t-$C_4H_9(Me)_2SiIH$	97/62	11	12
$(C_6H_{13})_3SiH$	101/82	14	14
$(C_6H_{13})_3SiH$ [b]	97/63	8	14
$(C_6H_{13})_3SiH$ [c]	93/58	7	10

All reactions were carried out in the vapor phase at 65-70 °C for a day or as otherwise noted

[b] Reaction time is 2 days

[c] Reaction time is 3 days

Table 3.3 Water contact angle (θ_A/θ_B) in degrees (deg) and layer thickness (from XPS) in angstroms (Å) for silicon-supported titanium surfaces treated with hydridosilanes in the vapor phase

Hydridosilane	XPS Atomic (%)[a]			
	Ti	C	Si	O
None (TiO_2)	29.80	<.1	0.10	70.10
O_2 cleaned	31.30	1.00	0.20	67.60
n-$C_{18}H_{37}SiH_3$	2.59	79.83	4.97	12.61
	10.58	53.22	3.76	32.44
$C_6H_{13}SiH_3$	8.68	52.24	5.96	33.12
	17.86	21.16	3.99	56.99
$(C_6H_5)_2SiH_2$	2.63	63.25	12.73	21.39
	14.50	34.23	4.20	47.07
n-$C_{18}H_{37}(Me)_2SiH$	9.75	55.67	3.30	31.28
	18.38	27.94	1.77	51.91
$(C_6H_5)_3SiH$	9.44	53.48	2.85	34.23
	19.80	28.02	1.67	50.50
$(C_6H_5)_2MeSiH$	5.26	56.60	11.08	27.06
	16.46	30.92	4.33	48.28
$(i\text{-}C_3H_7)_3SiH$	4.53	52.59	11.34	31.33
	11.98	31.58	7.06	49.38
$(n\text{-}C_3H_7)_3SiH$	8.70	53.31	6.51	31.48
	17.20	27.53	2.80	52.47
t-$C_4H_9(Me)_2SiH$	3.76	59.51	10.69	26.04
	16.99	26.49	4.78	51.73
$(C_6H_{13})_3SiH$	1.91	69.07	5.96	23.32
	15.24	33.96	3.57	47.24
$(C_6H_{13})_3SiH$[b]	5.89	58.70	6.60	25.49
	15.30	34.00	2.72	45.78
$(C_6H_{13})_3SiH$[c]	7.68	52.09	8.29	31.97
	18.54	28.33	2.61	50.52

[a] Upper rows are 15° takeoff angle data and lower rows are 75° data.
All reactions were carried out in the vapor phase at 65-70 °C for a day or as otherwise noted
[b] Reaction time is 2 days
[c] Reaction time is 3 days

Table 3.4 XPS analysis for silicon-supported titanium surfaces treated with hydridosilanes in the vapor phase

3.5 Conclusions

In this chapter, it is shown that the mono-, di and trihydridosilanes react with titanium surfaces in heptane at elevated temperatures and in the vapor phase at elevated temperature. The monolayers show high contact angle results. The thickness of the layers is calculated using the attenuation of the Ti_{2p} signal. The kinetics of the octadecylsilane reaction in heptane at 65-70 ^{o}C show that significant hydrophobization occurs in an hour, but that the reaction is not complete until 1-2 days.

3.6 References

(1) Plueddemann, E. P. *Silane Coupling Agents*, Plenum Press: New York, 1991.

(2) Leyden, D. E. *Silanes, Surfaces, and Interfaces*, Gordon and Breach: New York, 1986.

(3) Mittal, K. L.; Plueddemann, E. P. *Silanes and Other Coupling Agents*, Vsp: Utrecht, 1992.

(4) Ulman, A. *Chemical Reviews* **1996**, *96*, 1533-1554.

(5) Sagiv, J. *Israel Journal of Chemistry* **1979**, *18*, 346-353.

(6) Sagiv, J. *Journal of the American Chemical Society* **1980**, *102*, 92-98.

(7) Wasserman, S. R.; Tao, Y. T.; Whitesides, G. M. *Langmuir* **1989**, *5*, 1074-1087.

(8) Fadeev, A. Y.; McCarthy, T. J. *Langmuir* **1999**, *15*, 3759-3766.

(9) Boksanyi, L.; Liardon, O.; Kovats, E. S. *Advances in Colloid and Interface Science* **1976**, *6*, 95-137.

(10) Fadeev, A. Y.; McCarthy, T. J. *Langmuir* **2000**, *16*, 7268-7274.

(11) Kasemo, B. *Journal of Prosthetic Dentistry* **1983**, *49*, 832-837.

(12) Cacciafesta, P.; Hallam, K. R.; Oyedepo, C. A.; Humphris, A. D. L.; Miles, M. J.; Jandt, K. D. *Chemistry of Materials* **2002**, *14*, 777-789.

(13) Lausmaa, J. *Journal of Electron Spectroscopy and Related Phenomena* **1996**, *81*, 343-361.

(14) Pearson, W. B. *A Handbook of Lattice Spacings and Structures of Metals and Alloys*, Pergamon Press: New York., 1958.

(15) Henrich, V. E.; Cox, P. A. *The Surface Science of Metal Oxides*, Cambridge University Press: Cambridge ; New York, 1994.

(16) Fadeev, A. Y.; McCarthy, T. J. *Journal of the American Chemical Society* **1999**, *121*, 12184-12185.

(17) Aarik, J.; Aidla, A.; Uustare, T.; Sammelselg, V. *Journal of Crystal Growth* **1995**, *148*, 268-275.

(18) Steinemann, S. G. *Periodontology 2000* **1998**, *17*, 7-21.

(19) Cossement, D.; Delrue, Y.; Mekhalif, Z.; Delhalle, J.; Hevesi, L. *Surface and Interface Analysis* **2000**, *30*, 56-60.

(20) Cossement, D.; Pierard, C.; Delhalle, J.; Pireaux, J. J.; Hevesi, L.; Mekhalif, Z. *Surface and Interface Analysis* **2001**, *31*, 18-22.

(21) Gamble, L.; Henderson, M. A.; Campbell, C. T. *Journal of Physical Chemistry B* **1998**, *102*, 4536-4543.

(22) Fadeev, A. Y.; Helmy, R.; Marcinko, S. *Langmuir* **2002**, *18*, 7521-7529.

(23) Andrianov, K. A.; Sobolevsky, M. V. *High-Molecular Weight Organosilicon Compounds*, Oborongiz: Moskow, 1949.

(24) Voronkov, M. G.; Kalugin, N. B. *Zhurnal Prikladnoi Khimi* **1956**, *31*, 1390.

(25) Voronkov, M. G. *Zhurnal Prikladnoi Khimi* **1965**, *38*, 1483.

(26) Voronkov, M. G. *Zhurnal Prikladnoi Khimi* **1962**, *35*, 1093.

(27) Tada, H. *Langmuir* **1995**, *11*, 3281-3284.

(28) Tada, H. *Langmuir* **1996**, *12*, 966-971.

(29) Shafi, K. V. P. M.; Ulman, A.; Yan, X. Z.; Yang, N. L.; Himmelhaus, M.; Grunze, M. *Langmuir* **2001**, *17*, 1726-1730.

(30) Owens, T. M.; Nicholson, K. T.; Holl, M. M. B.; Suzer, S. *Journal of the American Chemical Society* **2002**, *124*, 6800-6801.

CHAPTER 4

MODIFICATION OF CHROMIUM SURFACES USING ORGANOSILANES

4.1 Introduction

A wide range of organic molecules are used to chemically modify metal oxide surfaces and this process has a wide range of applications such as improving adhesion at the interfaces of glass fiber-reinforced composites[1], generating low energy surfaces[2-9], and forming monolayers for lithography, micropatterning and sensors.[10-14] These modifications include the adsorption of alkanethiols[15,16], dialkyl disulfides[17,18] and dialkyl sulfides[19] on gold, alkanethiol and alkanedithiols on GaAs(001)[20], fatty acids on alumina[21,22], alcohols and amines on platinum[23], organosilicon hydrides, phosphates and alkanephosponic acids on titanium[24-29], and organosilanes on silicon surfaces.[5,30-33]

Organosilanes ($R_{3-n}SiX_{n+1}$) having one, two, or three hydrolyzable groups in the molecule (where X=Cl, OR and NMe_2) have been used to modify silicon surfaces.[5,30,31,33] Different structures on the surfaces are produced depending on the reaction conditions, chemistry of the organosilane and surface prehistory. Monofunctional organosilanes (R_3SiX) form reproducible covalently attached monolayers. Trifunctional silanes ($RSiX_3$) are more reactive and they can polymerize in the presence of water. This gives rise to different structures such as covalent attachment, 2-D self assembly and 3-D surface-induced polymerization. Difunctional organosilanes (R_2SiX_2) form covalently attached monolayers and grafted polysiloxane layers by surface-induced polymerization. (Figure 4.1)

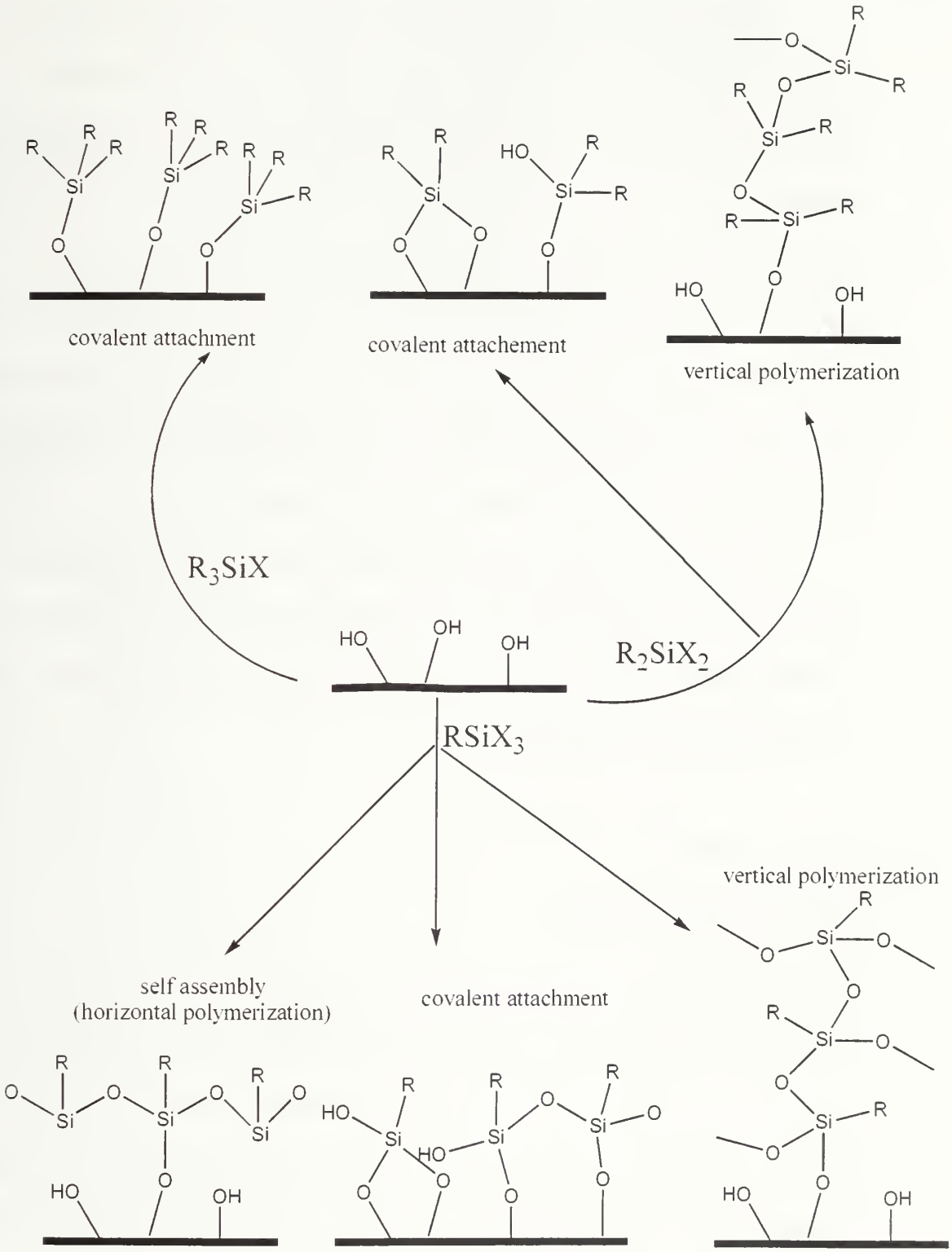

Figure 4.1 Possible products of reaction of organosilanes with silicon surfaces

Only a few studies of the formation of organic thin films on Cr have been reported: these include the assembly of surfactants such as myristic acid[34] and dodecylsulfate[35], deposition of Langmuir –Blodgett films of organic species such as phthalocyanines[36] and polyimides[37] on Cr electrodes, and the adsorption of electroactive species containing isonitrile and thiol functional groups[38], on Cr surfaces. The formation of organosilane (octadecylsilane[24] and octadecyltriethoxysilane[39]) layers has been reported, but the effects of temperature, solvent, reaction conditions (vapor phase reaction versus solution phase reaction), and leaving group have not been studied in any detail nor has the kinetics of the reactions been investigated.

In this chapter, silicon-supported chromium surfaces are modified by the reaction of mono- (R_3SiX where X=Cl, OEt, H), di- (R_2SiX_2 where X=Cl, OEt, H) and tri- ($RSiX_3$ where X=Cl, OEt, H) functional alkylsilanes under two different conditions: in solution and in the vapor phase.

4.2 Experimental

4.2.1 Materials and Methods

All chemicals were used as received unless noted otherwise. Toluene, hexane (HPLC grade), heptane (HPLC grade), methylene chloride (HPLC grade), 2-propanol and acetone were purchased from Fisher. Ethanol was purchased from VWR. All silane reagents, n-octadecylsilane (n-$C_{18}H_{37}SiH_3$), n-octadecyltrichlorosilane (n-$C_{18}H_{37}SiCl_3$), n-octyltichlorosilane (n-$C_8H_{17}SiCl_3$), n-octylsilane (n-$C_8H_{17}SiH_3$), benzyldimethylsilane (n-$C_7H_7(CH_3)_2SiH$), n-octylmethyldichlorosilane (n-$C_8H_{17}CH_3SiCl_2$),

n-hexylmethyldichlorosilane (n-$C_6H_{13}CH_3SiCl_2$), n-octadecyldimethylchlorosilane, (n-$C_{18}H_{37}(CH_3)_2SiCl$), octadecyltriethoxysilane (n-$C_{18}H_{37}(OC_2H_3)_3$), octyldimethyltriethoxysilane (n-$C_8H_{17}(OC_2H_3)_3$), n-propyltriethoxysilane (n-$C_3H_7(OC_2H_3)_3$), n-octadecylmethyldiethoxysilane (n-$C_{18}H_{37}CH_3(OC_2H_3)_2$), diphenylsilane ($(C_6H_5)_2SiH_2$), tri-isopropylsilane ((i-$C_3H_7)_3SiH$), tri-n-propylsilane ((n-$C_3H_7)_3SiH$), hexylsilane ($C_6H_{13}SiH_3$), triphenylsilane ($(C_6H_5)_3SiH$), diphenylmethylsilane ($(C_6H_5)_2CH_3SiH$), and trihexylsilane ($(C_6H_{13})_3SiH$), were purchased from Gelest. Octadecyldimethylsilane (n-$C_{18}H_{37}(CH_3)_2SiH$), phenylmethylsilane ($C_6H_5CH_3SiH_2$) and t-butyldimethylsilane (t-$C_4H_9(CH_3)_2SiH$) were purchased from Aldrich. Anhydrous heptane, anhydrous toluene and ethyldiisopropyl amine (EDIPA) were purchased from Aldrich. Water was purified using a Millipore Milli-Q system that involves reverse osmosis, ion exchange and filtration steps. Silicon-supported chromium wafers (the chromium layer on the silicon was ~1000 Å thick) were obtained from Schick and cleaned by a Harrick Scientific O_2 plasma cleaner at high power settings for 5 minutes prior to use. X-ray photoelectron spectra (XPS) were obtained on a Physical Electronics Quantum 2000 Scanning ESCA Microprobe. Depth profiling was done by collecting spectra at 15° and 75° take-off angles with respect to the plane of the sample surface. The analysis at 15° has a penetration depth of ~10 Å and that at 75 °corresponds to a penetration depth of ~40 Å. Contact angle measurements were made with a Ramè-Hart telescopic goniometer and a Gilmont syringe with a 24-gauge flat-tipped needle. Water was used as a probe liquid. Advancing and receding contact angles were recorded while the water was added and

withdrawn from the drop, respectively. Reported values are averages of 4-5 measurements made on different areas of a sample.

4.2.2. Reaction of Chromium Surfaces with Alkylchlorosilanes and Alkylethoxysilanes in the Vapor Phase

Chromium wafers were cleaned as described above. The wafers were immediately placed in the reaction tube containing the alkylchlorosilane or alkylethoxysilane of choice. Samples were placed in a custom-made wafer holder and suspended in a Schlenk tube containg 0.5 mL of silane (Figure 4.2). There was no contact between the silane and the silicon substrates. The reaction tube was placed in an oil bath and heated to 65-70 °C for 3 days. After the reaction, the wafers were rinsed with toluene, 2-propanol, ethanol, ethanol-water (1:1), and distilled water in this order, and then dried in a clean oven at 125 °C for 10 min. (Octadecyl samples were extracted with hexane in a Soxhlet apparatus for 2 hours before the rinsing steps).

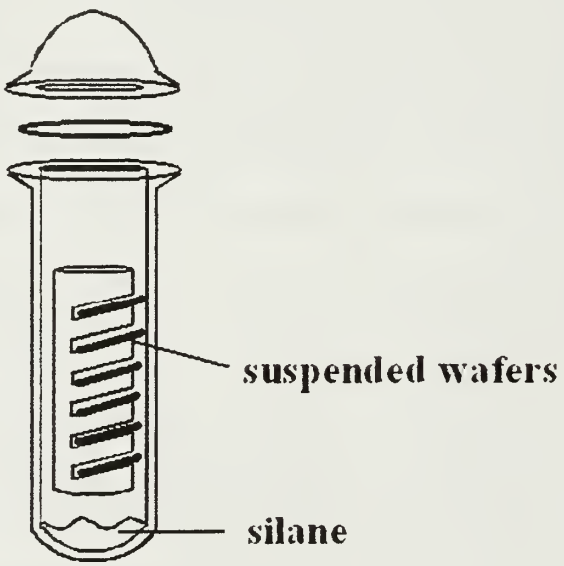

Figure 4.2 Schematic of the Schlenk tube used for the vapor phase reaction of alkylchlorosilanes , alkylethoxysilanes and hydridosilanes

Silicon wafers were also treated in the same way as above as control experiments.

4.2.3 Reaction of Chromium Surfaces with Octadecyltrichlorosilanes in Solution

Chromium wafers were cleaned as described above. The wafers were immediately placed into the reaction flask. The reaction flask was similar to the one that was used for the vapor phase reactions with the exception that the top included a 4 mm Teflon stopcock and joint capped with a rubber septum to facilitate cannulation and additions via syringe under an inert atmosphere. Clean wafers were covered with anhydrous toluene (10-15 mL) containing ethyldiisopropylamine (EDIPA) (0.17 mL; 10^{-3} mol). Octadecyltrichlorosilane (0.5 mL) was added via syringe. The reaction tube was placed in an oil bath and heated to 65-70 ^{o}C for 3 days or as otherwise noted. After the reaction, the samples were extracted with hexane in a Soxhlet apparatus for 2 hours and the wafers were rinsed with toluene, 2-propanol, ethanol, ethanol-water (1:1), and distilled water in this order, and then dried in a clean oven at 125 ^{o}C for 10 min. Silicon wafers were also treated in the same way as above as control experiments.

4.2.4 Reaction of Chromium Surfaces with Hydridosilanes in the Vapor Phase

Chromium wafers were cleaned as described above. The wafers were immediately placed in the reaction tube containing the hydridosilane of choice. Samples were placed in a custom-made wafer holder and suspended in a Schlenk tube containg 1 mL of silane (Figure 4.2). There was no contact between the silane and the silicon substrates. The reaction tube was placed in an oil bath and heated to 65-70 ^{o}C for 3

days. After the reaction, the wafers were rinsed with heptane, methylene chloride, ethanol, acetone and water, and then dried in a clean oven at 125 °C for 10 min.

4.2.5 Reaction of Chromium Wafers with Hydridosilanes in Solution

Chromium wafers were cleaned as described above. The wafers were immediately placed into the reaction flask. The reaction flask was similar to the one that was used for the vapor phase reactions with the exception that the top included a 4 mm Teflon stopcock and joint capped with a rubber septum to facilitate cannulation and additions via syringe under an inert atmosphere. Anhydrous heptane (~25 mL) was cannulated into the reaction tube and the hydridosilane (1 mL) of choice was added via syringe. The reaction tube was placed in an oil bath and heated to 65-70 °C for 3 days, unless otherwise noted. After the reaction, the wafers were rinsed with heptane, methylene chloride, ethanol, acetone, and distilled water in this order, and then dried in a clean oven at 125 °C for 10 min.

4.3 Results and Discussion

4.3.1 Reaction of Chromium Surfaces with Alkylchlorosilanes

Reaction of chromium surfaces with alkylchlorosilanes were studied in the vapor phase at 65-70 °C and in toluene in the presence of an amine catalyst at 65-70 °C. Toluene was chosen because toluene was reported[5,30] to prepare monolayers, oligomeric layers and polymeric layers on silicon surfaces with alkylchlorosilanes and alkylethoxysilanes. Ethyldiisopropylamine (EDIPA) was chosen as a base to prevent the silylation of the amine, which can take place with less sterically congested amines.

Silicon surfaces were also modified with alkylchlorosilanes using the same conditions to compare the results. Two kinds of mono-, di- and trichloroalkylsilanes were used to modify chromium surfaces in the vapor phase. Water contact angle data for covalently attached layers derived from alkylchlorosilanes (in solution and in the vapor phase) on chromium and silicon surfaces are shown in table 4.1. Octadecyltrichlorosilane was the only reagent used for the modification of the chromium surface in solution. Octadecyltrichlorosilane-derived layers on chromium (prepared either in the vapor phase or in toluene) have similar water contact angle values as octadecylchlorosilane-derived layers on silicon. Contact angle values of octadecyltrichlorosilane-derived layers on chromium (prepared either in the vapor phase or in toluene) are lower than the best self-assembled, most-close packed monolayers reported in the literature[30,31,40]. In the self-assembled monolayers, water interacts only with methyl groups on the surface. In octadecylchlorosilane-derived monolayers on chromium, the water interacts with a mixture of methyl and methylene groups. The composition of methyl and methylene groups can be calculated by the Israelachvilli-Gee equation (Equation 1).

$$(1+\cos\theta)^2 = f_1(1+\cos\theta_1)^2 + f_2(1+\cos\theta_2)^2$$

$$f_1 + f_2 = 1 \qquad (1)$$

The surfaces prepared from octadecyltrichlorosilanes on chromium can be treated as a mixture of methyl and methylene groups (contact angle of pure methyl and methylene surfaces are θ_1=110° and θ_2=94°, respectively. Equation (1) gives a mixture of 65% methyl and 35% methylene groups for the advancing angle of 103° (advancing contact angle of octadecyltrichlorosilane-derived layers on chromium).

alkylchlorosilane	conditions	on Cr	on Si
		Water Contact angle ($\theta_A/\theta_R(^o)$)	
n-$C_{18}H_{37}SiCl_3$	Vapor Phase, 70 °C 3days, O_2 plasma	105/83	103/87
n-$C_{18}H_{37}SiCl_3$	Toluene,EDIPA, 70 °C 3days, O_2 plasma	103/80	103/87
n-$C_8H_{17}SiCl_3$	Vapor Phase, 70 °C 3days, O_2 plasma	110/84	107/93
n-$C_8H_{17}CH_3SiCl_2$	Vapor Phase, 70 °C 3days, O_2 plasma	86/48	100/88
n-$C_6H_{13}CH_3SiCl_2$	Vapor Phase, 70 °C 3days, O_2 plasma	82/38	97/89
n-$C_{18}H_{37}(CH_3)_2SiCl$	Vapor Phase, 70 °C 3days, O_2 plasma	76/48	103/88
n-$C_8H_{37}(CH_3)_2SiCl$	Vapor Phase, 70 °C 3days, O_2 plasma	97/81	100/92

Table 4.1 Water contact angle data (θ_A/θ_R) in degrees (deg) for silicon and chromium surfaces treated with alkylchlorosilanes

The chromium surfaces prepared by the reaction of octyltrichlorosilane have a higher advancing contact angle value than the silicon surfaces prepared by the reaction of octyltrichlorosilane. The advancing contact angle value of octyltrichlorosilane-derived layers on chromium ($110^o/84^o$) is as high as the values of self assembled monolayers reported in the literature ($110^o/95^o$)[30]. The higher hysteresis can be due to molecular scale roughness and the rigidity of the layer that is a result of a crosslinked structure that the trifunctional reagents can form. Alkylmethyldichlorosilane and alkyldimethylchlorosilanes-derived layers show lower contact angle values on chromium than silicon. The layers are disordered and water penetrates the layers and interacts with the surface silanols.

Ellipsometry was attempted to measure the thickness of the layers on chromium surfaces. Unfortunately the results obtained were variable and inconsistent with the XPS data. Some of the surfaces showed zero thickness.

Alkylchlorosilane	Conditions	XPS Atomic (%)[a]			
		Si	C	Cr	O
chromium surface	O_2 plasma cleaned	~0	17.90	33.50	48.60
		~0	9.60	41.40	49.00
n-$C_{18}H_{37}SiCl_3$	Vapor Phase. 70 °C	12.10	51.30	4.50	32.10
	3days, O_2 plasma	12.10	26.30	11.00	49.60
n-$C_{18}H_{37}SiCl_3$	Toluene.EDIPA. 70 °C	3.45	43.10	16.55	36.85
	3days. O_2 plasma	2.25	27.55	25.85	44.70
n-$C_8H_{17}SiCl_3$	Vapor Phase. 70 °C	14.20	54.10	2.65	29.05
	3days. O_2 plasma	10.35	41.80	9.75	38.05
n-$C_8H_{17}CH_3SiCl_2$	Vapor Phase. 70 °C	4.60	48.90	15.30	31.20
	3days. O_2 plasma	2. 30	35.70	24.25	37.75
n-$C_6H_{13}CH_3SiCl_2$	Vapor Phase. 70 °C	3.35	34.55	23.00	39.15
	3days. O_2 plasma	3.05	19.00	32.60	45.35
n-$C_{18}H_{37}(CH_3)_2SiCl$	Vapor Phase. 70 °C	<.1	20.45	31.75	47.80
	3days. O_2 plasma	<.1	14.70	35.25	50.00
n-$C_8H_{37}(CH_3)_2SiCl$	Vapor Phase. 70 °C	0.35	20.75	29.70	49.15
	3days. O_2 plasma	0.40	19.45	33.75	51.45

[a] Upper rows are 15° takeoff angle data and lower rows are 75° data.

Table 4 2 XPS analysis of alkylchlorosilane-derived layers on chromium surfaces

Table 4.2 shows XPS data for alkylchlorosilane layers on chromium surfaces. The chromium surfaces prepared with alkylmethyldichorosilanes and alkyltrichlorosilanes all show an increase in carbon content and decrase in chromium surfaces. due to the layer formation. Also an appearance of a Si_{2p} peak is observed in the surfaces. The layers prepared with alkyldimethylchlorosilanes show a very small decrease in chromium content and a very small increase in carbon content. The XPS

results of the layers prepared from alkyldimethylchlorosilanes supports the idea that these layers are incomplete and the bonding densities in these layers are very low.

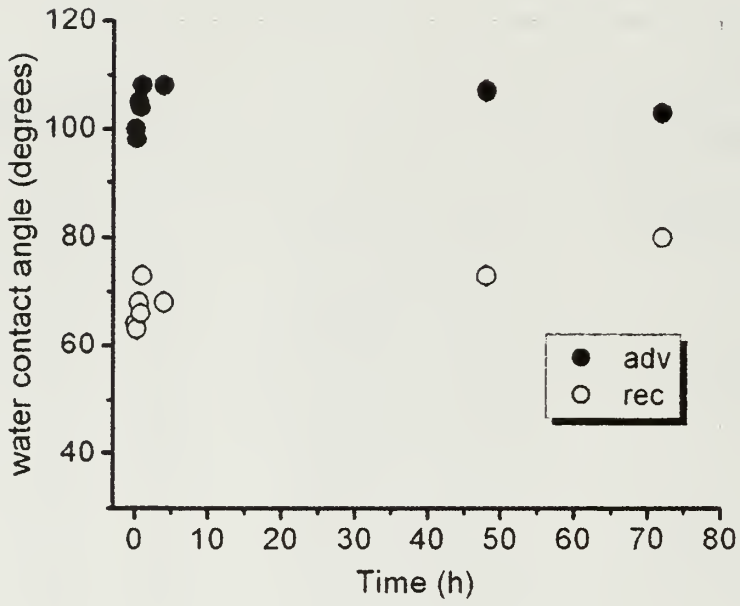

Figure 4.3 Water contact angle (θ_A/θ_B) data versus reaction time of grafted octadecyltrichlorosilane (Samples were prepared in toluene at 65-70 °C.) on chromium surfaces. The closed symbols are advancing angles and the open symbols are receding angles

The kinetics of the reaction of octadecyltrichlorosilane with chromium wafers in toluene in the presence of amine catalyst (EDIPA) at 65-70 °C was determined using contact angle measurements and XPS carbon content data. The data are plotted in figures 4.3 and 4.4. Each reaction time represents data from an individual sample. Significant hydrophobization occurs rapidly (to 98°/63°) after 15 min of reaction. The reaction is complete in an hour. At longer reaction times (72 h), a decrease in advancing contact angle data and an increase in receding contact angle data are observed. A decrease in advancing angle data can be due to the oxidative degradation of already modified layer.

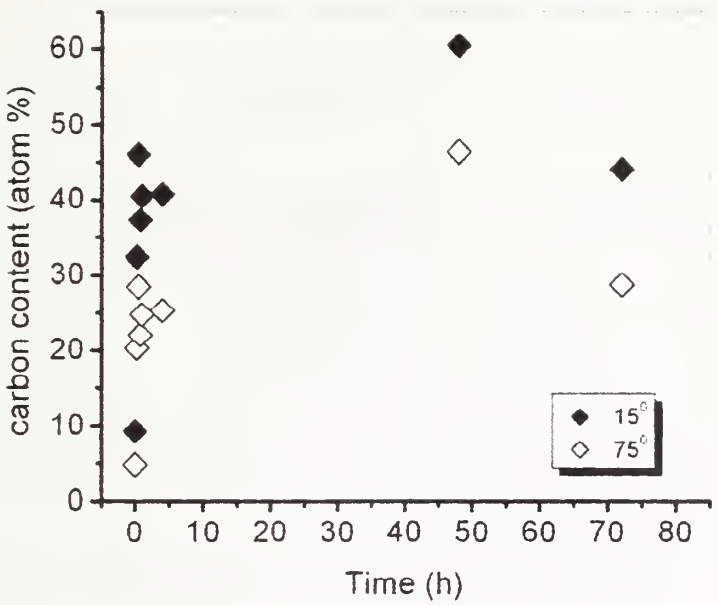

Figure 4.4 Carbon content (determined by XPS) for octadecyltrichlorosilane-derived chromium surfaces (♦, 15° take off angle. ◊, 75° take off angle) as a function of reaction time (Samples were prepared in toluene in the presence of EDIPA at 65-70 °C.)

Figure 4.4 shows carbon content (determined from XPS) for octadecytrichlorosilane-derived chromium surfaces at 15° and 75° take off angles as a function of reaction time. Carbon content increases as the reaction time increases until 48 hours. After 48 hours. a decrease in carbon content is observed. XPS data is consistent with the contact angle data. supporting the oxidative degradation of the already modified layer at longer reaction times.

4.3.2 Reaction of Chromium Surface with Alkylethoxysilanes.

The reactions of chromium surfaces with alklyldiethoxysilanes and

alkylethoxysilane	conditions	on Cr	on Si
		Water Contact angle (θ_A/θ_R (°))	
n-$C_{18}H_{37}Si(OC_2H_3)_3$	Vapor Phase, 70 °C 3days, O_2 plasma	100/77	101/83
n-$C_8H_{17}Si(OC_2H_3)_3$	Vapor Phase, 70 °C 3days, O_2 plasma	100/83	92/78
n-$C_3H_7Si(OC_2H_3)_3$	Vapor Phase, 70 °C 3days, O_2 plasma	98/62	83/72
n-$C_{18}H_{37}MeSi(OC_2H_3)_2$	Vapor Phase, 70 °C 3days, O_2 plasma	101/80	99/83

Table 4.3 Water contact angle data (θ_A/θ_R) in degrees (deg) for silicon and chromium surfaces treated with alkylethoxysilanes in the vapor phase

alkylethoxysilane	conditions	XPS Atomic (%)[a]			
		Si	C	Cr	O
chromium surface	O_2 plasma cleaned	~0	17.90	33.50	48.60
		~0	9.60	41.40	49.00
n-$C_{18}H_{37}Si(OC_2H_3)_3$	Vapor Phase, 70 °C	5.25	56.70	8.55	29.55
	3days, O_2 plasma	4.25	37.55	17.50	40.65
n-$C_8H_{17}Si(OC_2H_3)_3$	Vapor Phase, 70 °C	8.85	18.45	16.45	56.00
	3days, O_2 plasma	5.95	11.85	24.85	57.35
n-$C_{18}H_{37}MeSi(OC_2H_3)_2$	Vapor Phase, 70 °C	7.25	68.75	4.45	19.55
	3days, O_2 plasma	5.7	51.20	12.25	30.85
n-$C_3H_7Si(OC_2H_3)_3$	Vapor Phase, 70 °C	4.30	22.90	23.80	49.00
	3days, O_2 plasma	2.55	16.60	29.95	50.95

[a] Upper rows are 15° takeoff angle data and lower rows are 75° data.

Table 4.4 XPS analysis of alkylethoxysilane-derived layers on chromium surfaces

alkyltriethoxysilanes were studied in the vapor phase at 65-70 °C. The silicon surfaces are also modified in the same way to compare the results. The water contact angle data for alkylethoxysilane-derived layers on chromium and silicon are shown in table 4.3.

Alkylethoxysilane-derived layers on chromium show higher contact angle values than the alkylethoxysilane–derived layers on silicon. Hysterises is consistently is higher for the chromium surfaces prepared from alkylethoxysilanes than the silicon surfaces. The surfaces were also characterized by XPS. Table 4.4 shows XPS atomic composition data of chromium surfaces prepared from alkylethoxysilanes. After silanization, all the surfaces show an increase in carbon content and a decrease in chromium content due to layer formation. The appearance of silicon on the surfaces is also observed after reaction, which also supports layer formation.

4.3.3 Reaction of Chromium Surfaces with Hydridosilanes

Reaction of chromium surfaces with hydridosilanes was studied in the vapor phase at 65-70 °C for 3 days and in heptane at 65-70 °C for 3 days. Three kinds of mono- and trihydridosilanes and two kinds of dihydridosilanes were used to modify chromium surfaces in the vapor phase and in heptane. Water contact angle data for covalently attached layers from hydridosilanes in the heptane and in the vapor phase are shown in table 4.5 and 4.6, respectively. All mono-, di- and tri-hydridosilanes react with chromium surfaces as assessed by high water contact angle values (Table 4.5 and 4.6). Contact angle values for the trihydridosilane-derived layer prepared by solution reaction increase with chain length. In the case of the hexylsilane-derived layer, water probably penetrates the layer and interacts with the surface –OH groups. In the vapor phase reactions, contact angles for hydridosilane-derived layers decrease with chain length.

hydridosilanes	Reaction conditions	Water Contact angle (θ_A/θ_R (°))
n-$C_{18}H_{37}SiH_3$	Heptane, 70 °C 3days, O_2 plasma	108/85
n-$C_8H_{17}SiH_3$	Heptane, 70 °C 3days, O_2 plasma	95/58
n-$C_6H_{13}SiH_3$	Heptane, 70 °C 3days, O_2 plasma	86/42
$(C_6H_5)_2SiH_2$	Heptane, 70 °C 3days, O_2 plasma	93/61
$C_6H_5CH_3SiH_2$	Heptane, 70 °C 3days, O_2 plasma	96/55
$C_7H_7(CH_3)_2SiH$	Heptane, 70 °C 3days, O_2 plasma	77/24
$(n\text{-}C_6H_{13})_3SiH$	Heptane, 70 °C 3days, O_2 plasma	103/60
$(i\text{-}C_3H_7)_3SiH$	Heptane, 70 °C 3days, O_2 plasma	92/52

Table 4.5 Water contact angle data (θ_A/θ_R) in degrees (deg) for chromium surfaces treated with hydridosilanes in solution

hydridosilanes	conditions	Water Contact angle (θ_A/θ_R (°))
n-$C_{18}H_{37}SiH_3$	Vapor Phase, 70 °C 3days, O_2 plasma	101/87
n-$C_8H_{17}SiH_3$	Vapor Phase, 70 °C 3days, O_2 plasma	103/88
n-$C_6H_{13}SiH_3$	Vapor Phase, 70 °C 3days, O_2 plasma	108/81
$(C_6H_5)_2SiH_2$	Vapor Phase, 70 °C 3days, O_2 plasma	93/62
$C_6H_5CH_3SiH_2$	Vapor Phase, 70 °C 3days, O_2 plasma	94/63
$C_7H_7(CH_3)_2SiH$	Vapor Phase, 70 °C 3days, O_2 plasma	89/50
$(n\text{-}C_6H_{13})_3SiH$	Vapor Phase, 70 °C 3days, O_2 plasma	90/50
$(i\text{-}C_3H_7)_3SiH$	Vapor Phase, 70 °C 3days, O_2 plasma	94/64

Table 4.6 Water contact angle data (θ_A/θ_R) in degrees (deg) for chromium surfaces treated with hydridosilanes in the vapor phase

Hydridosilane	Reaction conditions	XPS Atomic (%)[a]			
		Si	C	Cr	O
chromium surface	O_2 plasma cleaned	~0	17.90	33.50	48.60
		~0	9.60	41.40	49.00
$n\text{-}C_{18}H_{37}SiH_3$	Heptane, 70 °C	3.45	43.10	16.55	36.85
	3days, O_2 plasma	2.25	27.55	26.85	44.70
$n\text{-}C_8H_{17}SiH_3$	Heptane, 70 °C	1.80	35.20	21.00	42.00
	3days, O_2 plasma	0.90	18.10	33.30	47.70
$n\text{-}C_6H_{13}SiH_3$	Heptane, 70 °C	3.40	41.20	15.65	41.00
	3days, O_2 plasma	3.20	25.25	28.25	43.35
$(C_6H_5)_2SiH_2$	Heptane, 70 °C	2.50	41.20	18.20	41.20
	3days, O_2 plasma	1.90	27.30	27.00	43.80
$C_6H_5CH_3SiH_2$	Heptane, 70 °C	6.30	42.00	13.60	38.10
	3days, O_2 plasma	4.50	28.00	21.70	45.10
$C_7H_7(CH_3)_2SiH$	Heptane, 70 °C	1.40	52.60	10.70	35.30
	3days, O_2 plasma	0.80	34.10	23.00	42.00
$(n\text{-}C_6H_{13})_3SiH$	Heptane, 70 °C	0.90	37.80	21.30	39.90
	3days, O_2 plasma	1.90	24.30	28.50	45.30
$(i\text{-}C_3H_7)_3SiH$	Heptane, 70 °C	6.20	28.40	18.30	47.10
	3days, O_2 plasma	2.80	16.90	28.30	51.00

[a] Upper rows are 15° takeoff angle data and lower rows are 75° data.

Table 4.7 XPS analysis of hydridosilane-derived layers prepared in solution on chromium surfaces

Hexylsilane layers prepared from vapor phase reactions exhibit contact angle values of 108°/81°, indicating that water interacts mostly with methyl groups.

Tables 4.7 and 4.8 show XPS atomic composition data prepared by reaction of hydridosilanes in heptane and in the vapor phase, respectively. After silanization, all surfaces show an increase in carbon content and a decrease in chromium content due to layer formation. An appearance of silicon on most of the surfaces is observed after the reactions.

Hydridosilane	Reaction conditions	XPS Atomic (%)[a]			
		Si	C	Cr	O
chromium surface	O_2 plasma cleaned	~0	17.90	33.50	48.60
		~0	9.60	41.40	49.00
n-$C_{18}H_{37}SiH_3$	Vapor Phase, 70 °C	5.90	57.85	8.45	27.80
	3days, O_2 plasma	4.75	36.95	18.65	39.75
n-$C_8H_{17}SiH_3$	Vapor Phase, 70 °C	10.70	70.90	0.40	17.90
	3days, O_2 plasma	10.90	65.10	1.10	22.90
n-$C_6H_{13}SiH_3$	Vapor Phase, 70 °C	13.60	46.90	2.50	37.00
	3days, O_2 plasma	12.50	26.00	12.50	46.90
$(C_6H_5)_2SiH_2$	Vapor Phase, 70 °C	2.50	34.25	22.15	41.15
	3days, O_2 plasma	1.75	19.4	32.80	46.05
$C_6H_5CH_3SiH_2$	Vapor Phase, 70 °C	4.95	41.85	14.65	38.55
	3days, O_2 plasma	2.90	26.45	25.35	45.25
$C_7H_7(CH_3)_2SiH$	Vapor Phase, 70 °C	0.3	26.00	27.50	46.25
	3days, O_2 plasma	0.7	14.95	36.30	48.00
$(n\text{-}C_6H_{13})_3SiH$	Vapor Phase, 70 °C	<.1	26.25	28.15	45.55
	3days, O_2 plasma	<.1	17.4	34.30	46.95
$(i\text{-}C_3H_7)_3SiH$	Vapor Phase, 70 °C	6.95	27.30	18.55	47.15
	3days, O_2 plasma	4.15	16.05	30.00	49.75

[a] Upper rows are 15° takeoff angle data and lower rows are 75° data.

Table 4.8 XPS analysis of hydridosilane-derived layers prepared in the vapor phase on chromium surfaces

Octadecylsilane was chosen to study the kinetics of solution phase reaction. The kinetics was followed by water contact angle (figure 4.5) and carbon content (determined by XPS, at 15° and 75°) (figure 4.6). Significant hydrophobization occurs in an hour, but the reaction is not complete until 24 hours. The reaction of chromium surfaces with octadecyltrichlorosilane is faster than with octadecylsilane. Decrease in water contact angle values at longer reaction times is not observed in the reaction of chromium surfaces with octadecylsilane as it was in octadecytrichorosilane-derived layers due the oxidation of already formed layers.

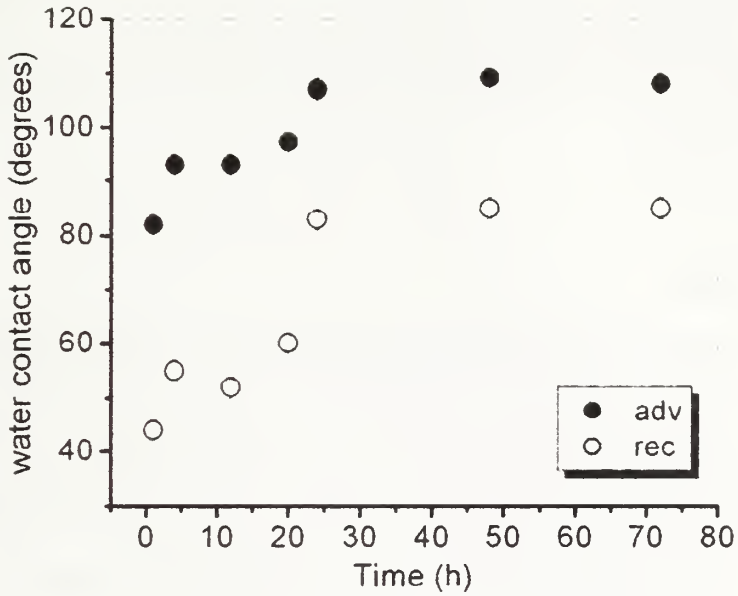

Figure 4.5 Water contact angle (θ_A/θ_R) data versus reaction time of grafted octadecylsilane (Samples were prepared in heptane at 70 °C.) on chromium surfaces. The closed symbols are advancing angles and the open symbols are receding angles.

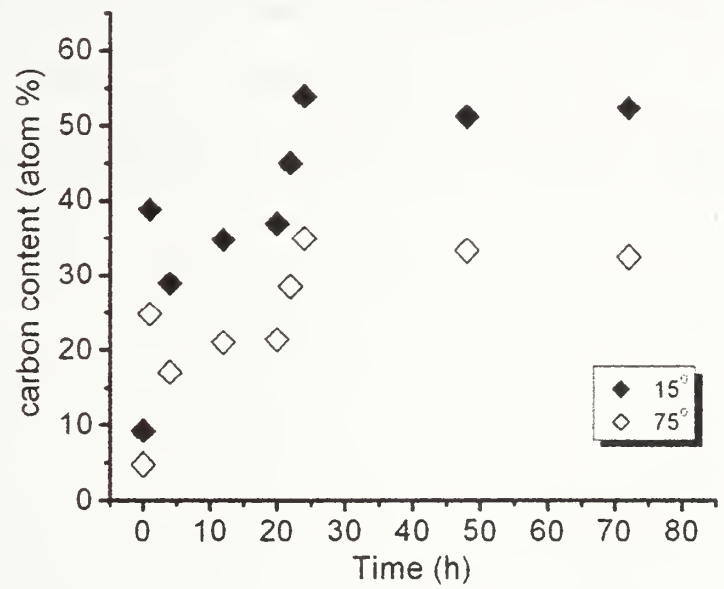

Figure 4.6 Carbon content (determined by XPS) for octadecylsilane-derived chromium surfaces (♦, 15° take off angle, ◊, 75° take off angle) as a function of reaction time (Samples were prepared in heptane at 65-70 °C)

Figure 4.6 shows carbon content (determined by XPS) for chromium surfaces prepared by the reaction of octadecylsilane in heptane at 65-70 ^{0}C as a function of reaction time. Carbon content increases as the reaction time increases and reaches a plateau at 24 hours.

4.4 Conclusions

In this chapter, it is shown that alkylchlorosilanes and hydridosilanes react with chromium surfaces in solution and in the vapor phase at elevated temperatures. Alkylethoxysilanes also react with chromium surfaces in the vapor phase. The layers all show high contact angle results. The XPS results in all cases show an increase in carbon content and a decrease in chromium content due to the layer formation. The kinetics of octadecylchlorosilane in toluene in the presence of amine at 65-70 ^{o}C shows that the reaction is fast and complete in an hour as assessed by contact angle measurements, whereas the kinetics with octadecylsilane in heptane show that the reaction is not as fast as the reaction of octadecylchlorosilane in toluene in the presence of amine at 65-70 ^{o}C and the reaction is complete in 2 days as assessed by contact angle measurements.

4.5 References

(1) Plueddemann. E. P. *Silane Coupling Agents*. Plenum Press: New York. 1991.

(2) Chen. W.: Fadeev. A. Y.: Hsieh. M. C.: Oner. D.: Youngblood. J.: McCarthy. T. J. *Langmuir* **1999**. *15*. 3395-3399.

(3) Sagiv. J. *Israel Journal of Chemistry* **1979**. *18*. 346-353.

(4) Sagiv. J. *Journal of the American Chemical Society* **1980**. *102*. 92-98.

(5) Fadeev. A. Y.: McCarthy. T. J. *Langmuir* **1999**. *15*. 3759-3766.

(6) Tada. H.: Nagayama. H. *Langmuir* **1994**. *10*. 1472-1476.

(7) Korosi. G.: Kovats. E. S. *Colloids and Surfaces* **1981**. *2*. 315-355.

(8) Brzoska. J. B.: Benazouz. I.: Rondelez. F. *Langmuir* **1994**. *10*. 4367-4373.

(9) Fadeev. A. Y.: Soboleva. O. A.: Summ. B. D. *Colloid Journal* **1997**. *59*. 222-225.

(10) Dulcey. C. S.: Georger. J. H.: Krauthamer. V.: Stenger. D. A.: Fare. T. L.: Calvert. J. M. *Science* **1991**. *252*. 551-554.

(11) Ross. C. B.: Sun. L.: Crooks. R. M. *Langmuir* **1993**. *9*. 632-636.

(12) Xia. Y. N.: Zhao. X. M.: Whitesides. G. M. *Microelectronic Engineering* **1996**. *32*. 255-268.

(13) Jeon. N. L.: Finnie. K.: Branshaw. K.: Nuzzo. R. G. *Langmuir* **1997**. *13*. 3382-3391.

(14) Allara. D. L. *Biosensors & Bioelectronics* **1995**. *10*. 771-783.

(15) Bain, C. D.; Whitesides, G. M. *Journal of the American Chemical Society* **1988**, *110*, 6560-6561.

(16) Bain, C. D.; Whitesides, G. M. *Journal of the American Chemical Society* **1988**, *110*, 5897-5898.

(17) Nuzzo, R. G.; Allara, D. L. *Journal of the American Chemical Society* **1983**, *105*, 4481-4483.

(18) Nuzzo, R. G.; Fusco, F. A.; Allara, D. L. *Journal of the American Chemical Society* **1987**, *109*, 2358-2368.

(19) Troughton, E. B.; Bain, C. D.; Whitesides, G. M.; Nuzzo, R. G.; Allara, D. L.; Porter, M. D. *Langmuir* **1988**, *4*, 365-385.

(20) Jun, K.; Zhu, X. Y.; Hsu, J. W. P. *Langmuir* **2000**, *22*, 3627-3636-3632.

(21) Allara, D. L.; Nuzzo, R. G. *Langmuir* **1985**, *1*, 45-52.

(22) Allara, D. L.; Nuzzo, R. G. *Langmuir* **1985**, *1*, 52-66.

(23) Bigelow, W. C.; Pickett, D. L.; Zisman, W. A. *Journal of Colloid Science* **1946**, *1*, 513-538.

(24) Fadeev, A. Y.; McCarthy, T. J. *Journal of the American Chemical Society* **1999**, *121*, 12184-12185.

(25) Fadeev, A. Y.; Helmy, R.; Marcinko, S. *Langmuir* **2002**, *18*, 7521-7529.

(26) Helmy, R.; Fadeev, A. Y. *Langmuir* **2002**, *18*, 8924-8928.

(27) Helmy, R.; Wenslow, R. W.; Fadeev, A. Y. *Journal of the American Chemical Society* **2004**, *126*, 7595-7600.

(28) Gawalt, E. S.; Avaltroni, M. J.; Koch, N.; Schwartz, J. *Langmuir* **2001**, *17*, 5736-5738.

(29) Tosatti, S.; Michel, R.; Textor, M.; Spencer, N. D. *Langmuir* **2002**, *18*, 3537-3548.

(30) Fadeev, A. Y.; McCarthy, T. J. *Langmuir* **2000**, *16*, 7268-7274.

(31) Wasserman, S. R.; Tao, Y. T.; Whitesides, G. M. *Langmuir* **1989**, *5*, 1074-1087.

(32) Cao, T. B.; Chen, J. Y.; Yang, C. H.; Cao, W. X. *New Journal of Chemistry* **2001**, *25*, 305-307.

(33) Wasserman, S. R.; Whitesides, G. M.; Tidswell, I. M.; Ocko, B. M.; Pershan, P. S.; Axe, J. D. *Journal of the American Chemical Society* **1989**, *111*, 5852-5861.

(34) Boerio, F. J.; Boerio, J. P.; Bozian, R. C. *Applied Surface Science* **1988**, *31*, 42-58.

(35) Arnebrant, T.; Backstrom, K.; Jonsson, B.; Nylander, T. *Journal of Colloid and Interface Science* **1989**, *128*, 303-312.

(36) Itoh, E.; Kokubo, H.; Shouriki, S.; Iwamoto, M. *Journal of Applied Physics* **1998**, *83*, 372-376.

(37) Iwamoto, M.; Yoneda, Y.; Fukuda, A. *Japanese Journal of Applied Physics Part 1-Regular Papers Short Notes & Review Papers* **1992**, *31*, 3671-3674.

(38) Clot, O.; Wolf, M. O. *Langmuir* **1999**, *15*, 8549-8551.

(39) Hild, R.; David, C.; Muller, H. U.; Volkel, B.; Kayser, D. R.; Grunze, M. *Langmuir* **1998**, *14*, 342-346.

(40) Ulman, A. *Chemical Reviews* **1996**, *96*, 1533-1554.

CHAPTER 5

REACTION OF HYDRIDOSILANES WITH OXIDIZED SILICON

5.1 Introduction

Modification of surface properties of inorganic materials with reactive organosilanes is a process that is widely used in both research and technology.[1-5] Organosilanes with the general formula (R_nSiX_{4-n}) (where X=Cl or OAlk or NMe_2) have been used to modify silicon.[6-12](R can be methyl group, long alkyl chains, perfluoroalkyl chains and other end-functionalized long chains.) Reports that have appeared used different reaction conditions (vapor phase and solution phase) and different substrates (silica. glass. quartz. silicon wafer).

It has been shown that the monofunctional organosilanes (having only one-hydrozable groups) give reproducible surface structures because there is only one type of grafting possible. covalent attachment to the surface by chemical bonds (Si_s-O-Si). The structure of these monolayers has been studied extensively for porous and nonporous highly dispersed silicas. The results of reaction conditions [13-17], bonded layer structure and dynamics[13-15.18-20], phase transitions of bonded layers[21-23] have been discussed in number of publications. Silica contains[24] ~5 silanol groups per $nm^2$and ~60% can react with alkyldimethylsilanes. The maximum bonding density of alkyldimethylsilyl groups is limited by the size of dimethylsilyl group and decreases slightly with larger alkyl groups[25]. The cross-sectional area of an alkyldimethyl group in a densely packed monolayer[13.25] is 32-38 $Å^2$. This value is almost the twice the area per alkyl chain in dense monolayers of self assembled alkyltrichlorosilane monolayers. (~20 $Å^2$).[11.26] The McCarthy group has reported detailed wettability studies of monolayers prepared with

monofunctional silanes.[9] Dense monolayers of monofunctional silanes project disordered alkyl chains toward the probe liquid. Water contact angles (θ_A/θ_B= ~105°/~94°) do not change as the alkyl chain length increases, indicating that water does not penetrate the monolayers.[9] Hydrophobization is achieved topologically, and monolayers prevent the water from penetrating and interacting with the residual silanols. The studies also indicate that the complete monolayers (of the same silane) can differ in bonding density depending on the reaction conditions.

Trifunctional silanes ($RSiX_3$) are more reactive than monofunctional silanes. They have the capability of polymerizing in the presence of water, which gives a number of possible structures. (These are discussed in the introduction section of Chapter 4.) The self assembly process of alkyltrichlorosilanes is well understood. The anchoring groups in self assembled monolayers (SAMs) are impelled together by strong lateral siloxane bonds and van der Waals interaction between the alkyl chains. The bonding with the surface is very small in self-assembled monolayers (SAMs) so monolayers of the same quality can be prepared on different substrates.[27,28] The structure of SAMs has been characterized by different techniques, and the highly ordered and densest monolayers contain closed-packed[27-31] 4.5-5 groups per nm^2. All chains attain vertical all-trans conformation. The water advancing and receding contact angles of SAMs derived from long-chain alkyl trichlorosilanes are reported as ~ 110-115° and ~100° respectively, indicating pure methyl–terminated surfaces.

Under certain conditions, trifunctional and difunctional silanes react with the surface silanol groups in a covalent attachment manner. The covalent attachment has been referred to as poor self-assembly due to its lower bonding density. Covalently

attached monolayers have been prepared with dry silica at elevated temperatures[32,33] and in the presence of amines at room[34,35] or elevated temperatures.[10,36] The McCarthy group has shown that the covalently attached monolayers (prepared by alkylmethyldichlorosilanes and alkyltrichlorosilanes with silicon wafers in toluene with base catalyst at elevated temperatures) are thinner than the fully stretched alkyl chains (SAMs) and the alkyl chains are disordered.[36] The average number of bonds with the silica surface per silane molecule is not completely clear yet in the covalently attachment process. According to the some characterization reports[1,23,34]. 1:1 (one Si_s-O-Si bond) as well as 1:2 (two Si_s-O-Si bonds) grafted structures are present on the on the surfaces but structures (1:3) with three Si_s-O-Si bonds (when trifunctional silanes are used) are not formed due to steric reasons.

Polymeric or oligomeric grafted layers were reported for the reaction of methyltrichlorosilanes[37] and dimethylchlorosilanes[38,39] with glass in the vapor phase. the reaction of alkylchlorosilanes with high surface area silicas[40]. and the reaction of alkyltrichlorosilanes and alkyldimethylchlorosilanes[10] (which have high vapor pressure) with silicon wafers in the vapor phase.

As society raises concerns about the environmental issues, research on the reducing the use of volatile compounds and the generation of aqueous waste become important. The McCarthy group[41] has reported modification of silica surfaces with alkylchlorosilane by using liquid and supercritical carbon dioxide as a solvent. Monochlorosilanes yielded monolayers; dichloro- and trichlorosilanes yielded oligomeric layers on the surfaces

	Contact angle ($\theta_A/\theta_R(^o)$)	Thickness (λ(Å))	reference
n-$C_8H_{17}SiCl_3$ Vapor Phase, 70 ^oC , 3 days (SiO_2)	111/97	22.3	[10]
n-$C_8H_{17}SiCl_3$ in liquid CO_2 at 1200 psi, 23 ^oC, 1 day (SiO_2)	107/90	21	[41]
n- $C_{18}H_{37}SiCl_3$ Vapor Phase, 70 ^oC , 3 days (SiO_2)	104/80	18.2	[10]
n-$C_8H_{17}SiCl_3$ toluene in EDIPA,70 ^oC, 3 days (SiO_2)	103/89	13.2	[10]
n-$C_{18}H_{37}SiCl_3$ toluene in EDIPA ,70 ^oC, 3 days (SiO_2)	103/85	20.1	[10]
n-$C_8H_{17}SiCl_3$ self assembly in CCl_4, 25 ^oC,1 hour(SiO_2)	110/95	16.5	[10]
n-$C_{18}H_{37}SiCl_3$ self assembly in CCl_4, 25 ^oC, 1 hour(SiO_2)	110/98	28.1	[10]
n-$C_8H_{17}SiCl_3$ in hexadecane or bicyclohexyl, 2 days (SiO_2)	-	14.8	[8]
n-$C_{18}H_{37}SiCl_3$ in hexadecane or bicyclohexyl, 2 days (SiO_2)	-	27.5	[8]
n-$C_8H_{17}SiCl_3$ in Isopar-g/CCl_4 (SiO_2)	111(static)	26	[42]

Table 5.1 Water contact angle and layer thickness data for $C_{18}H_{37}Si$ and $C_8H_{17}Si$ layers (supported on silicon oxide surfaces) reported in the literature

Table 5.1 shows the water contact angle and layer thickness data for $C_8H_{17}Si$ and $C_{18}H_{37}Si$ layers (supported on silicon dioxide) reported in the literature. The layer structure depends on the preparation method and reaction conditions. N-octyltrichlorosilane was shown to react with silica surfaces yielding oligomeric layers. covalently attached monolayers and SAMs. Covalently attached monolayers and SAMs are reported for the reaction of n-octadecyltrichlorosilane with silica surfaces.

Until now, modification of silicon surfaces with hydridosilanes has not been reported. In this chapter, the modification of oxidized silicon surfaces with mono- and trihydridosilanes under three different conditions (in vapor phase, in toluene and in $ScCO_2$) is described. The silylation of silica surfaces with hydridosilanes is illustrated below.

$$Si_{solid} - OH + R_{3-n}SiH_{n+1} \longrightarrow Si_{solid} - O - SiR_{3-n}H_n + H_2$$

5.1.1 Supercritical CO_2 ($ScCO_2$)

The diagram in figure 5.1 is a phase diagram of a pure substrate. The supercritical fluid (SCF)[43-46] is defined as a substance above its critical pressure (P_c) and critical temperature (T_c). In this region, the boundary between liquid and gas disappears. SCFs generally have gas-like diffusivity and have liquid like density. The density of SCFs can be adjusted by temperature and pressure. Carbon dioxide (CO_2) has a fairly low critical point at 31.1 °C and 72.8 atm. Its ability to achieve its supercritical state under mild conditions makes CO_2 a good candidate for fundamental research and applications of supercritical fluids. CO_2 is non-toxic, nonflammable, abundant and inexpensive. CO_2 can be recycled because it is gas at ambient conditions. CO_2 reduces the time

and cost of solvent separation and drying because after releasing CO_2, no solvent residue is left. CO_2 has a very high diffusivity, relatively low viscosity, and zero surface tension. A comparison of some physical properties among liquids, gases and supercritical fluids are listed in table 5.2. Even for liquid CO_2 at room temperature, the self-diffusivity is 10^{-3}-10^{-4} cm^2/sec, an order of magnitude higher than the diffusivity of solutes in normal liquids.[43]

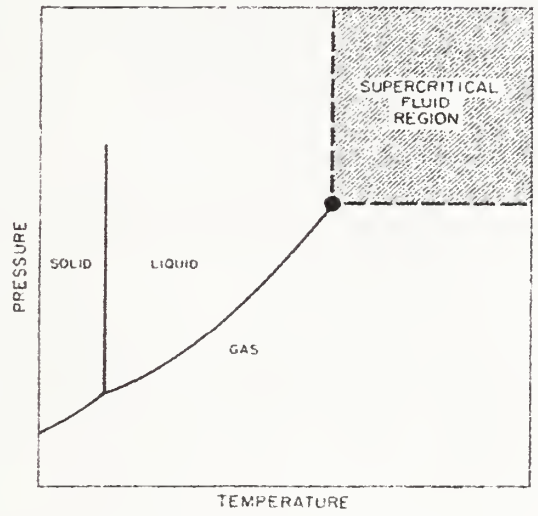

Figure 5.1 Phase diagram of a pure substance

	diffusivity (cm^2/sec)	viscosity (cps)	density (g/mL)	surface tension (dyn/cm)
Liquid	10^{-5}	1	1.0	20-50
Supercritical Fluid	10^{-3}	0.03	0.2-0.8	0
Gas	10^{-1}	10^{-5}	10^{-3}	-

Table 5.2 Physical properties comparison for liquids, gases and supercritical fluids[45]

CO_2 can dissolve many organic molecules to some extent but not most polar molecules and high molecular weight molecules. However by adding co-solvent and surfactants, the solubility of other molecules in CO_2 can be enhanced. $ScCO_2$ has a tunable solvent strength and by external control of temperature and pressure, molecules and fractions can be selectively dissolved or precipitated in $ScCO_2$

5.2 Experimental

5.2.1 Materials and Methods

All chemicals were used as received as unless noted otherwise. Toluene (HPLC), methylene chloride (HPLC), sulfuric acid, hydrogen peroxide (H_2O_2), sodium dichromate, ethanol and acetone were purchased from Fisher. All silane reagents, n-octadecylsilane (n-$C_{18}H_{37}SiH_3$), n-octylsilane (n-$C_8H_{17}SiH_3$), and tri-n-hexylsilane ($(C_6H_{13})_3SiH$) were purchased from Gelest. Anhydrous toluene was purchased from Aldrich. Water was purified using a Millipore Milli-Q system that involves reverse osmosis, ion exchange and filtration steps. Carbon dioxide (Coleman grade 99.99%, Merrian grade) was passed trough columns containing activated aluminum and copper catalyst (Engelhard Q-5) to remove water and oxygen respectively. A motorized syringe pump (ISCO model 100DM) was used to pressurize the carbon dioxide. Silicon wafers were obtained from International Wafer Service (<100>orientation, P/B doped, 20-40 Ω cm, thickness 450-575 μm). Ellipsometric measurements were done using a Rudolph Auto El-II automatic ellipsometer. The light source is He-Ne laser($\lambda = 623.8$ nm), the incident angle is 70° and the compensator is-45°. Measurements were performed on three to five spots on each sample. The thicknesses was calculated by transparent double layer model using a dafBM software (silicon substrate / silicon oxide / alkylsilanelayer /air) with the following parameters: silicon substrate $n_s = 3.858$, $k_s = 0.018$ (imaginary part of the refractive index); air, $n_o = 1$; alkylsilane layer, $n_1 = 1.45$; silicon oxide layer: $n_2 = 1.462$. Contact angle measurements were made with a Ramè-Hart telescopic goniometer and a Gilmont syringe with a 24-gauge flat-tipped needle. Water was used as the probe

liquid. Advancing and receding contact angle was recorded while the water was added and withdrawn from the drop, respectively. The values are averages of 4-5 measurements made on different areas of samples.

5.2.2 Pretreatment of Silicon Substrates

Silicon substrates used in this study were cleaned by two different methods. In the first method, wafers were cleaned by a Harrick Scientific O_2 plasma cleaner at high power settings for 5 minutes prior to use. The oxide layer on the wafers after plasma treatment was determined to be ~25 Å by ellipsometry. In the second method, the wafers were held in a custom designed holder and were rinsed with water and put in a freshly prepared mixture of 7 parts of concentrated sulfuric acid containing dissolved sodium dichromate (~3-5 wt %) and 3 parts of 30% hydrogen peroxide. Upon preparation, the solution turns from red-brown to green, warms to 80-90 ^{0}C, and foams extensively due to the formation of oxygen and ozone. Wafers are submerged in solution overnight, rinsed with copious water and placed in oven at 125 ^{o}C for 1-2 hours. Silanizations were carried out immediately after treating wafers in this fashion. The oxide layer on the wafers after this treatment was determined to be 22 Å by ellipsometry.

5.2.3 Reaction of Silicon Wafers with Hydridosilanes in the vapor phase

Silicon wafers were cleaned as described above. The wafers were immediately placed in the reaction tube containing the hydridosilane of choice. Samples were placed in a custom-made wafer holder and suspended in a Schlenk tube containing 1 mL of silane.(Figure 5.2) There was no contact between the silane and the silicon substrates. The reaction tube was placed in an oil bath and heated to 65-70 ^{o}C for a day. After the

reaction, the wafers were rinsed with toluene, methylene chloride, ethanol and distilled water in this order, and then dried in a clean oven at 125 °C for 10 minutes.

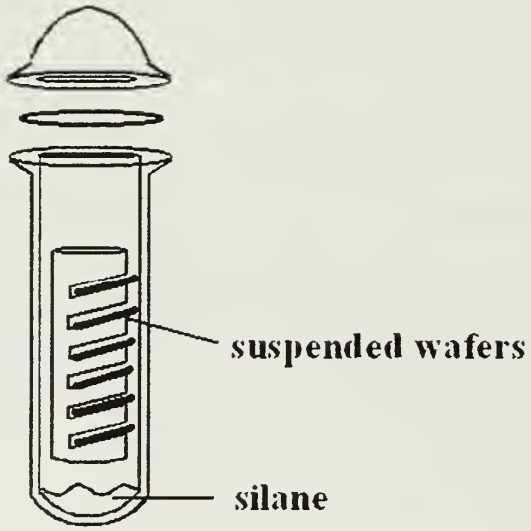

Figure 5.2 Schematic of the Schlenk tube used for the vapor phase reaction of hydridosilanes.

5.2.4 Reaction of Silicon wafers with Hydridosilanes in Solution

Silicon wafers were cleaned as described above. The wafers were immediately placed into the reaction flask. The reaction flask was similar to the one that was used for the vapor phase reactions with the exception that the top included a 4 mm Teflon stopcock and joint capped with a rubber septum to facilitate cannulation and additions via syringe under an inert atmosphere. Anhydrous toluene (~25 mL) was cannulated into the reaction tube and the hydridosilane (1 mL) of choice was added via syringe. The reaction tube was placed in an oil bath and heated to 65-70 °C for 3 days, unless otherwise noted. After the reaction the wafers were rinsed with toluene, methylene chloride, ethanol and distilled water in this order, and then dried in a clean oven at 125 °C for 10 minutes.

5.2.5 Reaction of Silicon wafers with Hydridosilanes in $ScCO_2$

Silicon wafers were cleaned as described above. Wafers were placed in a 8.5 mL stainless steel high-pressure vessel that contains the hydridosilane (1 mL)of choice. The vessel was filled through a needle valve with ~5 g of CO_2 (40 °C, 1385 psi). The vessels were placed in oil bath at 40 °C for 3 days unless otherwise noted. After the desired time, the silane/CO_2 was vented into ethanol. The wafers were removed and rinsed with toluene, methylene chloride, ethanol and distilled water in this order, and then dried in a clean oven at 125 °C for 10 minutes.

5.3 Results and Discussion

5.3.1 Reaction of Silicon surfaces with Tri-n-Hexylsilane

Chemically grafted monolayers of tri-n-hexylsilane were prepared by reaction of tri-n-hexylsilane with silicon wafers under three conditions: (1) in the vapor phase at 65-70 °C, (2) in toluene at 65-70 °C and (3) in $ScCO_2$ at 40 °C (1385 psi).(Figure 5.3) The surfaces were cleaned using two different methods: (1) O_2 plasma for 5 minutes and (2) piranha solution overnight.

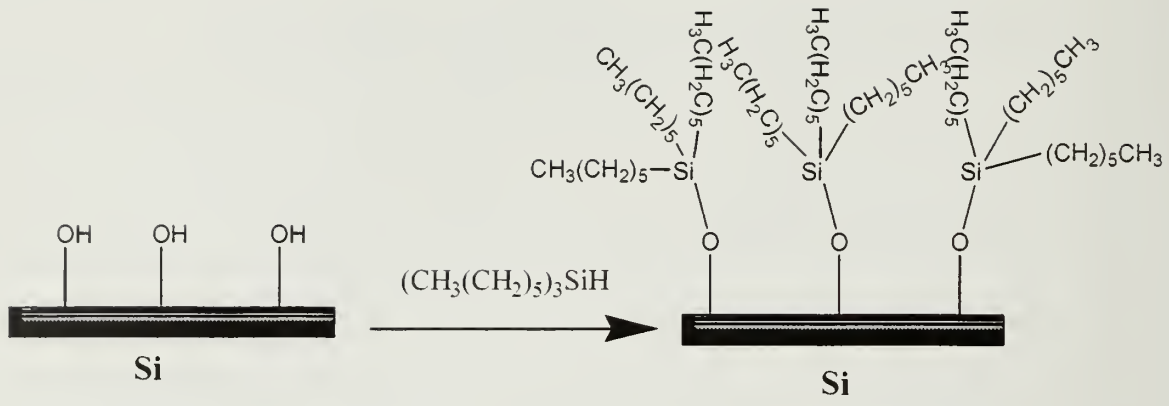

Figure 5.3 Schematic representation of the reaction of tri-n-hexylsilane with the Si/SiO_2

Table 5.3 shows water contact angle data and layer thickness data of tri-n-hexylsilane-derived monolayers on silicon prepared under different conditions . Tri-n-hexylsilane reacts with silicon surfaces cleaned with O_2 plasma (OPCSS) under all conditions as assessed by water contact angle and ellipsometry data. Tri-n-hexylsilane-derived monolayers on OPCSS have thicknesses of ~6-7 Å. independent of reaction conditions. The most hydrophobic surface is obtained from the vapor phase reaction ($94^{\circ}/79^{\circ}$). Monolayers prepared from toluene and $ScCO_2$ on OPCSS exhibit contact angle values of $86^{\circ}/66^{\circ}$ and $86^{\circ}/67^{\circ}$, respectively. This indicates that water interacts with silanols on the surfaces and bonding density is low on the surfaces. Tri-n-hexylsilane only reacts with silicon surfaces cleaned with piranha solution (PCSS) in the vapor phase at elevated temperatures. Tri-n-hexylsilane-derived monolayers on OPCSS and PCSS prepared from vapor phase show similar water contact angle values and thicknesses.

Reaction conditions	Cleaning Conditions			
	O_2 plasma		Piranha solution	
	Contact angle (θ_A/θ_R (°))	Thickness (λ(Å))	Contact angle (θ_A/θ_R (°))	Thickness (λ(Å))
Vapor phase 3 days, at 65-70 °C	94/79	6	93/77	6
Toluene , 3days, at 65-70 °C	86/66	7	59/34	0
$ScCO_2$, 3 days, 1385 psi at 40 °C	86/67	6	-	-

Table 5.3 Water contact angle data (θ_A/θ_R) in degrees (deg) and layer thickness (from ellipsomety) in angstroms (Å) for surfaces prepared by reaction of tri-n-hexylsilane under different conditions

The kinetics of the reaction of tri-n-hexylsilane with OPCSS and PCSS in the vapor phase was followed by water contact angle; the data are plotted in figure 5.4 and 5.5. The reaction of tri-n-hexylsilane with OPCSS shows significant hydrophobization in an hour and the reaction is completes in 24 hours. The reaction of tri-n-hexylsilane with PCSS is slower than the reaction of tri-n-hexylsilane with OCDSS. The reaction with PCSS is complete in 48 hours.

Figure 5.6 and 5.7 show monolayer thickness on OPCSS and PCSS as a function of reaction time. In both cases the thickness increases as the reaction time increases. The monolayer thickness on both of the surfaces was ~7 Å at longer reaction times.

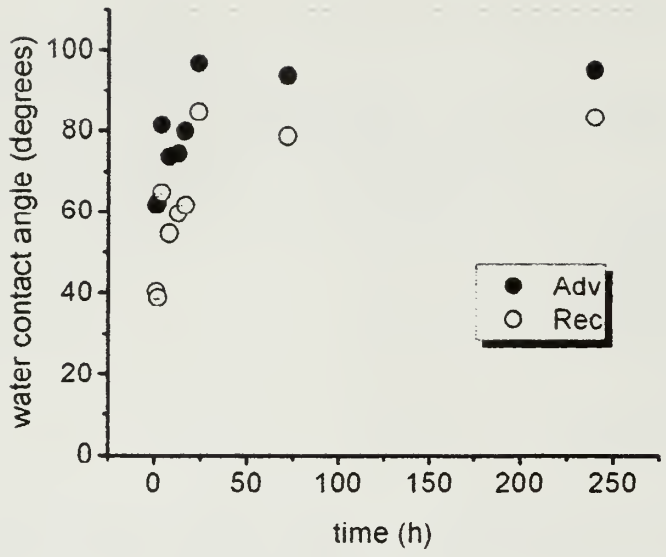

Figure 5.4 Water contact angle (θ_A/θ_R) data versus reaction time of Si/SiO_2-grafted tri-n-hexylsilane (Samples were prepared in the vapor phase at 65-70 °C. Prior to reaction, the wafers were treated with O_2 plasma.) The closed symbols are advancing angles and the open symbols are receding angles

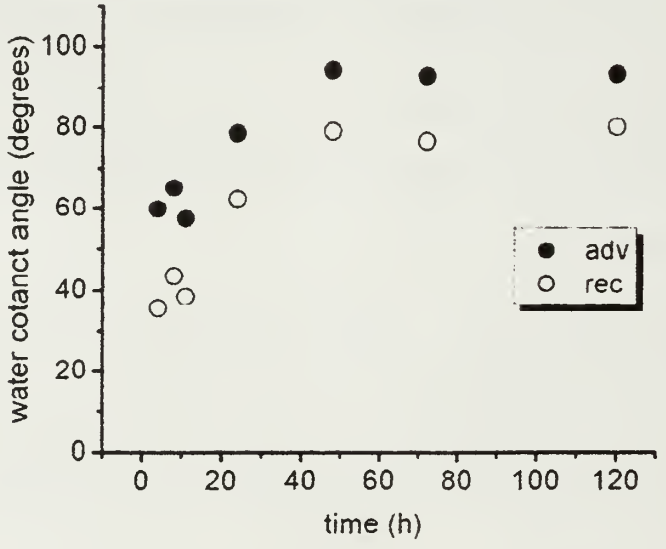

Figure 5.5 Water contact angle (θ_A/θ_R) data versus reaction time of Si/SiO_2-grafted tri-n-hexylsilane (Samples were prepared in the vapor phase at 65-70 °C. Prior to reaction, the wafers were cleaned with piranha solution.) The closed symbols are advancing angles and the open symbols are receding angles

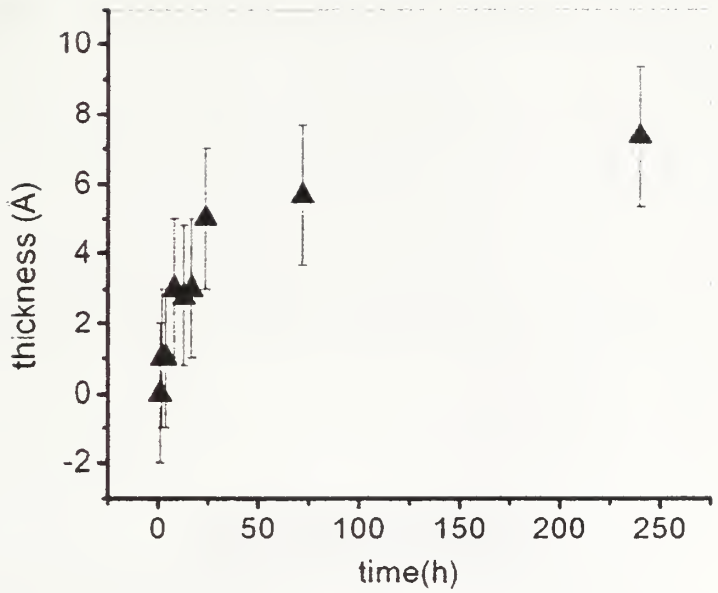

Figure 5.6 Layer thickness (from ellipsometry) versus reaction time of Si/SiO_2-grafted tri-n-hexylsilane (Samples were prepared in the vapor phase at 65-70 °C. Prior to reaction. the wafers were cleaned with O_2 plasma.)

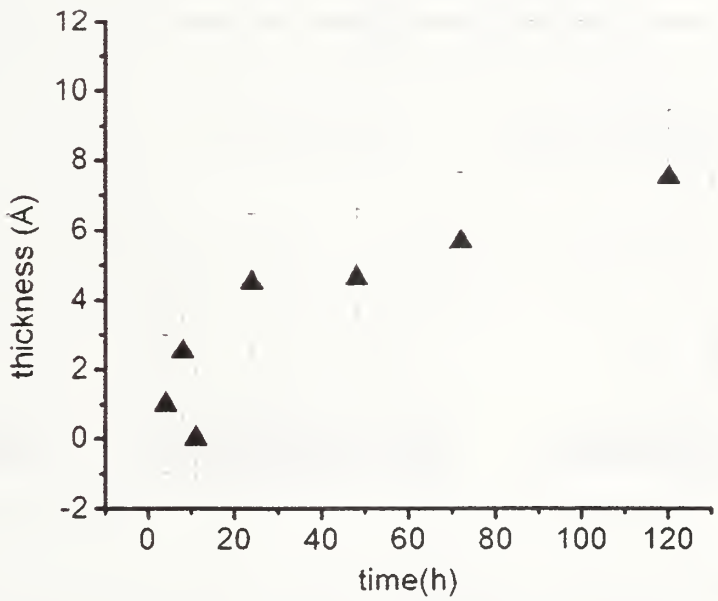

Figure 5.7 Layer thickness (from ellipsometry) vs reaction time of Si/SiO_2-grafted tri-n-hexylsilane (Samples were prepared in the vapor phase at 65-70 °C. Prior to reaction. the wafers were cleaned with piranha solution.)

5.3.2 Reaction of Silicon Surfaces with n-Octylsilane and n-Octadecylsilane

Silicon-supported alkylsiloxane layers were prepared by reaction of octadecylsilane (in the vapor phase at 65-70 °C and in toluene at 65-70 °C) and octylsilane ((in the vapor phase at 65-70 °C, in toluene at 65-70 °C and in $ScCO_2$ at 40 °C) with silicon wafers. The wafers were cleaned by O_2 plasma for 5 minutes. Figure 5.8 shows the different structures of layers that can form on the surfaces as a result of different reaction conditions.

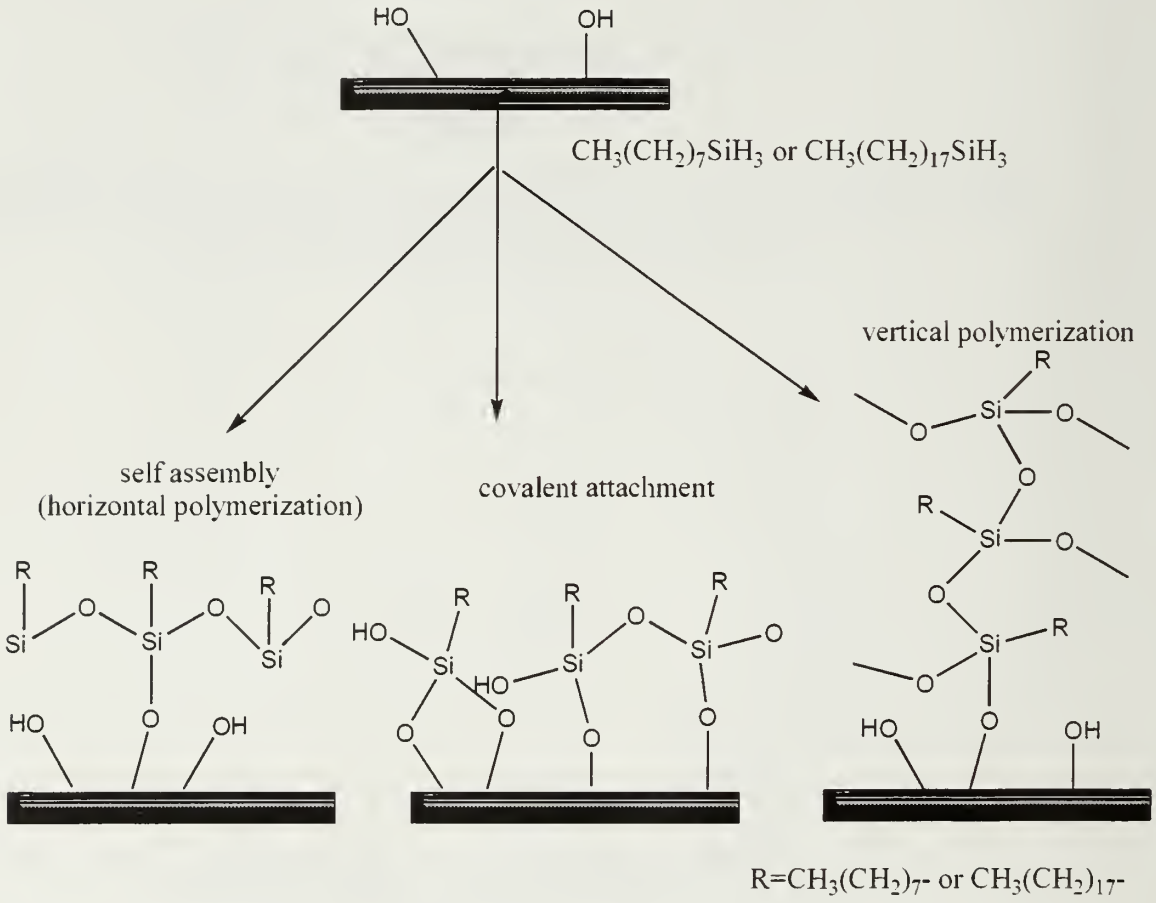

Figure 5.8 Schematic representation of the reaction of octylsilane and octadecylsilane with silicon surfaces and possible products of the reactions

Reaction conditions	$CH_3(CH_2)_7SiH_3$		$CH_3(CH_2)_{17}SiH_3$	
	Contact angle (θ_A/θ_R (°))	Thickness (λ(Å))	Contact angle (θ_A/θ_R (°))	Thickness (λ(Å))
Vapor phase, 1 day, at 65-70 °C	102/97	10	107/87	16
Toluene, 1 day, at 65-70 °C	81/51	10	96/63	20
Vapor phase, 2 days, 65-70 °C	102/95	11	100/75	14
Toluene, 2 days, at 65-70 °C	87/61	22	95/76	32
Vapor Phase, 3 days, at 65-70 °C	102/96	9	-	-
$ScCO_2$ 1385 psi 3 days,at 40 °C	115/97	13	-	-

Silicon wafers are cleaned with O_2 plasma for 5 minutes

Table 5.4 Water contact angle data (θ_A/θ_R) in degrees (deg) and layer thickness (from ellipsomety) in angstroms (Å) for surfaces prepared by reaction of octylsilane and octadecylsilane under different conditions

Table 5.4 shows the water contact angle and layer thickness data for surfaces prepared by reactions of octylsilane and octadecylsilane under different conditions. Reaction of silicon wafers with octylsilane in the vapor phase at 65-70 °C creates covalently attached monolayers and contact angle data indicates that water does not interact with the surface silanols. The hysteresis values in water contact angle data for n-octylsilane-derived monolayers prepared in the vapor phase are very low (5-7°). The octylsilane-derived layers in toluene show lower contact angle values than the monolayers prepared in the vapor phase. This indicates that water penerates through the layer and interacts with the surface silanols. Layers prepared in toluene at 65-70 °C for 2 days are oligomeric as assessed by thickness results. The octylsilane-derived monolayer prepared in $ScCO_2$ exhibits contact angle values higher than the self assembled monolayers

reported in the literature.[10] Octadecylsilane-derived monolayers prepared in the vapor phase show disordered and incomplete monolayer structure, and the residual silanols are apparent by the low receding contact angles. Surfaces prepared from octadecylsilane in toluene exhibit very low water contact angle data due to an incomplete reaction.

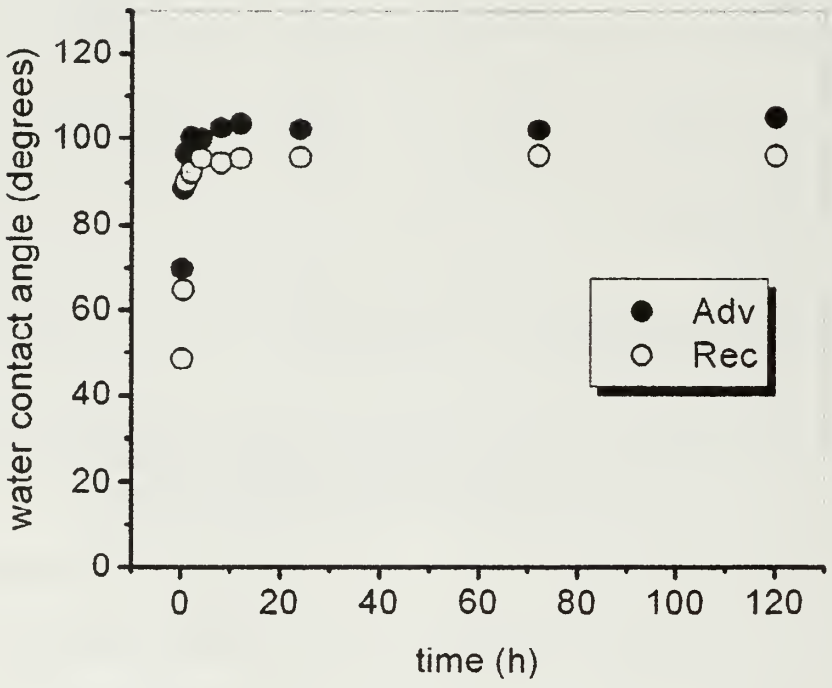

Figure 5.9 Water contact angle (θ_A/θ_R) data versus reaction time of Si/SiO_2-grafted octylsilane (Samples were prepared in the vapor phase at 65-70 °C. Prior to reaction, the wafers were treated with O_2 plasma.)The closed symbols are advancing angles and the open symbols are receding angles

The kinetics of the reaction of silicon wafers cleaned with O_2 plasma with octylsilane in the vapor phase and in $ScCO_2$ are followed by water contact angle data; and the data are plotted in Figure 5.9 and 5.10, respectively. The reaction in the vapor phase is very fast and is complete in 4 hours. The hysteresis of the octylsilane-derived monolayers prepared in the vapor phase is very low and the hysteresis does not increase at longer reaction times. The contact angle values show that the octylsilane-derived

monolayers consist of methyl and methylene groups on the surface and these monolayers are disordered. The reaction in $ScCO_2$ is also very fast and is complete within a couple of hours. The slight changes in contact angle values are observed for the octylsilane-derived monolayers prepeared in $ScCO_2$ as the reaction time increases.

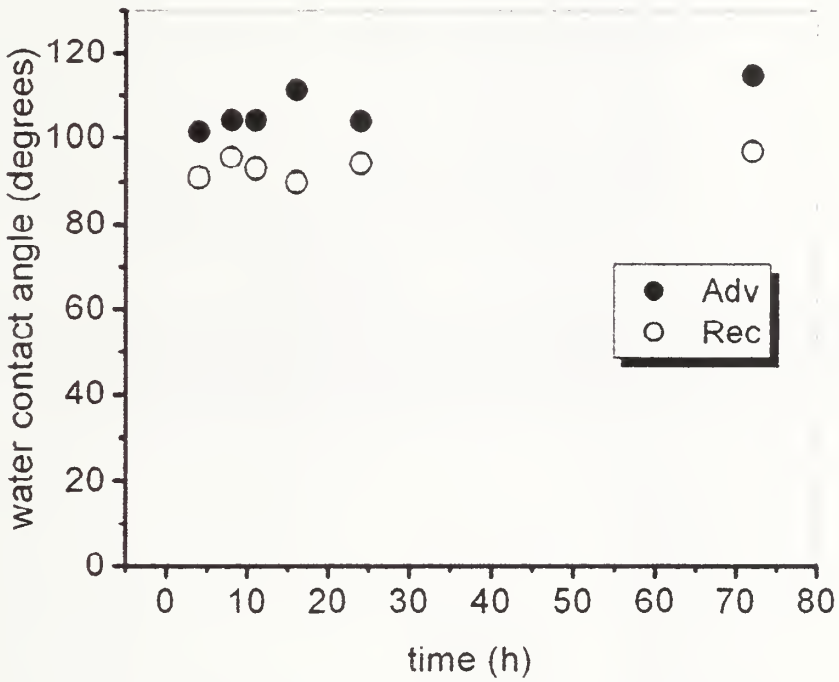

Figure 5.10 Water contact angle (θ_A/θ_R) data versus reaction time of Si/SiO_2-grafted octylsilane (Samples were prepared in $ScCO_2$ a 1385 psi at 40 °C. Prior to reaction, the wafers were treated with O_2 plasma). The closed symbols are advancing angles and the open symbols are receding angles

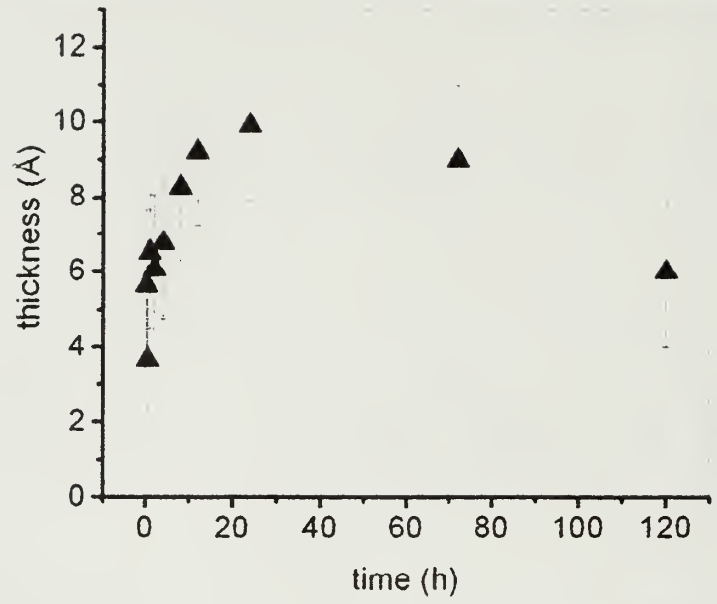

Figure 5.11 Layer thickness (from ellipsometry) versus reaction time of Si/SiO_2-grafted octylsilane (Samples were prepared in the vapor phase at 65-70 °C. Prior to reaction; the wafers were cleaned with O_2 plasma.)

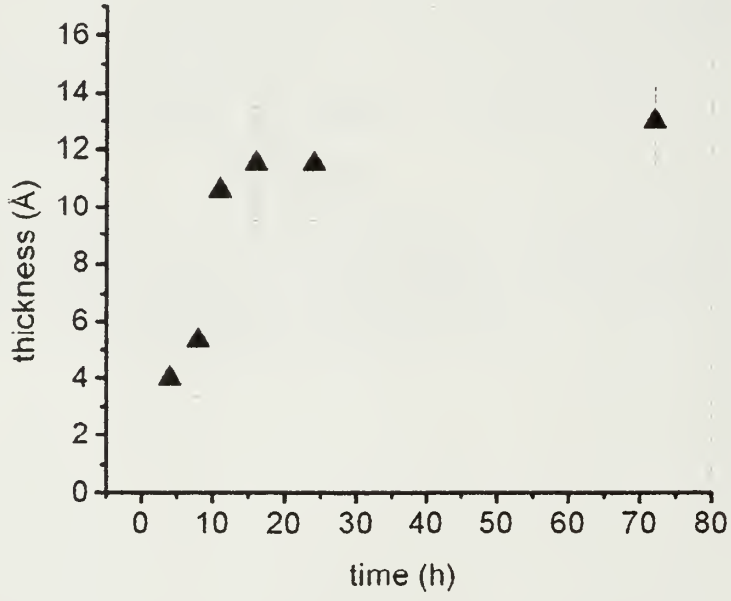

Figure 5.12 Layer thickness (from ellipsometry) vs reaction time of Si/SiO_2-grafted octylsilane (Samples were prepared in $ScCO_2$ at 1385 psi at 40°C .Prior to reaction; the wafers were cleaned with O_2 plasma.)

Figures 5.11 and 5.12 show layer thickness data of octylsilane-derived monolayers in the vapor phase and in $ScCO_2$ as a function of reaction time, respectively. In the vapor phase reactions, the monolayer thickness increases as the reaction time increases until some point, and after that time a slight decrease is observed (Figure 5.12). The thickness of these monolayers is consistently less than the length of fully stretched octylsilane, which argues for a disordered monolayer structure. The monolayer thickness increases as the reaction time increases in $ScCO_2$ and at high reaction times the thickness is 13 Å which is the value of the length of a fully stretched octylsilane. This is also consistent with the water contact angle data.

5.4 Conclusions

Silicon-supported alkylsiloxane layers are prepared by the reaction of tri-n-hexylsilane and n-octylsilane in the vapor phase, in toluene and in $ScCO_2$ at elevated temperatures, and n-octadecylsilane in the vapor phase and in toluene. The layer structure depends on the reaction conditions. The kinetics of reaction of tri-n-hexylsilane in the vapor phase with silicon wafers (O_2 plasma or piranha solution cleaned) was investigated. The kinetics of the reaction of octylsilane in the vapor phase and in $ScCO_2$ at elevated temperatures with silicon wafers (O_2 plasma cleaned) was also investigated.

5.5 References

(1) Unger, K. K. *Porous Silica, Its Properties and Use As Support In Column Liquid Chromatography*, Elsevier Scientific Pub. Co.;: New York, 1979.

(2) Plueddemann, E. P. *Silane Coupling agents*, Plenum Press: New York, 1991.

(3) Mittal, K. L.: Plueddemann, E. P. *Silanes and Other Coupling Agents*, Vsp: Utrecht, 1992.

(4) Leyden, D. E. *Silanes, Surfaces, and Interfaces*, Gordon and Breach: New York, 1986.

(5) Pesek, J. J.: Matyska, M. T.; Abuelafiya, R. R. *Chemically Modified Surfaces : Recent Developments*, Royal Society of Chemistry: Cambridge, 1996.

(6) Sagiv, J. *Israel Journal of Chemistry* **1979**, *18*, 346-353.

(7) Sagiv, J. *Journal of the American Chemical Society* **1980**, *102*, 92-98.

(8) Wasserman, S. R.; Tao, Y. T.; Whitesides, G. M. *Langmuir* **1989**, *5*, 1074-1087.

(9) Fadeev, A. Y.; McCarthy, T. J. *Langmuir* **1999**, *15*, 3759-3766.

(10) Fadeev, A. Y.; McCarthy, T. J. *Langmuir* **2000**, *16*, 7268-7274.

(11) Wasserman, S. R.; Whitesides, G. M.; Tidswell, I. M.; Ocko, B. M.; Pershan, P. S.; Axe, J. D. *Journal of the American Chemical Society* **1989**, *111*, 5852-5861.

(12) Tada, H.; Nagayama, H. *Langmuir* **1994**, *10*, 1472-1476.

(13) Boksanyi, L.; Liardon, O.; Kovats, E. S. *Advances in Colloid and Interface Science* **1976**, *6*, 95-137.

(14) Berendsen, G. E.; Pikaart, K. A.; Galan, L. D. *Journal of Liquid Chromatography* **1980**, *3*, 1437-1464.

(15) Sindorf, D. W.; Maciel, G. E. *Journal of Physical Chemistry* **1982**, *86*, 5208-5219.

(16) Szabo, K.; Leha, N.; Schneider, P.; Zeltner, P.; Kovats, E. S. *Helvetica Chimica Acta* **1984**, *67*, 2128-2142.

(17) Kinkel, J. N.; Unger, K. K. *Journal of Chromatography* **1984**, *316*, 193-200.

(18) Sander, L. C.; Callis, J. B.; Field, L. R. *Analytical Chemistry* **1983**, *55*, 1068-1075.

(19) Staroverov, S. M.; Fadeev, A. Y. *Journal of Chromatography* **1991**, *544*, 77-98.

(20) Fadeev, A. Y.; Eroshenko, V. A. *Journal of Colloid and Interface Science* **1997**, *187*, 275-282.

(21) Gilpin, R. K.; Gangoda, M. E. *Analytical Chemistry* **1984**, *56*, 1470-1473.

(22) Lochmuller, C. H.; Hunnicutt, M. L. *Journal of Physical Chemistry* **1986**, *90*, 4318-4322.

(23) Albert, K.; Bayer, E. *Journal of Chromatography* **1991**, *544*, 345-370.

(24) Zhuravlev, L. T. *Langmuir* **1987**, *3*, 316-318.

(25) Claudy, P.; Letoffe, J. M.; Gaget, C.; Morel, D.; Serpinet, J. *Journal of Chromatography* **1985**, *329*, 331-349.

(26) Maoz, R.; Sagiv, J. *Journal of Colloid and Interface Science* **1984**, *100*, 465-496.

(27) Kessel, C. R.; Granick, S. *Langmuir* **1991**, *7*, 532-538.

(28) Allara, D. L.; Parikh, A. N.; Rondelez, F. *Langmuir* **1995**, *11*, 2357-2360.

(29) Brzoska, J. B.; Benazouz, I.; Rondelez, F. *Langmuir* **1994**, *10*, 4367-4373.

(30) Parikh, A. N.; Liedberg, B.; Atre, S. V.; Ho, M.; Allara, D. L. *Journal of Physical Chemistry* **1995**, *99*, 9996-10008.

(31) Ulman, A. *Chemical Reviews* **1996**, *96*, 1533-1554.

(32) Hair, M. L.; Hertl, W. *Journal of Physical Chemistry* **1969**, *73*, 2372-&.

(33) Legrange, J. D.; Markham, J. L.; Kurkjian, C. R. *Langmuir* **1993**, *9*, 1749-1753.

(34) Hair, M. L.; Tripp, C. P. *Colloids and Surfaces a-Physicochemical and Engineering Aspects* **1995**, *105*, 95-103.

(35) Tripp, C. P.; Hair, M. L. *Journal of Physical Chemistry* **1993**, *97*, 5693-5698.

(36) Fadeev, A. Y.; McCarthy, T. J. *Langmuir* **1999**, *15*, 3759-3766.

(37) Trau, M.; Murray, B. S.; Grant, K.; Grieser, F. *Journal of Colloid and Interface Science* **1992**, *148*, 182-189.

(38) Herzberg, W. J.; Marian, J. E.; Vermeule.T. *Journal of Colloid and Interface Science* **1970**, *33*, 164-&.

(39) Ruhe, J.; Novotny, V. J.; Kanazawa, K. K.; Clarke, T.; Street, G. B. *Langmuir* **1993**, *9*, 2383-2388.

(40) Verzele, M.; Mussche, P. *Journal of Chromatography* **1983**, *254*, 117-122.

(41) Cao, C.; *New Developments Using Carbon Dioxide As a Solvent : Monolayers and Nanocomposites*, PhD Dissertation, University of Massachusetts, 2002

(42) Tillman, N.; Ulman, A.; Penner, T. L. *Langmuir* **1989**, *5*, 101-111.

(43) McHugh, M. A.; Krukonis, V. J. *Supercritical Fluid Extraction : Principles and Practice*, Butterworths: Boston, 1986.

(44) Leitner, W.; Jessop, P. G. *Chemical Synthesis Using Supercritical Fluids*, Wiley-VCH: New York, 1999.

(45) Hayes, H. J.: *Heterogeneous polymer modification : polyolefin maleation in supercritical carbon dioxide and amorphous fluoropolymer surface modification*, PhD Dissertation, University of Massachusetts, 1999

(46) Noyori, R. *Chemical Reviews* **1999**, *99*, 353-354.

BIBLIOGRAPHY

Aarik, J.;Aidla, A.;Uustare, T.;Sammelselg, V. *Journal of Crystal Growth* **1995**, *148*, 268-275

Adamson, A. W. *Physical Chemistry of Surfaces*; Wiley: New York, 1990.

Albert, K.;Bayer, E. *Journal of Chromatography* **1991**, *544*, 345-370

Allara, D. L. *Biosensors & Bioelectronics* **1995**, *10*, 771-783

Allara, D. L.;Nuzzo, R. G. *Langmuir* **1985**, *1*, 45-52

Allara, D. L.;Nuzzo, R. G. *Langmuir* **1985**, *1*, 52-66

Allara, D. L.;Parikh, A. N.;Rondelez, F. *Langmuir* **1995**, *11*, 2357-2360

Andrade, J. D. *Surface and Interfacial Aspects of Biomedical Polymers*; Plenum Press: New York, 1985.

Andrianov, K. A.;Sobolevsky, M. V. *High-Molecular Weight Organosilicon Compounds*; Oborongiz: Moskow, 1949.

Arnebrant, T.;Backstrom, K.;Jonsson, B.;Nylander, T. *Journal of Colloid and Interface Science* **1989**, *128*, 303-312

Awan, M. A.;Dimonie, V. L.;Elasser, M. S. *Polymer Preprints (American Chemical Society, Division of Polymer Chemistry)* **1994**, *35*, 551-552

Azzam, R. M. A.;Bashara, N. M. *Ellipsometry and Polarized Light*; North-Holland Pub. Co.: New York, 1977.

Bain, C. D.;Whitesides, G. M. *Journal of the American Chemical Society* **1988**, *110*, 6560-6561

Bain, C. D.;Whitesides, G. M. *Journal of the American Chemical Society* **1988**, *110*, 5897-5898

Berendsen, G. E.:Pikaart, K. A.:Galan, L. D. *Journal of Liquid Chromatography* **1980**, *3*, 1437-1464

Berg, J. C. *Wettability*; M. Dekker: New York, 1993.

Bertrand, P.:Jonas, A.:Laschewsky, A.:Legras, R. *Macromolecular Rapid Communications* **2000**, *21*, 319-348

Bigelow, W. C.:Pickett, D. L.:Zisman, W. A. *Journal of Colloid Science* **1946**, *1*, 513-538

Boerio, F. J.:Boerio, J. P.:Bozian, R. C. *Applied Surface Science* **1988**, *31*, 42-58

Boksanyi, L.:Liardon, O.:Kovats, E. S. *Advances in Colloid and Interface Science* **1976**, *6*, 95-137

Brzoska, J. B.:Benazouz, I.:Rondelez, F. *Langmuir* **1994**, *10*, 4367-4373

Cacciafesta, P.:Hallam, K. R.:Oyedepo, C. A.; Humphris, A. D. L.:Miles, M. J.;Jandt, K. D. *Chemistry of Materials* **2002**, *14*, 777-789

Cais, R. E.:Kometani, J. M. *Macromolecules* **1984**, *17*, 1932-1939

Cao, C.: *New Developments Using Carbon Dioxide As a Solvent : Monolayers and Nanocomposites*, PhD Dissertation, University of Massachusetts, 2002

Cao, T. B.; Chen, J. Y.; Yang, C. H.:Cao, W. X. *New Journal of Chemistry* **2001**, *25*, 305-307

Caruso, F.;Caruso, R. A.; Mohwald, H. *Chemistry of Materials* **1999**, *11*, 3309-3314

Chan, C. M. *Polymer surface modification and characterization*; Hanser ; Cincinnati, 1994.

Chen, W.:McCarthy, T. J. *Macromolecules* **1997**, *30*, 78-86

Chen, W.;Fadeev, A. Y.;Hsieh, M. C.;Oner, D.;Youngblood, J.;McCarthy, T. J. *Langmuir* **1999**, *15*, 3395-3399

Cho, J.;Caruso, F. *Macromolecules* **2003**, *36*, 2845-2851

Claudy, P.;Letoffe, J. M.;Gaget, C.;Morel, D.;Serpinet, J. *Journal of Chromatography* **1985**, *329*, 331-349

Clot, O.;Wolf, M. O. *Langmuir* **1999**, *15*, 8549-8551

Cossement, D.;Delrue, Y.;Mekhalif, Z.;Delhalle, J.;Hevesi, L. *Surface and Interface Analysis* **2000**, *30*, 56-60

Cossement, D.;Pierard, C.;Delhalle, J.;Pireaux, J. J.;Hevesi, L.;Mekhalif, Z. *Surface and Interface Analysis* **2001**, *31*, 18-22

Coupe, B.;Chen, W. *Macromolecules* **2001**, *34*, 1533-1535

Coupe, B.;Evangelista, M. E.;Yeung, R. M.;Chen, W. *Langmuir* **2001**, *17*, 1956-1960

Dante, S.;Hou, Z. Z.;Risbud, S.;Stroeve, P. *Langmuir* **1999**, *15*, 2176-2182

Davis, G. T.;Furukawa, T.;Lovinger, A. J.;Broadhurst, M. G. *Macromolecules* **1982**, *15*, 329-333

Decher, G. *Science* **1997**, *277*, 1232-1237

Decher, G.;Schlenoff, J. B. *Multilayer Thin Films : Sequential Assembly of Nanocomposite Materials*; Wiley-VCH: Weinheim, 2003.

Decher, G.;Hong, J. D.;Schmitt, J. *Thin Solid Films* **1992**, *210*, 831-835

Decher, G.;Lehr, B.;Lowack, K.;Lvov, Y.;Schmitt, J. *Biosensors & Bioelectronics* **1994**, *9*, 677-684

Degennes, P. G. *Macromolecules* **1981**, *14*, 1637-1644

Degennes, P. G. *Macromolecules* **1982**, *15*, 492-500

Dobiáš, B. *Coagulation and Flocculation : Theory and Applications*; M. Dekker: New York, 1993.

Dorinson, A.:Ludema, K. C. *Mechanics and Chemistry in Lubrication*; Elsevier: New York, 1985.

Dubas, S. T.;Schlenoff, J. B. *Macromolecules* **1999**, *32*, 8153-8160

Dulcey, C. S.:Georger, J. H.:Krauthamer, V.:Stenger, D. A.:Fare, T. L.:Calvert, J. M. *Science* **1991**, *252*, 551-554

Fadeev, A. Y.:Eroshenko, V. A. *Journal of Colloid and Interface Science* **1997**, *187*, 275-282

Fadeev, A. Y.;McCarthy, T. J. *Journal of the American Chemical Society* **1999**, *121*, 12184-12185

Fadeev, A. Y.:McCarthy, T. J. *Langmuir* **1999**, *15*, 3759-3766

Fadeev, A. Y.:McCarthy, T. J. *Langmuir* **2000**, *16*, 7268-7274

Fadeev, A. Y.:Soboleva, O. A.;Summ, B. D. *Colloid Journal* **1997**, *59*, 222-225

Fadeev, A. Y.:Helmy, R.:Marcinko, S. *Langmuir* **2002**, *18*, 7521-7529

Ferreira, M.:Cheung, J. H.;Rubner, M. F. *Thin Solid Films* **1994**, *244*, 806-809

Fowkes, F. M.:Zisman, W. A. *Contact Angle, Wettability and Adhesion*; American Chemical Society: Washington, 1964.

Fu, Y.:Bai, S. L.:Cui, S. X.;Qiu, D. L.;Wang, Z. Q.:Zhang, X. *Macromolecules* **2002**, *35*, 9451-9458

Furukawa, T.;Johnson, G. E.;Bair, H. E.;Tajitsu, Y.;Chiba, A.;Fukada, E. *Ferroelectrics* **1981**, *32*, 61-67

Gamble, L.;Henderson, M. A.;Campbell, C. T. *Journal of Physical Chemistry B* **1998**, *102*, 4536-4543

Garbassi, F.;Morra, M.;Occhiello, E. *Polymer Surfaces : From Physics to Technology*; Wiley: New York, 1998.

Gawalt, E. S.;Avaltroni, M. J.;Koch, N.;Schwartz, J. *Langmuir* **2001**, *17*, 5736-5738

Gilpin, R. K.;Gangoda, M. E. *Analytical Chemistry* **1984**, *56*, 1470-1473

Gramain, P.;Myard, P. *Macromolecules* **1981**, *14*, 180-184

Graul, T. W.;Schlenoff, J. B. *Analytical Chemistry* **1999**, *71*, 4007-4013

Guzonas, D. A.;Boils, D.;Tripp, C. P.;Hair, M. L. *Macromolecules* **1992**, *25*, 2434-2441

Hadziioannou, G.;Patel, S.;Granick, S.;Tirrell, M. *Journal of the American Chemical Society* **1986**, *108*, 2869-2876

Hair, M. L.;Hertl, W. *Journal of Physical Chemistry* **1969**, *73*, 2372-&

Hair, M. L.;Tripp, C. P. *Colloids and Surfaces A-Physicochemical and Engineering Aspects* **1995**, *105*, 95-103

Hao, E. C.;Lian, T. Q. *Chemistry of Materials* **2000**, *12*, 3392-3396

Hayes, H. J.;*Heterogeneous polymer modification : polyolefin maleation in supercritical carbon dioxide and amorphous fluoropolymer surface modification*, PhD Dissertation, University of Massachusetts, 1999

He, J. A.;Valluzzi, R.;Yang, K.;Dolukhanyan, T.;Sung, C. M.;Kumar, J.;Tripathy, S. K.;Samuelson, L.;Balogh, L.;Tomalia, D. A. *Chemistry of Materials* **1999**, *11*, 3268-3274

Helmy, R.;Fadeev, A. Y. *Langmuir* **2002**, *18*, 8924-8928

Helmy, R.;Wenslow, R. W.;Fadeev, A. Y. *Journal of the American Chemical Society* **2004**, *126*, 7595-7600

Henrich, V. E.;Cox, P. A. *The Surface Science of Metal Oxides*; Cambridge University Press: Cambridge ; New York, 1994.

Herzberg, W. J.;Marian, J. E.;Vermeule,T. *Journal of Colloid and Interface Science* **1970**, *33*, 164-&

Higashihata, Y.;Sako, J.;Yagi, T. *Ferroelectrics* **1981**, *32*, 85-92

Hild, R.;David, C.;Muller, H. U.;Volkel, B.;Kayser, D. R.;Grunze, M. *Langmuir* **1998**, *14*, 342-346

Hsieh, M. C.;*Polyelectrolyte Multilayer Assemblies*, PhD Dissertation, University of Massachusetts, 1999

Hsieh, M. C.;Farris, R. J.;McCarthy, T. J. *Polymer Preprints (American Chemical Society, Division of Polymer Chemistry)* **1997**, *38*, 670-671

Itoh, E.;Kokubo, H.;Shouriki, S.;Iwamoto, M. *Journal of Applied Physics* **1998**, *83*, 372-376

Iwamoto, M.;Yoneda, Y.;Fukuda, A. *Japanese Journal of Applied Physics Part 1-Regular Papers Short Notes & Review Papers* **1992**, *31*, 3671-3674

Iyengar, D. R.;McCarthy, T. J. *Polymer Preprints (American Chemical Society, Division of Polymer Chemistry)* **1989**, *30*, 154-155

Iyengar, D. R.;McCarthy, T. J. *Macromolecules* **1990**, *23*, 4344-4346

Jeon, N. L.;Finnie, K.;Branshaw, K.;Nuzzo, R. G. *Langmuir* **1997**, *13*, 3382-3391

Jun, K.;Zhu, X. Y.;Hsu, J. W. P. *Langmuir* **2000**, *22*, 3627-3636-3632

Kasemo, B. *Journal of Prosthetic Dentistry* **1983**, *49*, 832-837

Kawaguchi, M.;Mikura, M.;Takahashi, A. *Macromolecules* **1984**, *17*, 2063-2065

Kawaguchi, M.;Hayashi, K.;Takahashi, A. *Macromolecules* **1984**, *17*, 2066-2070

Kawaguchi, M.;Maeda, K.;Kato, T.;Takahashi, A. *Macromolecules* **1984**, *17*, 1666-1671

Kessel, C. R.;Granick, S. *Langmuir* **1991**, *7*, 532-538

Kharlampieva, E.;Sukhishvili, S. A. *Langmuir* **2003**, *19*, 1235-1243

Kinkel, J. N.;Unger, K. K. *Journal of Chromatography* **1984**, *316*, 193-200

Kleinfeld, E. R.;Ferguson, G. S. *Science* **1994**, *265*, 370-373

Kolb, B. U.;*Synthesis of Specifically Functionalized Polymers and Their Adsorption at the Solid-Solution Interface*, PhD Dissertation, University of Massachusetts, 1993

Kong, W.;Zhang, X.;Gao, M. L.;Zhou, H.;Li, W.;Shen, J. C. *Macromolecular Rapid Communications* **1994**, *15*, 805-805

Korosi, G.;Kovats, E. S. *Colloids and Surfaces* **1981**, *2*, 315-355

Kozlov, M.;McCarthy, T. J. *Langmuir* **2004**, *20*, 9170-9176

Kozlov, M.;Quarmyne, M.;Chen, W.;McCarthy, T. J. *Macromolecules* **2003**, *36*, 6054-6059

Kwok, D. Y.;Neumann, A. W. *Colloids and Surfaces a-Physicochemical and Engineering Aspects* **2000**, 161, 49-62.

Lausmaa, J. *Journal of Electron Spectroscopy and Related Phenomena* **1996**, *81*, 343-361

Lee, L.-H. *Adhesion and Adsorption of Polymers*; Plenum Press: New York, 1980.

Legrange, J. D.:Markham, J. L.:Kurkjian, C. R. *Langmuir* **1993**, *9*, 1749-1753

Leitner, W.:Jessop, P. G. *Chemical Synthesis Using Supercritical Fluids*; Wiley-VCH: New York, 1999.

Levasalmi, J. M.:McCarthy, T. J. *Macromolecules* **1997**, *30*, 1752-1757

Leyden, D. E. *Silanes, Surfaces, and Interfaces*; Gordon and Breach: New York, 1986.

Liu, S. Q.:Kurth, D. G.:Bredenkotter, B.:Volkmer, D. *Journal of the American Chemical Society* **2002**, *124*, 12279-12287

Liu, Y. J.:Wang, A. B.:Claus, R. O. *Applied Physics Letters* **1997**, *71*, 2265-2267

Lochmuller, C. H.:Hunnicutt, M. L. *Journal of Physical Chemistry* **1986**, *90*, 4318-4322

Lovinger, A. J.:Cais, R. E. *Macromolecules* **1984**, *17*, 1939-1945

Lovinger, A. J.:Davis, G. T.:Furukawa, T.:Broadhurst, M. G. *Macromolecules* **1982**, *15*, 323-328

Luckham, P. F.:Klein, J. *Macromolecules* **1985**, *18*, 721-728

Lvov, Y.:Ariga, K.:Ichinose, I.:Kunitake, T. *Langmuir* **1996**, *12*, 3038-3044

Maoz, R.:Sagiv, J. *Journal of Colloid and Interface Science* **1984**, *100*, 465-496

Marra, J.:Hair, M. L. *Macromolecules* **1988**, *21*, 2349-2355

McHugh, M. A.:Krukonis, V. J. *Supercritical Fluid Extraction : Principles and Practice*; Butterworths: Boston, 1986.

Mittal, K. L.;Plueddemann, E. P. *Silanes and Other Coupling Agents*; Vsp: Utrecht, 1992.

Mittal, K. L.;MST Conferences. *Adhesion Aspects of Polymeric Coatings*; Vsp Bv:; Boston, 2003.

Moore, J. A.;Kaur, S. *Macromolecules* **1998**, *31*, 328-335

Muthukumar, M.;Ho, J. S. *Macromolecules* **1989**, *22*, 965-973

Napper, D. H. *Polymeric Stabilization of Colloidal Dispersions*; Academic Press: New York, 1983.

Nathan, C. C.;Bregman, J. I. *Corrosion Inhibitors*; National Association of Corrosion Engineers: Houston, Tex., 1973.

Noyori, R. *Chemical Reviews* **1999**, *99*, 353-354

Nuzzo, R. G.;Allara, D. L. *Journal of the American Chemical Society* **1983**, *105*, 4481-4483

Nuzzo, R. G.;Fusco, F. A.;Allara, D. L. *Journal of the American Chemical Society* **1987**, *109*, 2358-2368

Ober, C. K.;Hair, M. L. *Journal of Polymer Science Part A-Polymer Chemistry* **1987**, *25*, 1395-1407

Ostrander, J. W.;Mamedov, A. A.;Kotov, N. A. *Journal of the American Chemical Society* **2001**, *123*, 1101-1110

Owens, T. M.;Nicholson, K. T.;Holl, M. M. B.;Suzer, S. *Journal of the American Chemical Society* **2002**, *124*, 6800-6801

Parikh, A. N.;Liedberg, B.;Atre, S. V.;Ho, M.;Allara, D. L. *Journal of Physical Chemistry* **1995**, *99*, 9996-10008

Parsonage, E.;Tirrell, M.;Watanabe, H.;Nuzzo, R. G. *Macromolecules* **1991**, *24*, 1987-1995

Pearson, W. B. *A Handbook of Lattice Spacings and Structures of Metals and Alloys*: Pergamon Press: New York,, 1958.

Pesek, J. J.;Matyska, M. T.;Abuelafiya, R. R. *Chemically Modified Surfaces : Recent Developments*: Royal Society of Chemistry: Cambridge, 1996.

Phuvanartnuruks, V.:*Polymer surface chemistry surface mixtures, supported polyelectrolyte multilayers and heterogeneous chemical modification*, PhD Dissertation, University of Massachusetts, 1997

Phuvanartnuruks, V.;McCarthy, T. J. *Macromolecules* **1998**, *31*, 1906-1914

Ploehn, H. J.;Russel, W. B. *Macromolecules* **1989**, *22*, 266-276

Plueddemann, E. P. *Silane Coupling Agents*: Plenum Press: New York, 1991.

Roe, R. J. *Journal of Chemical Physics* **1974**, *60*, 4192-4207

Ross, C. B.;Sun, L.;Crooks, R. M. *Langmuir* **1993**, *9*, 632-636

Ruhe, J.;Novotny, V. J.;Kanazawa, K. K.;Clarke, T.;Street, G. B. *Langmuir* **1993**, *9*, 2383-2388

Sagiv, J. *Israel Journal of Chemistry* **1979**, *18*, 346-353

Sagiv, J. *Journal of the American Chemical Society* **1980**, *102*, 92-98

Sander, L. C.;Callis, J. B.;Field, L. R. *Analytical Chemistry* **1983**, *55*, 1068-1075

Scheutjens, J. M. H. M.;Fleer, G. J. *Journal of Physical Chemistry* **1979**, *83*, 1619-1635

Scheutjens, J. M. H. M.;Fleer, G. J. *Journal of Physical Chemistry* **1980**, *84*, 178-190

Scheutjens, J. M. H. M.;Fleer, G. J. *Macromolecules* **1985**, *18*, 1882-1900

Schmitt, J.;Decher, G.;Dressick, W. J.;Brandow, S. L.;Geer, R. E.;Shashidhar, R.;Calvert, J. M. *Advanced Materials* **1997**, *9*, 61-&

Shafi, K. V. P. M.;Ulman, A.;Yan, X. Z.;Yang, N. L.;Himmelhaus, M.;Grunze, M. *Langmuir* **2001**, *17*, 1726-1730

Shiratori, S. S.;Rubner, M. F. *Macromolecules* **2000**, *33*, 4213-4219

Shoichet, M. S.;Mccarthy, T. J. *Macromolecules* **1991**, *24*, 1441-1442

Silberbe.A. *Journal of Chemical Physics* **1968**, *48*, 2835-&

Sindorf, D. W.;Maciel, G. E. *Journal of Physical Chemistry* **1982**, *86*, 5208-5219

Staroverov, S. M.;Fadeev, A. Y. *Journal of Chromatography* **1991**, *544*, 77-98

Steinemann, S. G. *Periodontology 2000* **1998**, *17*, 7-21

Stockton, W. B.;Rubner, M. F. *Macromolecules* **1997**, *30*, 2717-2725

Stouffer, J. M.;Mccarthy, T. J. *Macromolecules* **1988**, *21*, 1204-1208

Sukhishvili, S. A.;Granick, S. *Journal of the American Chemical Society* **2000**, *122*, 9550-9551

Sukhishvili, S. A.;Granick, S. *Macromolecules* **2002**, *35*, 301-310

Sukhorukov, G.;Dahne, L.;Hartmann, J.;Donath, E.;Mohwald, H. *Advanced Materials* **2000**, *12*, 112-115

Sun, J. Q.;Zou, S.;Wang, Z. Q.;Zhang, X.;Shen, J. C. *Materials Science & Engineering C-Biomimetic and Supramolecular Systems* **1999**, *10*, 123-126

Sun, J. Z.;Sun, J. Q.;Ma, Y. G.;Zhang, X.;Shen, J. C. *Materials Science & Engineering C-Biomimetic and Supramolecular Systems* **1999**, *10*, 83-86

Szabo, K.;Leha, N.;Schneider, P.;Zeltner, P.;Kovats, E. S. *Helvetica Chimica Acta* **1984**, *67*, 2128-2142

Tada, H. *Langmuir* **1995**, *11*, 3281-3284

Tada, H. *Langmuir* **1996**, *12*, 966-971

Tada, H.;Nagayama, H. *Langmuir* **1994**, *10*, 1472-1476

Tadros, T. F. *The Effect of Polymers on Dispersion properties*; Academic Press: London, 1982.

Takahashi, A.;Kawaguchi, M. *Advances in Polymer Science* **1982**, *46*, 1-65

Taton, T. A.;Mucic, R. C.;Mirkin, C. A.;Letsinger, R. L. *Journal of the American Chemical Society* **2000**, *122*, 6305-6306

Tian, J.;Wu, C. C.;Thompson, M. E.;Sturm, J. C.;Register, R. A. *Chemistry of Materials* **1995**, *7*, 2190-2198

Tian, J.;Wu, C. C.;Thompson, M. E.;Sturm, J. C.;Register, R. A.;Marsella, M. J.;Swager, T. M. *Advanced Materials* **1995**, *7*, 395-398

Tillman, N.;Ulman, A.;Penner, T. L. *Langmuir* **1989**, *5*, 101-111

Tompkins, H. G. *A User's Guide to Ellipsometry*; Academic Press: Boston, 1993.

Tosatti, S.;Michel, R.;Textor, M.;Spencer, N. D. *Langmuir* **2002**, *18*, 3537-3548

Trau, M.;Murray, B. S.;Grant, K.;Grieser, F. *Journal of Colloid and Interface Science* **1992**, *148*, 182-189

Tripp, C. P.;Hair, M. L. *Journal of Physical Chemistry* **1993**, *97*, 5693-5698

Troughton, E. B.:Bain, C. D.:Whitesides, G. M.:Nuzzo, R. G.:Allara, D. L.:Porter, M. D. *Langmuir* **1988**, *4*, 365-385

Tseng, C. M.:Lu, Y. Y.:Elaasser, M. S.:Vanderhoff, J. W. *Journal of Polymer Science Part a-Polymer Chemistry* **1986**, *24*, 2995-3007

Ulman, A. *An Introduction to Ultrathin Organic Films : From Langmuir-Blodgett to Self-assembly*; Academic Press: Boston, 1991.

Ulman, A. *Chemical Reviews* **1996**, *96*, 1533-1554

Unger, K. K. *Porous Silica, Its Properties and Use As Support In Column Liquid Chromatography*; Elsevier Scientific Pub. Co. :: New York, 1979.

van Ackern, F.;Krasemann, L.;Tieke, B. *Thin Solid Films* **1998**, *329*, 762-766

Vanderbeek, G. P.:Stuart, M. A. C.:Fleer, G. J.:Hofman, J. E. *Macromolecules* **1991**, *24*, 6600-6611

Verzele, M.;Mussche, P. *Journal of Chromatography* **1983**, *254*, 117-122

Viswanathan, N. K.;Balasubramanian, S.:Li, L.:Kumar, J.:Tripathy, S. K. *Journal of Physical Chemistry B* **1998**, *102*, 6064-6070

Voigt, A.:Lichtenfeld, H.:Sukhorukov, G. B.:Zastrow, H.:Donath, E.:Baumler, H.:Mohwald, H. *Industrial & Engineering Chemistry Research* **1999**, *38*, 4037-4043

Voronkov, M. G. *Zhurnal Prikladnoi Khimi* **1962**, *35*, 1093

Voronkov, M. G. *Zhurnal Prikladnoi Khimi* **1965**, *38*, 1483

Voronkov, M. G.;Kalugin, N. B. *Zhurnal Prikladnoi Khimi* **1956**, *31*, 1390

Wang, L. Y.:Wang, Z. Q.;Zhang, X.:Shen, J. C.;Chi, L. F.:Fuchs, H. *Macromolecular Rapid Communications* **1997**, *18*, 509-514

Wang, L. Y.;Fu, Y.;Wang, Z. Q.;Wang, Y.;Sun, C. Q.;Fan, Y. G.;Zhang, X. *Macromolecular Chemistry and Physics* **1999**, *200*, 1523-1527

Wang, M.;Jiang, M.;Ning, F. L.;Chen, D. Y.;Liu, S. Y.;Duan, H. W. *Macromolecules* **2002**, *35*, 5980-5989

Wasserman, S. R.;Tao, Y. T.;Whitesides, G. M. *Langmuir* **1989**, *5*, 1074-1087

Wasserman, S. R.;Whitesides, G. M.;Tidswell, I. M.;Ocko, B. M.;Pershan, P. S.;Axe, J. D. *Journal of the American Chemical Society* **1989**, *111*, 5852-5861

Xia, Y. N.;Zhao, X. M.;Whitesides, G. M. *Microelectronic Engineering* **1996**, *32*, 255-268

Yagi, T. *Polymer Journal* **1979**, *11*, 711-719

Yamada, T.;Kitayama, T. *Journal of Applied Physics* **1981**, *52*, 6859-6863

Yang, X.;Johnson, S.;Shi, J.;Holesinger, T.;Swanson, B. *Sensors and Actuators B-Chemical* **1997**, *45*, 87-92

Youngblood, J. P.:*Wettability of Polymer Surfaces : Effects of Chemistry and Topography*, PhD Dissertation, University of Massachusetts, 2001

Zhang, H. Y.;Wang, Z. Q.;Zhang, Y. Q.;Zhang, X. *Langmuir* **2004**, *20*, 9366-9370

Zhang, W. Q.;Shi, L. Q.;Gao, L. C.;An, Y. L.;Li, G. Y.;Wu, K.;Liu, Z. *Macromolecules* **2005**, *38*, 899-903

Zhang, X.;Gao, M. L.;Kong, X. X.;Sun, Y. P.;Shen, J. C. *Journal of the Chemical Society-Chemical Communications* **1994**, 1055-1056

Zhuravlev, L. T. *Langmuir* **1987**, *3*, 316-318